LUMA-GIS Thesis nr 30

Processing of MODIS Vegetation Indices for analysis of agricultural droughts in the southern Ukraine between the years 2000-2012

Oleksandr Nekrasov

2014

Department of

Physical Geography and Ecosystem Science

Lund University

Sölvegatan 12

S-223 62 Lund

Sweden

Processing of MODIS Vegetation Indices for analysis of agricultural droughts in the southern Ukraine between the years 2000-2012

Oleksandr Nekrasov

Master degree thesis, 30 credits in
Geographic Information Systems

Supervisor: Dr. David Tenenbaum

Abstract

In the current research, agricultural droughts were analyzed over the territory of Southern Ukraine for the period 2000-2012. Since agricultural drought is "insufficient soil moisture to meet the needs of a particular crop" according to a definition provided by the Food and Agricultural Organization of the United Nations (FAO), the conditions of crop vegetation along with surface soil moisture conditions were analyzed in this research. Analysis was performed using indices calculated from time series of remote sensing data acquired by the Moderate Resolution Imaging Spectroradiometer (MODIS). The Normalized Difference Vegetation Index (NDVI) was used as a proxy of agricultural vegetation conditions. Time series NDVI data used in the current research was acquired from the MODIS vegetation indices collection. Temperature-Vegetation Dryness Index (TVDI) was used to reflect surface moisture conditions. TVDI was calculated from surface temperature and MODIS-NDVI datasets using software developed during the present research. In order to have pixels representing signal from agricultural areas only, agricultural fields were classified and masked before the analysis. Winter and summer crops were classified and analyzed separately in the research, due to their different growing seasons and cultivation schedules. Analysis of vegetation and moisture conditions was performed on an annual basis. For this purpose, maximum NDVI values and integral NDVI values were calculated from NDVI profiles of the growing season for each year of the analysis. Since winter and summer crops are not often planted in the same fields in different years, and in order to have continues time series of winter and summer crop parameters, analysis in the present research was conducted based on 10 kilometer grid, cells which were coded with the Morton key index. In order to reflect changes between various years' standard deviation, inter-annual trends were calculated for each parameter in this research. Dependence of vegetation conditions on surface moisture was objectively assessed by Pearson's correlation coefficient. Standardized values were calculated for vegetation and moisture parameters and compared in order to subjectively investigate impacts of droughts on crops in particular years of the analysis.

As a result of the research, it was found that amount of green vegetation for winter and summer crops has generally decreased over the Southern Ukraine between the years 2000-2012. Parameters of vegetation performance strongly varied in space and in time. Trends of surface moisture were also found to be negative during that period. Correlation between vegetation and moisture was statistically significant over the majority of the study area. In many locations correlation between NDVI and TVDI metrics was particularly strong ranging, from -0.7 to -0.94. Five years with unusually dry surface moisture conditions were found during the study period – 2000, 2003, 2007, 2009 and 2012. Winter and summer crops were differently impacted in these years. Both crop types were largely damaged by droughts in years 2007 and 2012. In year 2003, winter crops survived in small areas only, according to crop classification results, and had unusually poor amount of green biomass over a vast area. In years 2000 and 2009 effects from dry conditions were not as strong and widespread.

Finally, it can be concluded that during the study period (2000-2012), strong agricultural drought occurred three times: in years 2003, 2007 and 2012. These droughts were characterized by unusually dry surface moisture and low phenologic performance of agricultural vegetation. In year 2012, both winter and summer crops were equally impacted, while in year 2003 summer crops were not influenced by drought and in year 2007 summer crops were damaged more than winter crops.

Acknowledgement

The present work was performed by me in order to complete my master's degree in Geographical Information Systems at Lund University, Sweden. The scope of the research of the present thesis includes development of algorithms for automated processing of vegetation indices in order to analyze agricultural droughts in the southern Ukraine over the period 2000-2012. Vegetation indices used as initial data in the research were calculated from remote sensed data acquired by the Moderate Resolution Imaging Spectroradiometer onboard of Terra, the NASA's scientific research satellite.

I want to thank my thesis supervisor, David Tenenbaum from Department of Physical Geography and Ecosystems Analysis for his advices and corrections. His help was essential for me to reach high quality of the current work.

I am grateful for help from my colleagues from SPC "Vector", who assisted me with advices regarding development of data processing algorithms. Especially, I want to thank doctor Leonid Grekov for providing me with datasets with the results of crop classification in the Kryvoozersky administrative district, Mykolaiv Oblast.

I want also to thank my former thesis supervisor docent Hans Hauska from the Geo-informatics division at the Department for Urban Planning and Environment, Royal Institute of Technologies, Stockholm. From his comments and guidelines, I learned how to conduct scientific research, which helped me during the work under the present thesis.

Table of content

List of figures

List of tables

List of abbreviations

AVHRR	Advanced Very High Resolution Radiometer
BT	Brightness Temperature
CRA-CIN	Research Centre for Industrial Crops
CSV	Comma Separated Value format
CWSI	Crop Water Stress Index
EEA	European Environment Agency
ETM+	Enhanced Thematic Mapper Plus, onboard Landsat 7
FAO	Food and Agriculture Organization of the United Nations
GDP	Gross domestic product
GEOG	Department of Geographical Sciences at the University of Maryland
GHCND	Global Historical Climatology Network
GWR	Geographically Weighted Regression
LULC	Land Use and Land Cover
MODIS	Moderate Resolution Imaging Spectroradiometer
MVC	Maximum Value Composites
MVR	Maximal Value Raster
NDVI	Normalized Difference Vegetation Index
NDWI	Normalized Difference Water Index
NIR	Near infrared spectrum of light
NOAA	National Oceanic and Atmospheric Administration
NPP	Net Primary Productivity
PELCOM	Pan-European land cover database
SPI	Standardized Precipitation Index
SPOT VGT	System for Earth Observation, Vegetation
SVI	Standardized Vegetation Index
Ta	Temperature of air
Ts	Temperature of land surface
TVDI	Temperature-Vegetation Dryness Index
UNFCCC	United Nations Framework Convention on Climate Change
USGS	U.S. Geological Survey
USWCL	U.S. Water Conservation Laboratory
VHI	Vegetation Health Index

1. Introduction

Ukraine is a young country situated in central Europe and was created after the collapse of the Soviet Union in year 1991. Ukraine has unique climatic and land resources, which are suitable for agriculture. Generally, the Ukrainian agriculture sector can be characterized by a strong focus on plant production, while meat is imported to certain extant (van Leeuwen et al., 2012). Before the year 1991, Ukraine played a role of the "breadbasket" of the Soviet Union (FAO, 2005). After the collapse of the USSR, Ukrainian territory was one of the most arable in Europe. In those times, 70% of all land was used for agriculture, 81 percent of which was cultivated (Saiko, 1995). In comparison, only 37% of the area of the former Soviet Union was used for agriculture, while 48% of land was used for agriculture in France and Germany. At the beginning of the new century, the share of agricultural land has increased to 75% (Martynenko, 2001). According to Saiko (1995), such abundance of cultivated area provides favorable conditions for crop production.

After the collapse of the Soviet Union, GDP of the agricultural sector declined by 51% till the year 1999. The reason for this was the end of government support and the transition from production targets to a market-oriented approach (FAO, 2005). This caused a lack of money, which reduced the effectiveness of farmers' activities. Lack of resources as well as insufficient experience and knowledge caused the use of obsolete techniques in farming (Martynenko, 2001). Usage of fertilizers has reduced by a factor of seven since the year 1990 (FAO, 2005), which caused very low yields in comparison to the rest of the Europe (van Leeuwen et al., 2012).

Currently, agricultural production accounts for one tenth of Ukrainian GDP and employs about 19% of people in Ukraine (World Bank, 2004). In the near future a steady increase is projected in the production of grain crops (van Leeuwen et al., 2012). However, according to van Leeuwen et al. (2012) growth in production is small and limited by the loss of fertility of soils and droughts. Thus, droughts and land degradation can be identified as two major problems of Ukrainian agriculture.

According to previous research, droughts in the Ukrainian territory happen every 2-4 years (Kogan et. al., 2011; Vojegova et al., 2013; Adamenko and Prokopenko, 2011). Also, mild droughts affect 20-40% of the Ukrainian territory every year. In the year 2007, 60% of the territory was hit by a severe drought (Kogan et. al., 2011), which destroyed crops in a vast area (Netis, 2007). Thus, weather variability and extreme weather conditions are the main risks for the Ukrainian agricultural sector (Kul'bida, 2009).

In the future, droughts may become even more frequent in Central and East European countries including Ukraine (AVEC, 2003). Increased climate variability and more frequent extreme climate events may cause downward trends in yields (McCarthy, 2009). Ukrainian agriculture is also vulnerable to droughts due to anthropogenic desertification processes developing according to a "Mediterranean scenario", with a high magnitude of erosion and disruption of feeding of ground water (Yatsyk et al., 2006). Netis (2009) has discovered that there was increase in precipitation and decrease in soil humidity over the last 35 years, which can be interpreted as evidence of the degraded ability of soil to hold water. Due to this, desertification may occur in Ukraine, even without an increase in the aridity of climate conditions (Yatsyk et al., 2006).

The ability of farmers to resist droughts in Ukraine is limited due to poor access to finances and uncertainty caused by political decisions (van Leeuwen et al., 2012). In this case, the production

systems of farmers is not flexible enough, which, according to FAO (2004), may be a reason for the inability to cope with strong climate variations and their consequences. In order to deal with increasing aridity and extreme weather events, sound drought management is required. Decisions regarding appropriate drought mitigation measures should be based on objective assessment, which must be based upon reliable information (Balint et al., 2011). Good knowledge of climate patterns and crop vulnerability may help farmers to develop optimal strategies for their activities (FAO, 2004). This knowledge can be obtained by studying previous droughts that will identify territories, that are most vulnerable to droughts. Such studies will also help to evaluate the drought risks to which Ukrainian agriculture is exposed.

Drought is an extreme weather event which, according to FAO (2013), can be defined as deficit of precipitation compared to the inter-annual average and which results in water shortage. If as a result of drought, soil moisture is insufficient for specific agricultural crops, drought is called agricultural drought (FAO, 2013). It is stated in Peters et al. (2002) that droughts are hard to monitor, since droughts have varying length, spatial extent and magnitude. Another challenge is that the onset of drought is slow and often hard to determine. Thus, it is not sufficient to use climate data only for drought monitoring. Climate data must be supplemented by satellite data (Peters et al., 2002), which "provides a synoptic view of the land and a spatial context for measuring drought impacts" (Gu et al., 2007). The Normalized Difference Vegetation Index (NDVI) is a comprehensive measure of photosynthetic activity, which has been widely used for monitoring vegetation response to climate variability in combination with weather data (Gesser et al., 2012; Propastin and Kappas, 2008; Runnström, 2000; Wang, et al., 2001; Aragón, et al., 2012; Ichii, et al., 2002; Peters et al., 2002; Gu, et al., 2007; Liu et al., 2011).

Although the combination of climate data and NDVI has been proven to be effective, there are some limitations to this approach. According to Gu et al. (2007), NDVI responds to changes in rainfall with a time lag. The slow response of NDVI to a lack of rainfall is caused by the fact that NDVI is sensitive to the amount of chlorophyll in the vegetation foliage. After vegetation experiences water stress, it remains green for some time, thus NDVI does not changing immediately (Sandholt et al., 2002). The amount of rainfall has also limited applicability to characterize agricultural drought. For this purpose, soil moisture is a better indicator. Poor yields are more related to soil dryness then to insufficiency of rainfall, since water may be lost from soil as a result of improper agricultural activities (FAO, 2004).

According to the surface energy balance law (Sandholt et al., 2002; Gonzalez et al, 2005; USWCL, 2001), soil moisture has influence on the temperature of the land surface, due to changes in evaporation. Also, the amount of water in the root zone has an influence on water transpiration from plants and the temperature of the canopy (Sandholt et al., 2002). In order to characterize water stress of plants the Crop Water Stress Index (CWSI) was developed, which represents the difference between actual and potential transpiration. Although CWSI has been widely and successfully used in crop monitoring, use of CWSI for areas with partial vegetation coverage may be limited. In order to overcome this limitation, surface temperature was combined with NDVI and the Temperature-Vegetation Dryness Index (TVDI) was developed (Sandholt et al., 2002). TVDI is simpler to calculate than CSWI since it does not require data on meteorological conditions.

1.1 Aim and objectives

According to Brown et al. (2008), monitoring of drought requires a series of observations at the same location. For this purpose, time series of remote sensed data have been widely used for drought monitoring and monitoring of crop water stress in previous research. However, these methods have, thusfar, had little application over Ukrainian territory. Previously, vegetation conditions in response to weather events were analyzed over Ukrainian territory using the Vegetation Health Index (VHI), which is the combination of NDVI and brightness temperature (calculated from IR4, 10.3–11.3 of NOAA AVHRR) (Kogan, et al. 2011; Kogan and Guo, 2011).

The purpose of the current research is to complement results acquired using VHI by investigating whether agricultural droughts is a driving force of poor performance of crop vegetation in certain years over part of the Ukrainian territory. In order to accomplish this, this research aims to analyze surface moisture conditions assessed using the Temperature-Vegetation Dryness Index (TVDI), and then to compare moisture conditions with vegetation performance assessed using NDVI.

The current research also complements the results of research conducted by Kogan (2011) and Kogan and Guo (2011), by analyzing conditions of crop vegetation only. Vegetation performance calculated in the current research must be related to agricultural fields and must not be contaminated with data from other land use types. Unlike the NOAA AVHRR sensor used in previous research, the MODIS sensor has spatial resolution sufficient to perform analysis on a field-by-field basis. This provides the possibility to separately analyze fields covered with winter and summer crops, which are exposed to different weather events due to different cultivation schedules.

The aim of the current research is to investigate the condition of crops over the period between the years 2000-2012 and to examine whether poor vegetation performance may be caused by unusually dry surface moisture conditions.

The objectives of this research are:

- to calculate the spatial distribution of variability and inter-annual trends of conditions of winter and summer crops and standardized deviation of crop conditions from normal
- to calculate the spatial distribution of variability and inter-annual trends of surface moisture conditions and standardized deviation of moisture conditions from normal
- to compare results of the analysis of vegetation performance and moisture conditions and suggest whether agricultural droughts according to the definition from FAO (2013) may be a driving force of poor vegetation performance.

Since summer and winter crops must be classified for every year of the analysis, this approach entails certain limitations on the extent of the study area, which covers the southern Oblasts of Ukraine only. The southern part of Ukraine was chosen for this research, since it is the most arid part of Ukraine (Rudenko, 2007) and is classified as semiarid (Verheye, 2006). The study period is limited by MODIS data availability, which is available since the year 2000. Also, this research is limited to being conducted on a yearly basis using metrics of NDVI and TVDI calculated from their respective time series.

2. Background and theory

2.1 Study area

2.1.1 Geography and climate

The current study is focused on the southern region of Ukraine (Figure 1) which includes Odessa oblast, Mykolaiv Oblast, Kherson Oblast, Zaporizja Oblast and Autonomous Republic of Crimea (Crimean Peninsula). The study area covers approximately 140 thousand square kilometers and stretches 686 kilometers from west to east and 425 kilometers from north to south. Terrain is predominantly plains and the majority of the study area lies on the Black Sea Lowland with elevations ranging from 90 to 150 meters above sea level. The eastern and north-western parts of the study area are at a higher elevation than the rest of the area. Elevations there are around 200 meters and reach 300 meters in some locations. In the southern part of the Crimea Peninsula, the Crimean Mountains are situated. The southern edge of the study area is bounded by the Danube River and the Black and Azov Seas. There are plenty of inland water bodies (Figure 1B) and two major rivers the Dnieper and Pivdenniy Bug, in the area. The study area is situated in the Steppe zone (Gumeniuk et al., 2010) with highly fertile Chernozem and Haplic Kastanozem soils, the thickness of which is 41–70 cm on average (FAO, 2005).

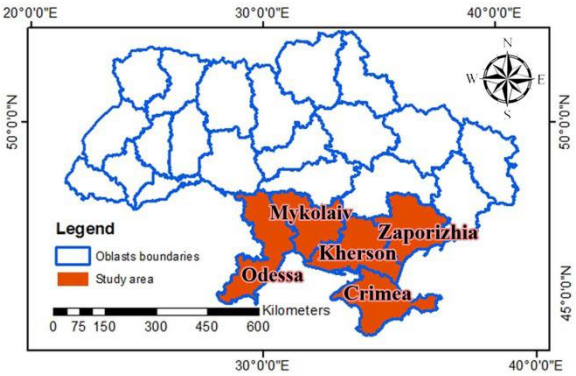

Figure 1. Location of the study area.

The climate of the study area is Atlantic-continental and characterized by continentally and aridity in comparison to other parts of Ukraine (UNFCCC, 1998). The annual amount of rainfall ranges from less than 400 mm to more than 550 mm, and the average annual temperature is 8 to 12 degrees centigrade (Rudenko, 2007). These variables change mainly from north to south. Due to low air humidity, dust storms and dry winds are frequent in the area (UNFCCC, 1998).

The study area lies in the temperate climatic zone with hot summers and cold winters. The temperature and amount of precipitation varies during the year. In the study area, there are 220-240 days in the year when temperature stays above +5 degrees centigrade and approximately 170 days when temperature is higher than +10 degrees, during which vegetation can grow (Rudenko, 2007). Figure 2 shows average monthly values of temperature and precipitation for Southern Ukraine for the period 1972-2006.

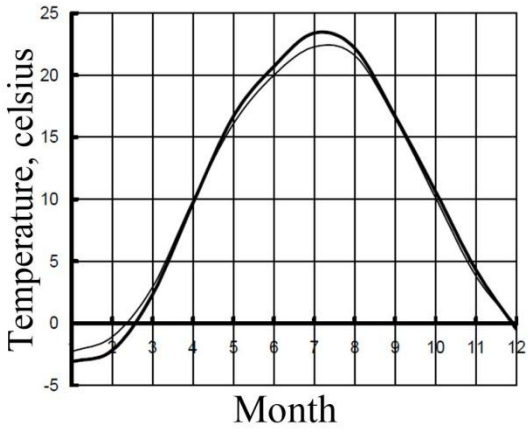

Month	Precipitation, mm
January	26,9
February	29
March	31
April	34,6
May	45,9
June	50,9
July	49,7
August	40,9
September	44,4
October	29,6
November	37,4
December	32,5

1972-2006

Figure 2. Variations in temperature and precipitation during the year in Southern Ukraine (Netis, 2009)

2.1.2 Agricultural sector

Administrative regions chosen as the study area are the most cultivated in Ukraine. As seen in Table 1, the share of arable land is around 70% of the total area. As in the other parts of Ukraine, the agricultural sector is mainly represented by large agricultural enterprises (agro-holdings), some of which cultivate as much as 20 thousand hectares of arable land (Martynenko et al., 2001).

The main crops cultivated in the study area are winter wheat and sunflower. In this area, 35% of all Ukrainian winter wheat and 37% of Ukrainian sunflower are produced (FAO, 2005). As seen in Table 1, these two crops together occupy more than half of the study area. The other half is occupied by winter barley, maize, rape, sugar beet, alfalfa etc. These crops are usually planted in a sequence, called a crop rotation scheme. In Ukraine, crop rotation schemes may include sequences of different lengths (from 2 to 6 years). For example, one of the most common crop rotation schemes is fallow, winter wheat, sunflowers, spring, barley and maize (FAO, 2005). During the fallow season, no crop is planted and land is regularly sown, which is required for land to replenish its moisture content. Unlike large agro-enterprises, private farmers cultivate vegetables and fruits rather than grain and industrial crops. Manual labor is required for the cultivation of these crops and there is a broader market for selling them (FAO, 2005).

The Ukrainian agricultural sector causes about 40% of environmental degradation in Ukraine, the majority of which is the degradation of Ukraine's famous highly fertile soils (World Bank, 2007). This is caused by deterioration of the humus balance in the soil (FAO, 2005). For example, only 61% of agriculture land in the year 1998 was of sufficient quality, 26% was classified as weak degraded and 4% was severely degraded (Martynenko et al., 2001). Although agricultural production has fallen since 1991 (World Bank, 2004), agro-holdings, which replaced state-owned farms during land privatization in 1992-2000, continue to overexploit the land (Martynenko et al., 2001).

	Share of arable land	Share of forest	Share of winter wheat	Share of sun flower
Odessa Oblast	66.5%	5-10%	40-50%	20-30%
Mykolayiv Oblast	73%	0-5%	30-40%	20-30%
Kherson Oblast	72.9%	0-5%	30-40%	10-20%
Zaporizja Oblast	75.4%	0-5%	20-30%	30-40%
Crimea	68.2%	10-15%	30-40%	0-10%

Table 1. Some agricultural features of administrative regions within the study area (FAO, 2005)

2.2 Literature review

2.2.1 Previous approaches in investigation of relations between vegetation and climate

During the investigation of relationships between vegetation activity and precipitation anomalies in Central Asia, NDVI has been used as a proxy for vegetation activity (Gesser et al., 2012). For this purpose, NDVI derived from the AVHRR sensor was compared to climate data using linear multi-temporal correlation analyses. As a result, it was found that vegetation is sensitive to precipitation variations in almost 80% of the study area. The strongest sensitivity was found in areas where the annual amount of rainfall is between 100 and 400 mm. Temporal lag between anomalies in rainfall and vegetation response was found to be between 1 to 3 months.

The spatial relationship between vegetation patterns and precipitation was investigated in the dry lands of Kazakhstan (Propastin and Kappas, 2008). In this research, NDVI-rainfall correlation was assessed using geographically weighted regression (GWR) for the period 1985-2000. NDVI was derived from the AVHRR sensor and climate data was taken from weather stations. Using GWR, maps of the study area were created showing spatial variations in the NDVI-rainfall relationship. In this research it was found that the NDVI-precipitation relationship varied spatially and temporally across the study area and period. Finally, it was concluded that the response of vegetation to changes in rainfall was a strong indicator of vegetation performance.

In his research, Runnström (2000) has examined biological productivity of vegetation in semi-arid areas in Northern West China over the period 1982-1993. NDVI derived from the AVHRR sensor was used in the research to calculate vegetation peak seasonal values. As argued by Runnström, vegetation peak values are a better metric for comparisons between years since they are not influenced by the timing of summer rain. Trends of vegetation peak values were also compared to amount of summer rainfall. In this research, a positive trend in biological productivity was found over the majority of the study area. It was also found that a correlation between biological production and rainfall was stronger in more arid areas. Runnström concluded that the calculation of linear trends from NDVI time series is a comprehensive way to assess vegetation changes at the regional level.

Bi-weekly NDVI, precipitation and temperature datasets were used in order to investigate spatial patterns of NDVI caused by climatic variability in the central Great Plains of the United States for the period 1989-1997 (Wang, et al., 2001). Based on these datasets, correlation coefficients were calculated for the relationships between NDVI and various climate factors. Seasonal relations, as well as relations between growing seasons, were examined in this research. As a result, a strong correlation was found between the variations of NDVI spatial patterns and deviations from the average amount of precipitation. Significant covariance between these variables was discovered in 60-95% of the study area. These results demonstrate that precipitation has a strong influence on the spatial patterns of vegetation productivity.

The NDVI-rainfall relationship was investigated over a portion of North Central Mexico for the period 2000-2010 (Aragón, et al., 2012). In this research, MODIS-NDVI images were combined into yearly maximum images, which were then utilized in principal component analysis. An inter-annual upward trend in the NDVI-rainfall relationship was found over the study area during the study period. This trend was validated by the data about crop harvest.

AVHRR NDVI data sets were also used to examine the relationship between vegetation and climate on the global scale during the period 1982-1990 (Ichii, et al., 2002). Correlations between NDVI and temperature and NDVI and precipitation were examined in this research, and maps of these correlations were made. It was discovered that NDVI trends can be explained by changes in temperature during the growing season in northern middle and high latitudes. In this area, a significant increase was found in annual average NDVI and for the spring to autumn period. Changes in rainfall explained variations in NDVI in semi-arid regions of the Southern Hemisphere, where precipitations had significantly decreased during the study period. The increase of NDVI in equatorial regions cannot be explained by trends in precipitation or temperature. Instead, the assumption was made that this increase was caused by an increase in nitrogen and carbon dioxide levels in the atmosphere.

NDVI was applied to drought monitoring by Peters et al. (2002). In this research the Standardized Vegetation Index (SVI) was used to describe deviations of vegetation conditions from normal. This index is based on weekly NDVI values acquired from the AVHRR sensor and derived using z-scores calculated for each pixel of each week during the period 1989 – 2000. In this study, the SVI index was applied to the central part of the U.S. By comparing maps showing SVI values with maps created during the Drought Monitor project, it was concluded that the SVI index is a useful indicator for evaluation of vegetation stress in response to weather conditions.

NDVI acquired from the MODIS datasets, in combination with normalized difference water index (NDWI), was used to assess droughts over the Great Plains of the U.S for a five-year period from 2001 to 2005 (Gu, et al., 2007). By analyzing relations between NDVI, NDWI and data from the drought monitor project, it was determined that NDWI has higher drought sensitivity than NDVI. According to Gu, et al. (2007), this means that vegetation loses water faster than it loses chlorophyll. Based on this phenomenon, a new index was presented in this research, which is calculated as the normalized difference between NDVI and NDWI values. The new index is more sensitive to droughts than NDVI or NDWI alone.

The relationships between NDVI as a proxy of vegetation activity and climate variables were investigated over Southwest China (Liu et al., 2011). Inter-annual variations in NDVI values acquired from the SPOT VGT 1-km resolution NDVI dataset were compared to variations in precipitation and temperature acquired from 31 weather stations scattered over the study area. Correlations were computed for the annual average values of these variables during the drought period. Then, the statistical significance of the correlation was tested. Based on the test results, correlation coefficients were arranged into four classes by their degree of significance. As a result, maps were produced, which show patterns of change of correlation significance. It was also found that the correlation between NDVI and temperature is more significant than between NDVI and precipitation.

Above in the current section, methods are summarized, which were used in previous researches as useful indicators of drought. These approaches were analyzed and based on the analysis method for the current research was designed. Although, the choice of method in the current research was strongly influenced by availability of open source data, inability to have field surveys and limited human resource, it follows the general principles of best practice described above.

2.2.2 Use of cropland masking

Various plant species respond differently to changes in environmental factors. In order to assess the effects of weather conditions on different vegetation types, phenology parameters can be used to discriminate between different vegetation cover (Hermance et al., 2007). Isolation of cropland in the analysis of NDVI time series is one of the factors that contributes to successful agricultural monitoring (Funk, et al., 2009). Cropland masking was extensively used in the prediction of yields, where it can substantially improve forecasts (Kastens et. al., 2005). Since masking of cultivated areas helps to limit the influence of non-agricultural areas on the result, it was used in the investigation of climate effects on agricultural vegetation. For example, the evaluation of response of soybean vegetation to climate variability was conducted using "soybean pure-pixels", which were determined as a result of land cover classification using images from Landsat 5 and 7 (Giarolla, et al., 2010). For this purpose, images were selected to represent two phenological stages in crop development, which correspond to sowing and grain maturation. In the investigation of variability of farming systems in Africa, previously produced crop masks were not used, since accurate and validated crop masks were not available for the territory and existing crop masks did not represent changes over time (Vrieling, et al., 2011). Instead, cropland areas were identified using thresholds applied to average NDVI values and seasonal variations in NDVI values.

Due to the enhanced spatial resolution of the MODIS sensor compared to AVHRR, it is possible to discover NDVI characteristics of specific crop types using MODIS datasets. This feature of MODIS was used during the large-area crop mapping in the Central Great Plains, U.S.A. (Wardlow et al., 2008). In this research, general crop types were identified using their seasonal NDVI profiles. As indicated in Wardlow, the spatial resolution of the MODIS sensor is sufficient to collect spatial-temporal signals of individual crop types in fields that are 32 hectares and larger. By visually comparing MODIS and Landsat ETM+ images, Wardlow has concluded that they represent similar field patterns.

2.2.3 Normalized Difference Vegetation Index (NDVI)

In order to examine the influence of climate on vegetation, NDVI derived from satellite imagery was used in the current research. According to Weier et al. (2000) NDVI is used to calculate the photosynthetic capacity of vegetation. This index is based on the fact that chlorophyll in plant leaves absorbs visible light (0.4-0.7 μm) and plant cell structures reflect near infrared light (0.7-1.1 μm). As shown in Equation 1, NDVI is calculated as "near-infrared radiation minus visible radiation divided by near-infrared radiation plus visible radiation".

$$NDVI = (NIR — VIS)/(NIR + VIS) \quad (1)$$

NDVI has been widely used to estimate influence of climatic condition on vegetation activities in different regions (Yuan et al., 2007). Time series of NDVI data is often used as a proxy for seasonal vegetation productivity and it provides information about seasonal and inter-annual response of vegetation to climate variability (van Leeuwen et al., 2013).

According to Huete et al. (1997), NDVI is sensitive to changes in absorbed photosynthetically active radiation. It is more sensitive to variations in visible spectrum reflectance and it becomes insensitive to variations in the near infrared spectrum in densely vegetated areas. The other limitation mentioned in Heute et al. (1997) is that NDVI values are significantly higher in darker spectral signatures when there are no significant changes in scatter within the red to NIR portion of the spectrum. This effect was observed in the humid season in semi-arid areas, when NDVI values increased without increases in biomass.

2.2.4 Calculation of phenological parameters using NDVI time series data and TIMESAT software

The scientific community is interested in employing satellite data to assess changes in land surface phenology in order to understand the response of terrestrial ecosystems to climate and other factors (Hermance et al., 2007). If one plots continuous NDVI time series data for the growing season, the result will be a curve that displays different growing stages. Parameters describing these stages can be calculated by the analysis of such curves (USGS, 2011). According to Reed et al. (1994), these parameters can be divided into three categories: temporal metrics, NDVI-value metrics and metrics derived from metrics from these two categories. In Reed et al. (1994) twelve seasonal vegetation parameters, which can be calculated from NDVI time-serieses were identified, including the onset of greenness, time of peak NDVI, maximum NDVI, rate of green up, rate of senescence and integrated NDVI.

Extraction of seasonality parameters can be problematic in the case where the quality of the time series is low (Jönsson and Eklundh, 2002). In order to solve this, Hermance et al. (2007) and Reed et al. (1994) have proposed that time series data must be smoothed before phenology information can be extracted from it. One of the ways to solve this problem is to calculate seasonality information based on a function fitted to the seasonal NDVI profile.

Currently, only limited approaches exist for extraction of seasonality information from an NDVI time series. The successful and widely used tool to extract this information is the TIMESAT software developed by Eklundh and Jönsson (2012). In this software, seasonality information is extracted from the fitted function. Prior to fitting the function, seasons are determined, which is often hard to do due to the high levels of noise in data (Jönsson and Eklundh, 2003). In order to improve the determination of seasons this software uses the Savitzky-Golay, Gaussian and logistic

functions. Savitzky-Golay filtering method based on a local polynomial fit. In the software, local functions are used to describe one growing season. They are merged with global functions that describe NDVI variability in all seasons. The local function consists of three parameters: the base level of NDVI, the amplitude of variations and the asymmetric Gaussian-like function. The Gaussian function has five additional parameters that describe the width and flatness of each half of the Gaussian curve (Jönsson and Eklundh, 2003). The global function is then used to derive seasonality parameters.

2.2.5 Surface temperature

According to USWCL (2001), the temperature of the canopy is related to plant water stress magnitude. This relation is based on the mechanism, by which plants transpire water in order to cool leaves. When there is not enough water, transpiration is reduced and leaf temperature is increased. Thus, the increase of canopy temperature is an indicator of plant water stress. The same condition is valid for the bare soil. Moist soil is cooler than dry soil because of water evaporation from its surface.

Measurement of leaf surface temperature is one of the most widely used methods for remote detection of water stress in crop vegetation.

$$R_n = H + G + \lambda E \quad (2)$$

$$H = \rho C_P \frac{T_s - T_a}{r_a} = A_t * (T_s - T_a) \quad (3)$$

$$G = R_n * C_l \quad (4)$$

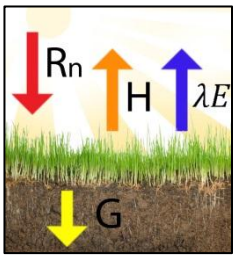

Figure 3. Scheme of energy balance

This method can be explained by the energy balance equation (Equation 2) (Figure 4). In this equation, net radiation (R_n) is amount of energy radiated from the sun. Soil heat flux (G) shows amount of energy that utilized for heating soil. Heat flux (H) is sensible heat radiated from the surface. Latent heat flux (λE) is energy acquired during evaporating water from surface of plants or soil. According to this equation, net radiation is equal to the sum of heat flux , soil heat flux and latent heat flux (Gonzalez et al, 2005). The values of these parameters depend on each other i.e. they are strongly interlinked (Sandholt et al., 2002).

Soil heat flux dependent on net radiation, soil properties and land cover (Oliver et al., 1987). According to CRA-CIN, (2009) soil heat flux can be simply described by net radiation multiplied with a constant related to the density of vegetation cover (D_{vc}) (Equation 3). Latent heat flux describes the energy required to transform water into vapor. According to Gonzalez et al, (2005), λE is highly dependent on plant water conditions and it is equal to zero for completely water stressed vegetation. Heat flux can be described by the aerodynamic characteristics of the air such as air density (ρ), aerodynamic resistance (r_a) that reflects resistance of air to heat transfer from surface, specific heat of the air (C_p) which shows amount of heat energy in the air with respect to air pressure and air moisture, and the difference between surface and air temperature (Equation 3) (Gonzalez et al, 2005). Based on these assumptions, Equation 2 can be transformed to Equation 5, where T_s and T_a are surface and air temperature, A_t is a coefficient related to thermodynamic characteristics of the air.

$$T_s - T_a = A_t[R_n(1 - D_{vc}) - \lambda E] \quad (5)$$

2.2.6 Temperature-Vegetation Dryness Index (TVDI)

Based on information from section 2.2.5, the difference between surface and air temperature can serve as an indication of water conditions of plants in fully vegetated areas. In practice, vegetation has varying density over the large territory. In the case of partial vegetation, the difference between temperatures of vegetation and soil visible to a sensor will affect surface temperature values (Sandholt et al., 2002). This is a significant problem for water stress estimation using this method. One of the solutions to overcome this limitation is to combine surface temperature with spectral vegetation indices (Gonzalez et al, 2005) one of which is NDVI, which is related to the percentage of vegetation cover on the land surface. In combination, surface temperature (Ts) and NDVI can reflect vegetation and moisture conditions of the surface (Sandholt et al., 2002).

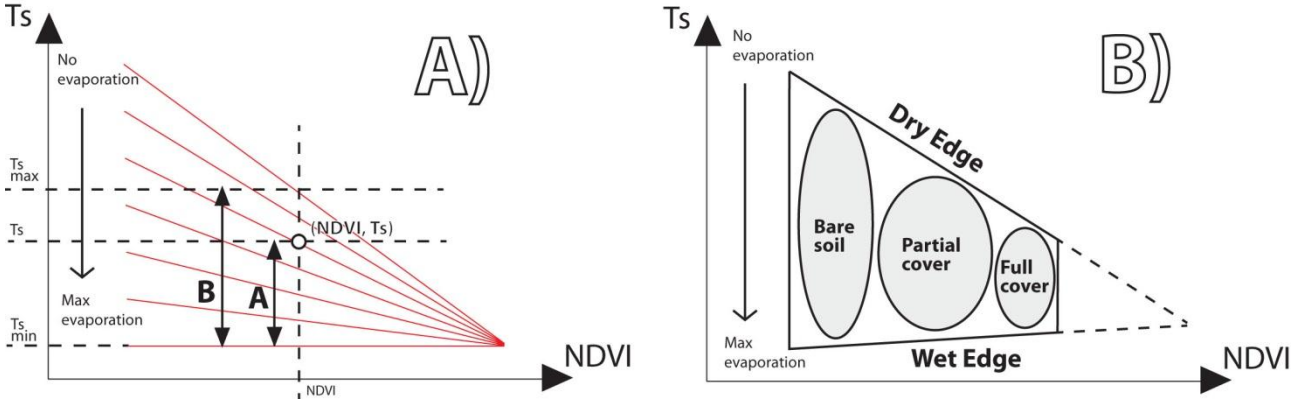

Figure 4. Scheme of Ts/NDVI space (based on Sandholt et al., 2002)

According to Nemani et al. (1992), Ts values are lower when values of NDVI are higher. Also it was suggested that for wet conditions, the difference between the temperature of leaves and bare soil is smaller than for dry conditions. However, there are some differences and, thus wet edge would not be parallel to NDVI axis as it was specified in TVDI formula. Further simplification of this space would assume that these lines are parallel. Isolines of Ts/NDVI relations drawn for different moisture conditions will form a triangle shape (Sandholt et al., 2002), as illustrated in Figure 5A. By plotting NDVI and surface temperature data against each other, the shape of a scatter plot will be either triangular or trapezoidal if "if a full range of fractional vegetation cover and soil water contents is represented in the data" (Min et al., 2010) (Figure 5B). This shape is called the Ts/NDVI space. The upper and lower limits of the Ts/NDVI space are called the dry and wet edges respectively, which mean that points found in upper left part of the Ts/NDVI space represent values collected over the dry bare soil and points in a lower left limit represent a fully vegetated dry area.

There are two possible methods for the estimation of these limits. According to Sandholt et al. (2002), the dry and wet edges of a Ts/NDVI space can be determined based on physical models or empirical results i.e. a scatterplot of Ts and NDVI measurements. The use of physical models is similar to an approach commonly used in CWSI (Crop Water Stress Index) calculations (Yuan et al., 2004; Gonzalez et al, 2005; USWCL, 2001), where maximal and minimal canopy temperature are determined by equations that include physical parameters like the vapor pressure deficit of the air, the heat capacity of air, aerodynamic resistance etc. These parameters can be determined via experiments in a controlled environment (Pinnok et al., 2002). Empirical estimation of the limits of

Ts/NDVI space is simpler, and it takes these parameters into account implicitly (Sandholt et al., 2002).

When the limits of the Ts/NDVI space are found, the Temperature-Vegetation Dryness Index (TVDI) can be calculated using Equation 6. T_s is a current value of surface temperature T_{s-min} is a minimal Ts value for current NDVI value and T_{s-max} is the maximal Ts value for current NDVI. The TVDI index can also be described as result of division of values A/B from Figure 5A.

$$TVDI = \frac{T_s - T_{s-min}}{T_{s-max} - T_{s-min}} \quad (6)$$

The TVDI index comprehensively reflects relation and changes between surface temperature and NDVI and it has many applications (Meng et al., 2010). This index is better applied to an area large enough to represent different vegetation and moisture conditions, where all portions of the Ts/NDVI space are defined (Sandholt et al., 2002).

2.3 Vegetation variability over Ukrainian territory

Although vegetation changes in relation to climate have been widely investigated in previous research, only a few research approaches have been applied on Ukrainian territory. One such study was conducted by Kogan et al. (2011). This study was performed using the Vegetation Health (VH) index, calculated using NDVI data and brightness temperature (BT) derived from the 10.3 to 11.3 mm IR4 channel of the AVHRR. The BT index estimates the hotness of the canopy and it is useful since high temperature and insufficient water supply in dry years cause overheating of the canopy. As mentioned in in this study, the VHI is a useful approach for drought assessment over Ukrainian territory due to its lack of dependence on extensive spatial coverage of weather stations in the area of interest.

The purpose of the research conducted by Kogan et al. (2011) was crop monitoring and early assessment of yield, which revealed the impact of climate on crop vegetation conditions. Calculated VHI was compared to national and regional Ukrainian yield statistics. Kogan et al. (2011) concluded that drought affects Ukrainian territory every 2-4 years and the most severe droughts occurred in years 2003 and 2007. As a result of the research, very strong vegetation stress occurred in Ukrainian territory in the year 2003 compared to years 2002 and 2004. Drought stress also caused crop yields in this year to be moderate.

In another publication, Kogan (2007) compared development of drought in year 2007 to drought in year 2003. As seen from the result of the research, droughts in years 2003 and 2007 have similar temporal profiles until June. However, unlike 2003, drought in 2007 continued until August.

Vegetation change over the Northern Eurasian grain belt was assessed for the period 2001-2008 using NDVI trends derived from MODIS-NDVI datasets (Wright et al., 2012). This research covers portion of central and southern Ukraine. As a result of the research it was found that NDVI trend was significantly negative over the study area as well as over Ukrainian territory.

3. Materials and methods

3.1. Vegetation data

3.1.2 MODIS-NDVI product

The MODIS-NDVI product was used in the current research (GEOG, 2013). It provides NDVI calculated from bands 1 and 2 of the Moderate Resolution Imaging Spectroradiometer (MODIS) instrument operated on board NASA's Terra and Aqua satellites (Carroll et al., 2004). Time-series of MODIS-NDVI datasets have a resolution of 250 meters and are available since the year 2000 (GEOG, 2013). NDVI data is provided in this product as grayscale images in the Sinusoidal projection, where NDVI values are recalculated and stretched from 50 to 250. In order to cover the study area, NDVI datasets for the region *Europe, East 2* were used in this research. MODIS-NDVI is available as 16-day maximum value composites (MVC). Compositing is used in order to select the most accurate value from 16-day observation periods. As mentioned in Heute et al., (2002) this method minimalizes contamination of values by clouds, heavy aerosols and view angle effects. In this research, 16-day composites for the period between Julian days 097 and 289 were used.

According to Brown et al., (2008), vegetation index products derived from MODIS are more useful than products generated from Advanced Very High Resolution Radiometer (AVHRR), since MODIS products have better spatial and spectral resolution, more precise geolocation, and they are better corrected for atmospheric errors. Heute et al. (2002) has concluded that MODIS vegetation indices, as well as MODIS-NDVI, are sensitive to seasonal vegetation variations, land cover and biological variations. MODIS-NDVI has good dynamic range and sensitivity for monitoring and assessment of vegetation conditions. It was effectively used in previous research in order to estimate vegetation response to climate variations (Gu, et al., 2007; Giarolla, et al., 2010; Aragón, et al., 2012).

In the current research, MODIS-NDVI datasets were used in original, scaled NDVI values, which relations to NDVI values can be described by the formula (7).

$$Scaled\ NDVI = (NDVI * 200.0) + 50.0 \quad (7)$$

3.1.2 Parameters of seasonal NDVI profile used in the current research

In the current research, inter-annual changes in vegetation conditions were analyzed. In order to characterize annual vegetation conditions, the parameters of the seasonal vegetation patterns observed from MODIS-NDVI time series were used. These parameters are illustrated in Figure 8. All calculations in the current research were made using 8-bit stretched NDVI values (0-255).

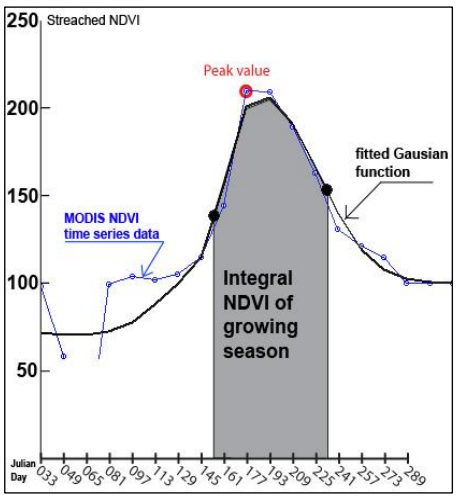

Figure 5. Parameters of seasonal NDVI profile

Cumulative NDVI or ΣNDVI has become a tool for monitoring Net Primary Productivity (NPP) on an annual basis (Ricotta et al., 1999). NPP is a parameter of special

interest for the assessment of phenological response to climate variability (Vrieling, et al., 2011). In order to analyze growing season parameters, values corresponding to the period before the beginning of the season must be removed i.e. the time series must be filtered from preseason noise (Funk, et al., 2009). Values of ΣNDVI parameters can also be contaminated by noise present in MODIS-NDVI datasets (Heute et al., 2002). In order to remove values that do not correspond to the growing season and to filter data from noise, the integral of a Gaussian function fitted to the growing season profile was used in the current research as a more stable substitute for ΣNDVI. Cumulative NDVI of the growing season was computed using the TIMESAT software package is referred to as the large integral hereafter (Figure 8) and was described in Yin et al. (2012) as closely related to NPP.

Another parameter used in this research is an annual peak NDVI value (Figure 4), which according to Hird and McDermid (2011) is one of the most used NDVI seasonality metrics found in the literature. Dou et al. (2008) has concluded that the effects of precipitation on vegetation are most readily observed using this variable. Since contaminated signal is characterized by degraded values (Heute et al., 2002), maximal annual NDVI values represent the least contaminated values in the growing season (Hird and McDermid, 2011). Reed et al. (1994) has insisted that peak NDVI values must be calculated from original unsmoothed data, since they are generally not affected by atmospheric and other errors. However maximum NDVI values may still be distorted by positively biased noise in NDVI.

3.2 Climate data

3.2.1 Data from the network of climate stations

Climate data for the current research was obtained from the NOAA (2013) Global Historical Climatology Network (GHCND). Stations used in this research are situated inside or around the study area and illustrated in Figure 9. In order to be used in the analysis, data was interpolated between these climate stations. Among 18 meteorological elements included in the NOAA database, average monthly temperature of air (Ta) was used in this research. Data was acquired for six months (April – September) for each year in the study period. Precipitation data was not used in the current research, instead TVDI index was used to assess moisture of soil.

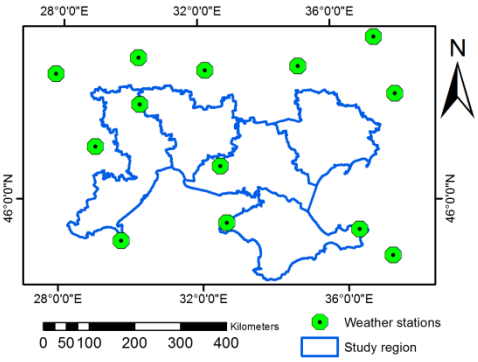

Figure 6. Location of climate stations used in the current research

3.2.3 Approach for TVDI calculations used in the current research

Two types of devices that can be used to measure surface temperature remotely are infrared thermometers and thermal scanners, on board aircraft and satellite platforms (USWCL, 2001). These devices measure the "amount of radiation emitted from a surface and relate it to temperature" (USWCL, 2001). One of the types of devices capable of remote measurements of surface temperature that is installed on a satellite platform is the MODIS sensor. The surface temperature (Ts) data product used in this research is MOD11A2, acquired from EROS (2011, 2012). Datasets of this product cover an 8-day period and they are composed from daily data as an average value of clear sky conditions. These datasets have 1 km spatial resolution.

As mentioned above, TVDI is usually implemented over large areas, with a range of different moisture conditions and land cover (Sandholt et al., 2002; Meng et al., 2010; Min et al., 2010). In the present research, the study area is comparatively small and in order to include different moisture conditions in calculations, TVDI was calculated on an inter-annual basis. In order to analyze changes between years, TVDI was calculated for particular dates (16-day periods) in each year during the growing season from April to October. The limits of the Ts/NDVI space for each date were defined for all studied years. In other words, Ts and NDVI values were sampled in a particular date in years 2000-2012 and one Ts/NDVI space was constructed from sampled values. Resulted Ts/NDVI space constructed using combined data from multiple years represents variations Ts and NDVI data not only in space, but also in time which is required to perform inter-annual analysis.

$$TVDI = \frac{(T_s - T_a) - (T_s - T_a)_{min}}{(T_s - T_a)_{max} - (T_s - T_a)_{min}} \quad (8)$$

Since air temperature on a particular date in different years can vary, surface temperature values and as a result TVDI calculations can be influenced by this difference. In order to account for this problem, Equation 6, was modified to Equation 8. In the new formula, air temperature was subtracted from surface temperature prior to constructing the Ts/NDVI space. Such an approach is already in use for calculations of CWSI (Yuan et al., 2004; Gonzalez et al, 2005; USWCL, 2001). In fact, Equation 8 is now quite similar to that for CWSI, with two key differences: The first difference is that Ts values are grouped for NDVI values. The second difference is that maximum and minimum $Ts - Ta$ values are determined empirically on the regional scale and on an inter-annual basis.

According to Equation 5, variations in surface air temperature differences will reflect variations in latent heat flux (λE). Net radiation will be almost the same for particular calendar date in different years, due to the same solar angle in these days. Since Ts values are sampled for a particular NDVI value, the density of vegetation (D_{vc}) is constant. If we assume that the thermodynamic factors of the air are constant, then the difference between surface and air temperature will be dependent on variations of latent heat flux, which reflects soil moisture conditions.

In the present research, the limits of Ts/NDVI space will not be modeled by a triangular or trapezoidal model. Instead, limits for *Ts* values will be empirically determined for each particular 8-bit stretched NDVI value. This approach will reduce errors of overestimation and underestimation of the minimum and maximum *Ts* values for a given NDVI value caused by the use of simple linear models of wet and dry edges used in previous research (Sandholt et al., 2002; Meng et al., 2010; Min et al., 2010).

In order to be compared on an inter-annual basis with vegetation characteristics represented by NDVI metrics, annual cumulative TVDI was calculated using TVDI values. For this purpose, TVDI values for a 16-day period within a given year were summed. Resulting cumulative TVDI was used in the further analysis.

3.3 Isolation of cultivated areas

3.3.1 Existing crop masks available for the Ukrainian territory

There are several Land Use Land Cover (LULC) datasets available for the Ukrainian territory. LULC classes of the Kryvoozersky administrative district, Mykolaiv Oblast were derived from three different datasets, illustrated in Figure 10. In Figure 10A, a dataset showing different crop types is illustrated; this was produced by Grekov (2011) using high resolution spatial imagery and extensive field surveys. Grekov's (2011) dataset covers the current administrative district and has high accuracy, thus it can be used as a ground truth dataset for LULC in this district. In Figures 10B and 10C, fragments of the Global Land Cover Dataset (EEA, 2008) and Pan-European Land Cover Database (PELCOM, 2001) are presented for the same area.

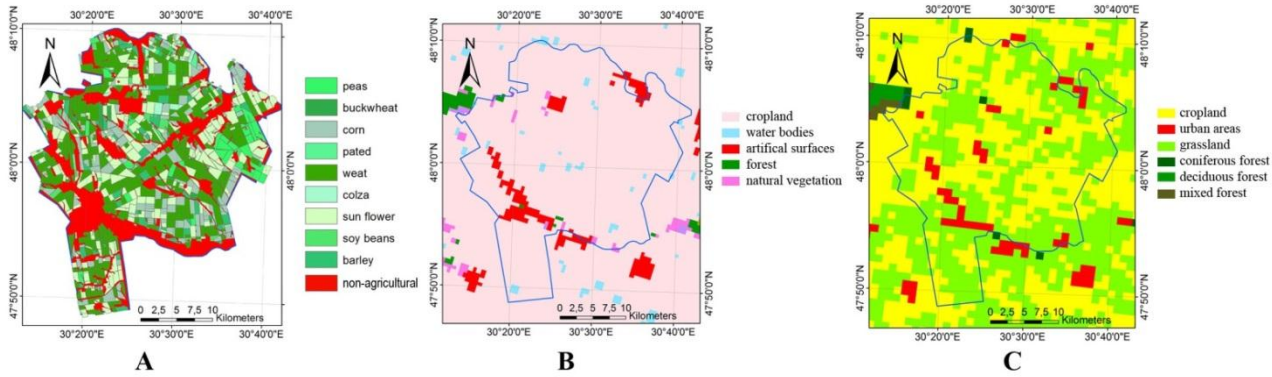

Figure 7. Comparison of land use datasets of Kryvoozersky district, Mykolaiv Oblast

The difference between the PELCOM and EEA datasets clearly demonstrates a problem similar to one described in Vrieling, et al. (2011). The PELCOM datasets does not reflect changes in LULC classes that take place over the time. By comparing the EEA dataset and the dataset derived by Grekov, it can be seen that a much smaller area is classified as non-agricultural in the EEA dataset. Agricultural areas in the EEA dataset have high classification accuracy i.e. there is a high probability that agricultural areas are classified as such in the EEA dataset. However, the object accuracy of agricultural areas is not as high, since some non-agricultural areas are also classified as agricultural. In order to have "pure agricultural" pixels for analysis, object accuracy is required i.e. all points classified as fields should represent fields on the ground. The requirement here is to have only agricultural pixels in the analysis, thus it is not as important that all agricultural fields will be classified as it is that other LULCs not be misclassified as agricultural. The other obstacle to using the EEA and PELCOM datasets in the current research is that summer and winter crops are not differentiated therein.

3.3.2 Crop masking approach implemented in the current research

Since, it is impossible to use existing winter and summer crop masks, summer/winter crop masking was conducted in the current research.

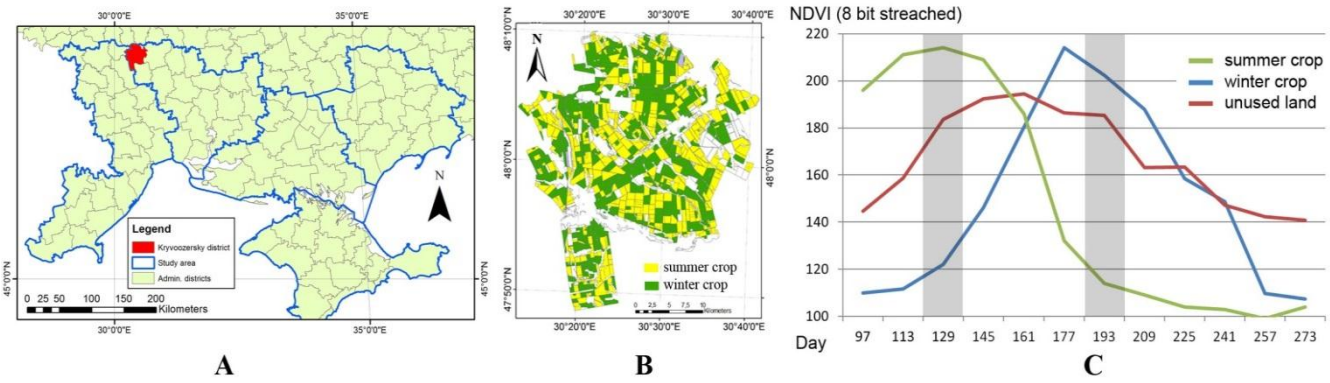

Figure 8. NDVI profiles of summer/winter crops in Kyvoozersky district, Mykolayivs'ka oblast

In Figure 11C, seasonal NDVI profiles for the year 2011 derived from MODIS-NDVI are illustrated for winter and summer crops. These profiles were created using a summer/winter crop map of Kyvoozersky district derived by the aggregation of respective crop types from Grekov's (2011) dataset (Figure 11B). As seen in Figure 11C, there is strong difference between the NDVI values of summer and winter crops on Julian days 129 and 177. On day 129, winter crops reach their maximum NDVI, while summer crops are at their early development stage. On day 177, summer crops are near their peak value, and winter crops have values close to their base value. This difference in crop development stages can be seen in Figure 12. In the figure, NDVI calculated from Landsat 5 TM images representing a small area in Mykolaiv Oblast is illustrated. As seen in the figure, fields that had low NDVI values in May had high NDVI values in July and vice-versa. These features of the growing season are also related to cultivation dates in the agricultural calendar for the Ukrainian steppe territories (Fedorenko, 2011) according to which winter crops are harvested in June and summer crops in August.

Based on observations discussed in previous paragraphs, a winter/summer crop classification methodology was defined. This methodology uses difference between NDVI values of summer and winter crops on days 129 and 177, and also the high seasonal variability of NDVI of agricultural areas as compared to unused areas. In cases when data is missing in a particular year for the 16-day composites related to days 129 and 177, those for days 113 and 193 are chosen instead.

$$\text{Seasonal variability index} = (NDVI_{129} - NDVI_{177})/(NDVI_{129} + NDVI_{177}) \quad (9)$$

As seen in Equation 9, if the index has a small value, then there is small seasonal variability of NDVI, and consequently, the area is not used in agriculture. This assumption is similar to one used in Vrieling et al. (2001). If this index has a high negative value, then a summer crop is planted in the area. If this index has a high positive value, then a winter crop is planted. Which values are small or large was determined through visual analysis of MODIS-NDVI datasets, based upon which threshold values of +0.3 and –0.3 were selected. The threshold can be used over the whole study territory, since it is situated in the same biome zone (temperate steppe) and phenological variations from West to East and from South to North are insignificant.

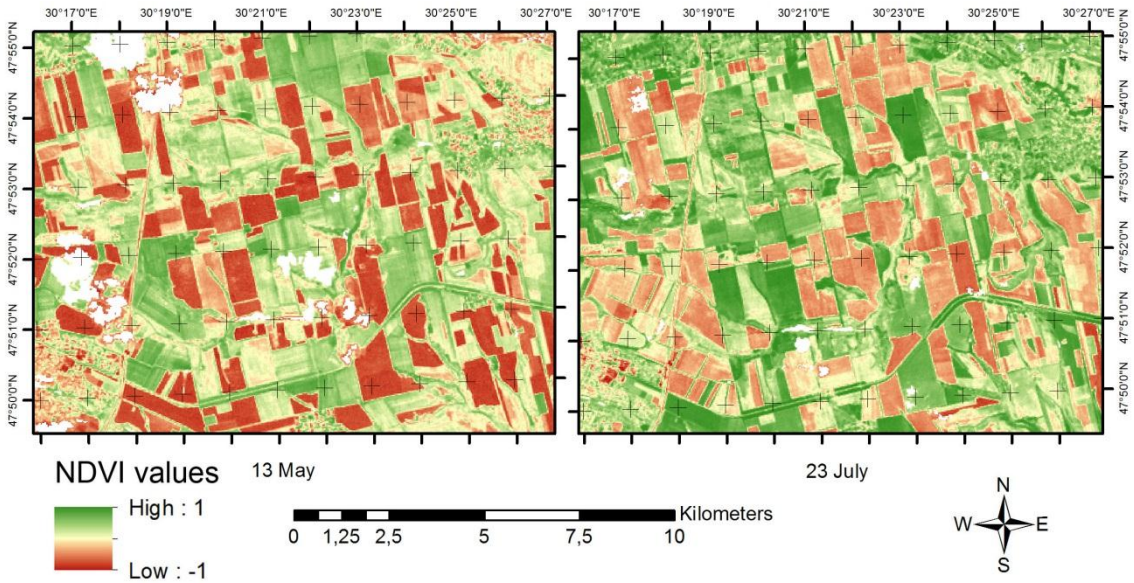

Figure 9. NDVI calculated from Landsat 5 images taken in spring and summer

3.4 Statistical analysis of vegetation and climate variables

3.4.1 Morton key as a basis for the analysis

Due to utilization of crop rotation schemes, summer and winter crops are not planted each year in the same fields. In other words, crop patterns change between seasons. In order to analyze inter-annual variability of phenology parameters of summer and winter crops, spatial data was aggregated to a rectangular grid with cells of size 10x10 km i.e. average or maximum value of values between pixels inside a cell was used. This is required in order to have continuous data for further analysis. Figure 33 illustrates the purpose of using grid cells to sample phenology parameters instead of simple pixel-by-pixel comparison. The grid was built in the same sinusoidal projection as MODIS-NDVI datasets used throughout this research. Cell size was chosen experimentally with the goal of having fewer value gaps. The grid covers the whole study area as shown in Figure 13A.

Cells in the grid were ordered by the Morton index (Figure 13B). Vegetation and climate data values were assigned to these cells using a zonal statistic function. As a result, values of variables ordered by Morton index were available in a tabular form for statistical analysis. This index was calculated in MS Excel using an algorithm illustrated in Figure 13C (Lawder et al., 2000).

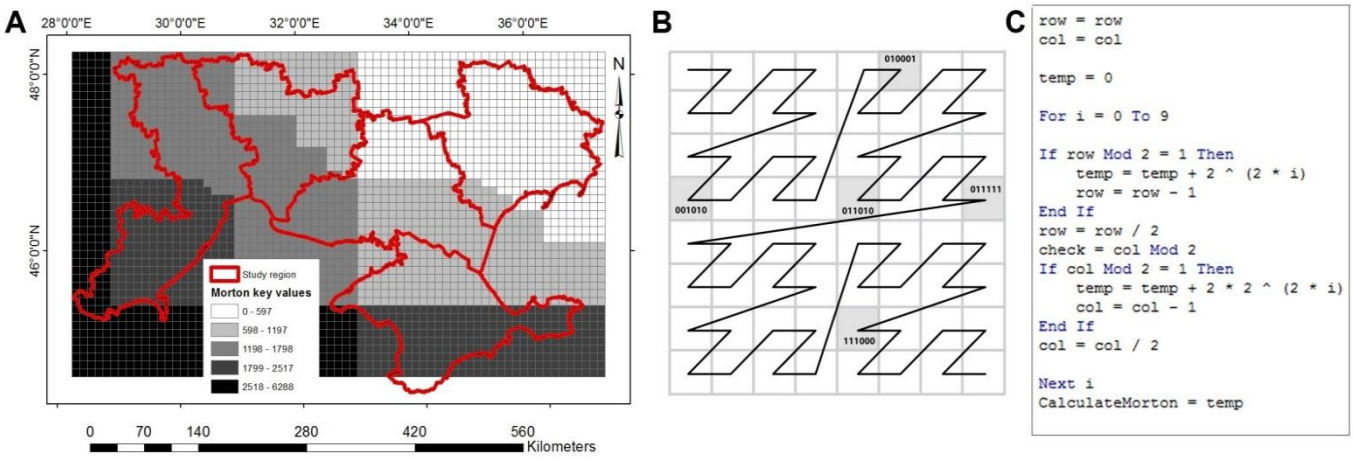

Figure 10. Morton key index developed for this study area

3.4.2 Standardization of measurements, calculation of trends and correlation

In order to explore the behavior of variables, and the values of variables acquired by different measurements, their attribute values must be standardized, since the values of variables in different measurement locations (grid cells) belong to different measurement populations with differing variability, mean and standard deviation characteristics. According to Rogerson (2001) this can be done by subtracting the mean value from each value and dividing it by the standard deviation (Equation 10). The result is called a Z-score and it shows how many standard deviations of value a variable is from a population mean. The population mean for the grid cell value is the all year average value of this cell for the study period 2000-2012. Using Z-score values -1 and +1, three categories for each variable were defined: They are negative deviations larger than a standard deviation, deviations within a standard deviation, and positive deviations larger than a standard deviation. In other words, the first category shows unusually low values and the third shows unusually high values.

$$z = \frac{X - \bar{X}}{STD}; \quad (10)$$

Standard deviation is the square root of squared deviations of observations from the mean (Rogerson, 2001). The STD shows absolute average deviation of observations from the mean regardless of sign. In Equation 11, calculation of standard deviation is shown for a population with *n* - samples.

$$STD = \sqrt{\frac{\sum_{i=1}^{n}(X_i - \bar{X})^2}{n-1}}; \quad (11)$$

STD was used in this research to evaluate the variability of variables over the study area and during the study period. It was calculated for non-standardized variables in their original units. In order to find relations between the variability in surface moisture and vegetation variables, standardized covariance or Pearson's correlation coefficient was used. The coefficient was estimated using Equation 12, which is the sum of the products of standardized moisture and vegetation variables (Equation 10) divided by the number of measurements minus one. Since temporal relations between

these variables are investigated in this research, the coefficient was calculated for each measurement location (grid cell) for variations in values during the 13-year study period. Thus, variables will have 11 degrees of freedom and assuming that correlation is negative and one directional, correlation -0.475 gives a probability of 0.05. Significance level was chosen to be 5%, thus correlation values more negative than -0.475 were regarded as significant results.

$$r = \frac{\sum_{i=1}^{n} Z_{moist} * Z_{veget}}{n-1}; \qquad (12)$$

Runnström (2000) and Peng et al. (2011), have used the slope of linear trend line as a representation of annual average vegetation gain. In Yin et al. (2012) trend analysis was used to analyze patterns of vegetation change. For the central-southern portion of Ukrainian territory, trend analysis was used by Wright et al. (2012) to examine vegetation changes. In the present research, this method was used as a tool to preliminarily estimate patterns and magnitudes of average annual changes in variables. It was calculated using Equation 13, and this equation was applied to each grid-cell in the study area.

$$gain_{NDVI} = \frac{number_{of_{Years}} * \sum NDVI_i * year_i - \sum NDVI_i * \sum year_i}{number_{of_{Years}} * \sum {year_i}^2 - (\sum year_i)^2}; \qquad (13)$$

3.4.3 Grouping of variables

In the current research, changes over the whole study area are investigated. Due to the size of the study area, it is not possible to plot variables against each other in separate graphs for all measurement locations. Instead, graphs representing a variable from all locations (all grid cells) were combined into a family of curves. Thus, temporal changes in variables were assessed by families of curves i.e. graphs representing all measurements within the study area. Each family of curves was illustrated by an envelope that contains 90% and 60% of the curves included in the family. In order to define such an envelope, values of variables were arranged in descending order and the lower bound of the envelope was identified as a value that splits off the lower 5% of values. The upper bound was calculated in a similar way, but 95% was used instead of 5%. The envelope that contains 60% of the curves was identified using 20% and 80% values as bounds. Then, calculated bounds were plotted for each year in the study period and connected with each other, thus forming continuous graphs.

3.5 Data processing

3.5.1 Data processing

In Figure 14, the steps of data processing that were undertaken in the current research are illustrated. As seen in the figure, MODIS-NDVI and Ts time series data are used as input data. Climatic data from the network of climate station, as well as the rectangular vector grid, are also used as input data in the research. After the operations described in following subsections of this section were completed, raster datasets representing maximum NDVI, integral NDVI and cumulative TVDI were computed for each year of the study period. These datasets were summarized by grid cells using zonal statistics. Resulting tabular data was analyzed in MS Excel and the results of the analysis were joined to grid cell layers based on the Morton key approach

described above. By specifying different legend properties, the results of the research are visualized and presented in the form of thematic maps.

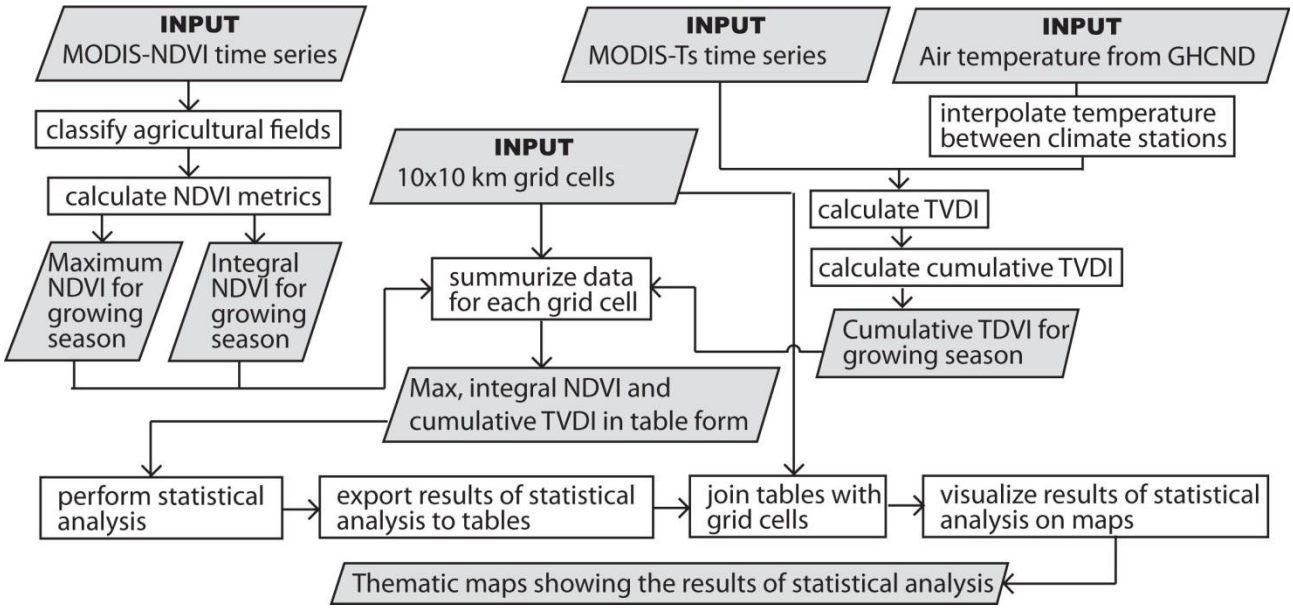

Figure 11. General steps in data processing

3.5.2 Classification of summer/winter crop fields

In order to classify summer and winter crop fields, the index calculated according to Equation 8 was used. As shown in Figure A.1 in Appendix A, this index was calculated for each year. In order to calculate the index, maps showing vegetation variability were compiled. Data in these maps was reclassified using threshold values +0.3 and -0.3, related to winter and summer crops respectively. Reclassification results were exported to new layers and vectorised in order to filter polygons smaller than 32 ha. This is done since 250m MODIS-NDVI datasets have been demonstrated to be useful in locating individual crop fields when they are 32 hectares or larger (Wardlow et al., 2008), so that smaller polygon might represent noisy data. The remaining vector polygons were rasterized. As a result, annual summer/winter crop maps were created.

3.5.3 Calculation of parameters of seasonal NDVI profiles

Maps showing peak NDVI values for each year were derived from NDVI time series for winter and summer crops through the algorithm illustrated in Figure A.2. The algorithm begins using the initialization of the maximal value raster (MVR). Then each raster is retrieved from the time series, verified for validity (NDVI stretched values should be between 50 and 250) and compared to MVR. If the NDVI value of a pixel in the retrieved raster is higher than that in MVR, the value in MVR is rewritten with the pixel value. In other cases, the value in MVR is not edited. As a result, after each image from the time series is compared with MVR, MVR represents the values of pixels, which are maximal for the time-series.

Integral NDVI for the growing period is derived as the integral of the seasonality function calculated by the TIMESAT software package as shown in Figure A.3. In order to process NDVI time series in the software, each image is converted to 16-bit binary image. Then, data processing was performed according to the TIMESAT specification (Jonsson and Eklundh, 2004). The

program delivered seasonality information as text files, in which rows and columns identify the locations of points. Each row in the file also has values of seasonality parameters. This data was imported to tables and positions described by rows and columns were converted to original coordinates. Then, coordinates were used to create point vector layers where points correspond to the pixels from initial datasets and have seasonality parameters associated with them as attribute information. Using point layers, raster datasets were created showing integral values of the growing season.

In this research, phenology data was assigned to 10x10 kilometer grid cells illustrated in Figure 13. As shown in Figure A.4, maximum NDVI values, as well as integral NDVI values for winter and summer crop fields, were sampled for grid cells using zonal statistics. As a result of this operation, tables were produced showing average values of phenology metrics for grid cells. The Morton key method was used in these tables for identification. Tables were then used in statistical analysis and the results of the analysis were visualized using maps. For this purpose, they were exported to DBF tables and joined with the grid cells layer based on the Morton key.

3.5.4 Automation of Vegetation data processing

Data used in the current research is available in the form of time serieses, which consist of 11 years of data with 13 images per year. As seen from previous sections, the sequences of data processing applied in the research include operations conducted multiple times. In order to save time and minimize errors, data processing procedures were automated. Implementation of these operations was organized into an object-oriented structure (Figure A.5) in order to encapsulate common features. Such an approach makes this structure less complicated and more effective in terms of the easy and accurate implementation of changes.

Algorithms for data processing were implemented as nested loops that retrieve each dataset in the time series. For example, the implementation of an algorithm for a maximum value raster (MVR) calculation (Figure A.2) is illustrated in Figure A.6. As seen in the figure, there are two nested *for* loops. The outer loop iterates through all years in the study period, while the inner loop iterates through the raster datasets for a certain year.

Map algebra operations were implemented using Arc Objects .NET libraries. Operations presented in Figure A.3, which created point vector layers from tabular data and create raster layers, were implemented using ArcGIS functionality in the Python environment.

3.6 TVDI calculations

3.6.1 General description

In the current research, TVDI was calculated using Equation 7. For this purpose, a software tool was developed. The tool uses time series Ts-Ta data and NDVI data as inputs.

3.6.2 Input data processing

Before the tool for TVDI calculations can be applied, the initial data must be processed. The main complication for use of the automatic tool for pixel-by-pixel TVDI calculation is that pixel positions must be identical in the temperature and NDVI rasters. In order to achieve this, Ts-Ta and NDVI

raster datasets must have the same spatial extent, the same size of pixel and the same number of pixels. In Figure A.7, the algorithm for the required data transformation is illustrated. In this algorithm, data from climate stations, the original Ts time series and the MODIS-NDVI time series are used as input data. The output data from the algorithm is two time series datasets of Ts-Ta and NDVI, which satisfy the condition mentioned above.

Data from climate stations were acquired from the GHCND network (NOAA, 2012) in a comma-separated value (CSV) format. As a first step, this data was imported to MS Excel where the data from climate stations was processed. The result was exported as a DBF table that was converted to a point vector layer in the ArcGIS environment. Average monthly temperature data, which is one of the attribute of the resulting point layer, was interpolated among climate stations for each month between April and October in the study period 2000-2012. The result of this stage is a time series of air temperature data.

Temperature data was acquired from EROS (2011, 2012) in the form of multilayer HDF files. As shown in Figure 19, Ts data was extracted and recalculated to degrees Celsius. Values derived for 8-day periods were combined to represent average values in 16-day period. It was done by combining two adjacent datasets of a temporal duration which was within the duration of the same MODIS-NDVI MVC. In this operation, values of pixel were determined as an average between two datasets. In the case when a value in one dataset is missing, the value from the other dataset was chosen. Finally, air temperature data was subtracted from the surface temperature data.

As was already mentioned in the first paragraph of this section, datasets of MODIS-NDVI time series must be transformed in order to have the same spatial reference, extent and pixel size as Ts-Ta data. In order to accomplish this, a dummy raster was created from a Ts-Ta dataset with the value of all pixels equal to one. As shown in Figure 19, this dataset was multiplied with each dataset from the NDVI time series. In the Environment Setting for this operation, the "MEAN" method was specified to solve values at coinciding locations. The resulting raster datasets from this procedure have the same spatial properties as Ts-Ta datasets and represent NDVI values, which satisfies the condition specified at the beginning of this section.

3.6.3 Calculation of limits of Ts/NDVI space

In the current research, TVDI was calculated using the limits of *Ts-Ta* values empirically determined for each 8-bit stretched NDVI value. For this purpose, zonal statistics were used, the result of which were grouped by dates. The result was limits for all years for particular dates. These were exported to SQL server tables in order to be used in the further analysis. The algorithm is illustrated in Figure A.8.

As seen in Figure A.8, the input data for the algorithm is MODIS-NDVI and *Ts-Ta* time series, which were produced by the algorithm illustrated in Figure A.7. First, zonal statistics were calculated for each dataset in the time series. Then the results of zonal statistics for all years were grouped by date. Grouping was performed by determining the maximum and minimum values for a particular 16-day period between all years. During this operation, 156 datasets were grouped in 12 datasets (one for each 16-day period). This data was grouped again in two tables, one representing inter-annual maximum *Ts-Ta* values for all time periods, and the other represent minimum values. These tables were exported to SQL server format in order to be used for TVDI calculations.

3.6.4 The tool for automated TVDI calculation

In order to calculate TVDI, a software tool was developed in C# using ArcObjects libraries. The complete static scheme of this software is illustrated in Figure A.11. It consists of four libraries, which encapsulate functions for process management, TVDI and raster calculations (*Calculations*), reading Ts-Ta limits from database (*EdgeDataBaseLibrary*), and operations with files on a hard drive (*RasterOpenSaveLibrary*).

The general description of the algorithm implemented in the software is illustrated in Figure A.9. The algorithm consists of two nested loops; one iterates through dates (16-day periods) of datasets in the time series, the other iterates through years in the study period. The algorithm revisits each dataset in the initial time series. In each iteration, data from current temperature and NDVI datasets are read and written to two arrays. Then, the limits of Ts-Ta/NDVI space are retrieved from a SQLserver database. Using this data, TVDI is calculated and written to a new raster dataset, which is then saved. The core functions for TVDI calculations are implemented in the *Calculations* library, which is illustrated in Figure A.10. The principle of TVDI calculation (comment frame in Figure A.10) is that it visits each record in the initial data arrays, calculates TVDI and stores result at the same index in the new array.

4. Results

4.1 Classification of agricultural fields for each year in the study period

In the beginning of this research, agricultural fields were classified using a variability index described in Equation 8, using threshold values of -0.3 for summer crop and +0.3 for winter crop. Classification was performed for each year in the study period (2000-2012). As a result of this classification, raster maps of summer crop and winter crop were created for each year. These maps were then used to eliminate other land cover types in order to gather phenological metrics specifically for summer crop and winter crop conditions.

In Figure 15, the total area of fields classified for each year is illustrated. These are not the total amount of winter and summer crop fields on the ground. These are rather those fields, which are larger than 35 hectares and satisfy conditions discussed in section 3.2. As seen from the figure, there are strong variations between area of fields classified for different years.

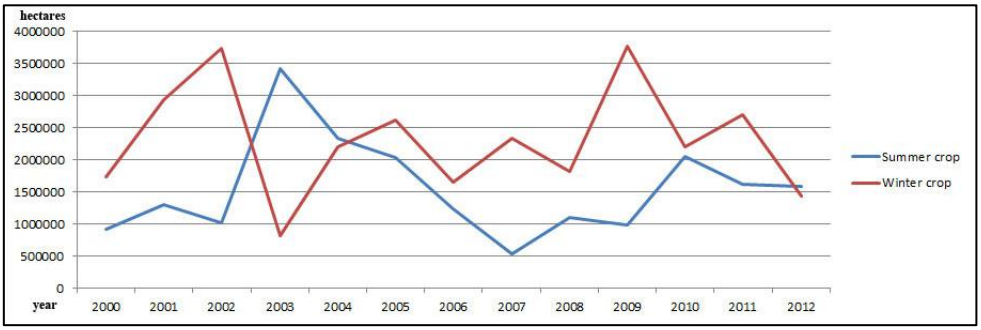

Figure 12. Total area of fields classified for years in the study period

Figure 16 shows the spatial distribution of summer and winter crop fields. In this figure, the area of agricultural fields inside grid cells is presented, which is averaged for the study period. This figure shows that there are more winter crop fields in the southern part of the study area than in the northern part. In the majority of the Crimean Peninsula, the southern part of Odessa Oblast and the south eastern part of Kherson Oblast, the area of agricultural fields exceeds 2000 hectares per cell. Summer crops were primarily classified in Zaporizhia Oblast and in the north east part of Mykolaiv Oblast. There is also a large area of summer crop fields classified in the center of Zaporizhia Oblast. In the eastern part of the study area, agricultural fields were rarely classified. Insignificant amounts of summer crops were located in the Crimean Peninsula.

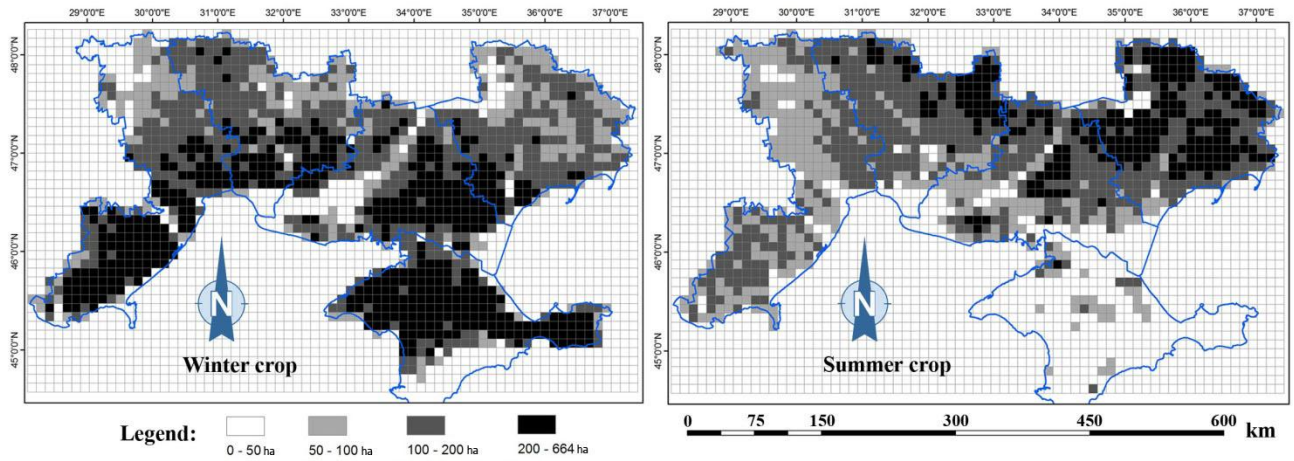

Figure 13. Average distribution of summer crop fields and winter crop fields over the study area during the study period

4.2 Seasonal NDVI profiles for summer and winter crops

After summer and winter crops were classified, clipping MODIS-NDVI time series with the results of crop classification produced crop specific time series. NDVI profiles of these time series are illustrated in figures in Appendix B. In these figures, NDVI curves are plotted as envelopes showing 90% and 60% of all measurements over the study area. Figure B.1 shows the seasonal NDVI profiles for winter crop fields and Figure B.2 shows the profile for summer crop fields. As seen from figures, seasonal NDVI profiles of winter/summer agricultural vegetation show distinct properties, as discussed in section 3.3.2 of the current report.

As seen from Figure B.1, winter crop reaches its maximum NDVI values around days 113, 129 and 145. After these dates, NDVI decreases sharply and reaches its minimum values around days 177 and 193. In year 2003, the NDVI profile of winter crop is bimodal, since there is a significant increase in NDVI values of winter crops after the end of growing season. A similar but not as strong NDVI seasonal pattern can be seen in the preceding and following years (2002 and 2004). Deviations from the usual pattern can also be seen in year 2007. In this year, NDVI shows low values at day 161 compared to the rest of the study period. In other years NDVI values stay around 150-200 (8-bit NDVI) while in year 2007, NDVI reaches a value of around 100-150 by day 161. Such a low value can be seen only in year 2003.

NDVI profiles of summer crops are different from the profiles of winter crops (Figure B.2). NDVI for summer crop fields reaches maximal values around days 177, 193 and 209. In day 129 and before, the NDVI profile shows relatively low values in range 100-150. After NDVI reaches peak values, it begins to decrease slightly to its background values until day 273. As is the case for winter crops, summer crop profiles show anomalously low NDVI values in year 2007 at the end of the growing season. In other years, NDVI ranges from 150 to 200 at day 209, and in the year 2007 it reaches values 30 points lower than average. In year 2002, NDVI shows relatively low peak NDVI values (less than 200). Also the date at which NDVI reaches its peak in this year in different locations spreads between days 161 and 225. Such a low maximum NDVI value can also be seen in the years 2007 and 2009.

4.3 Phenology parameters of summer and winter crops

4.3.1 Annual maximum NDVI value

In Figure 17, maximum annual NDVI values are illustrated for winter and summer crops for each year. The spatial distribution of this variable is illustrated in Figure 18. As seen in Figure 17, annual maximum NDVI values vary around 200 (8-bit stretched NDVI). For winter crops, values reach a minimum in year 2003, when they were approximately 12 points smaller than in other years. The highest maximum values for winter crops can be seen in years 2008 and 2001. For summer crops, there is no distinct inter annual peak of maximum NDVI values. In years 2007, 2009 and 2012, maximum NDVI values for summer crop reach their minima. The spatial distribution of standardized (unusually high and low) maximum NDVI values is illustrated in Appendix C (Figures C.1, C.2).

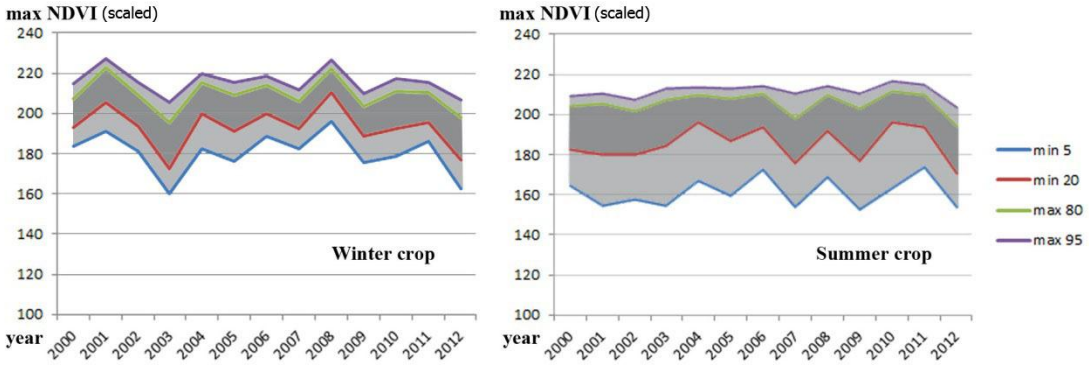

Figure 14. Maximum annual NDVI values for winter and summer crops

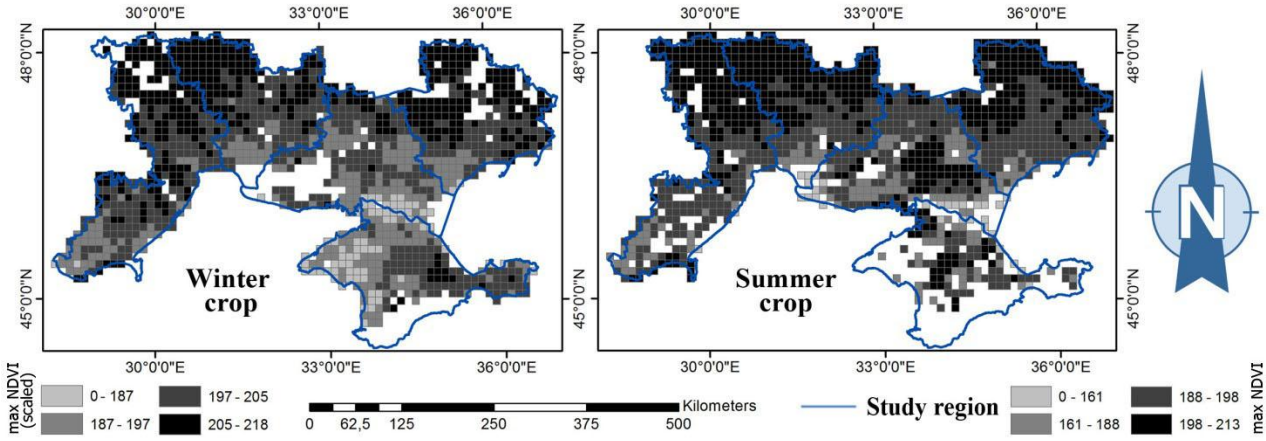

Figure 15. Mean max NDVI values for winter and summer crops

Standard deviation (STD) of maximum NDVI values between different measurement locations is illustrated in Figure 19. As seen in the figure, maximum NDVI values vary with higher amplitude for summer crops over the area than for winter crops. There is also a distinct minimum extreme around year 2007. The spatial distribution of inter-annual STD is shown in Figure 20. As seen in the figure, STD values for winter/summer crops are high in Cherson Oblast, where they reach values from 10 to 17 for the majority of the area. Deviations are relatively low for summer crops in Mykolaiv Oblast and Odessa Oblast (from 3 to 8 in the majority of areas) and for winter crops in Zaporizhia Oblast and Mykolaiv Oblast (from 6 to 10).

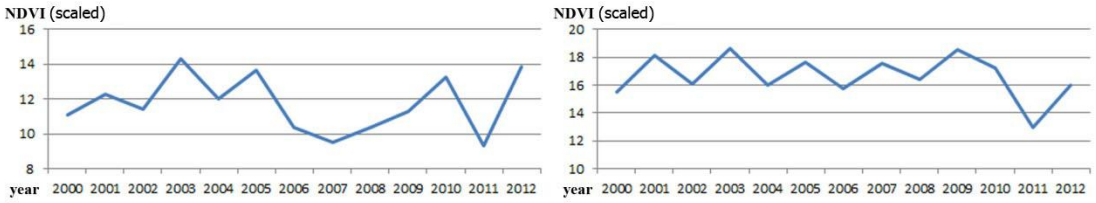

Figure 16. STD for maximum NDVI between measurement locations (grid cells)

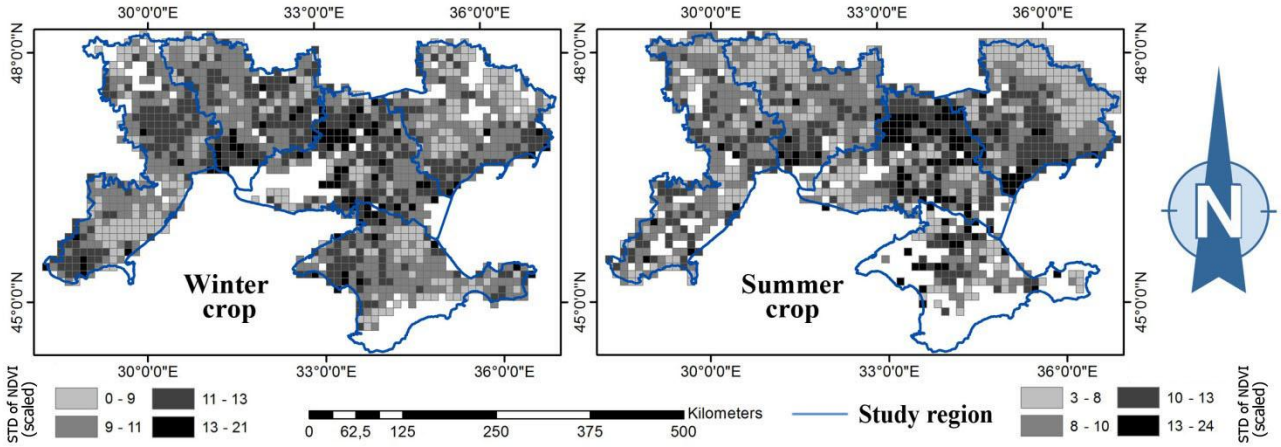

Figure 17. STD for maximum NDVI between years

Inter-annual trends for maximum NDVI values are shown in Figure 21. As seen in the figure, trends for summer crops were positive in almost the entire study area, while trends for winter crops were highly negative in the north-eastern and western parts, where they ranged from -2.7 to -0.4. Trends for winter crops in the southern part of Odessa Oblast, the central part of Cherson Oblast and in the Crimean Peninsula were positive. Highly positive trends are seen for summer crops in the center of Cherson Oblast (0.7-6).

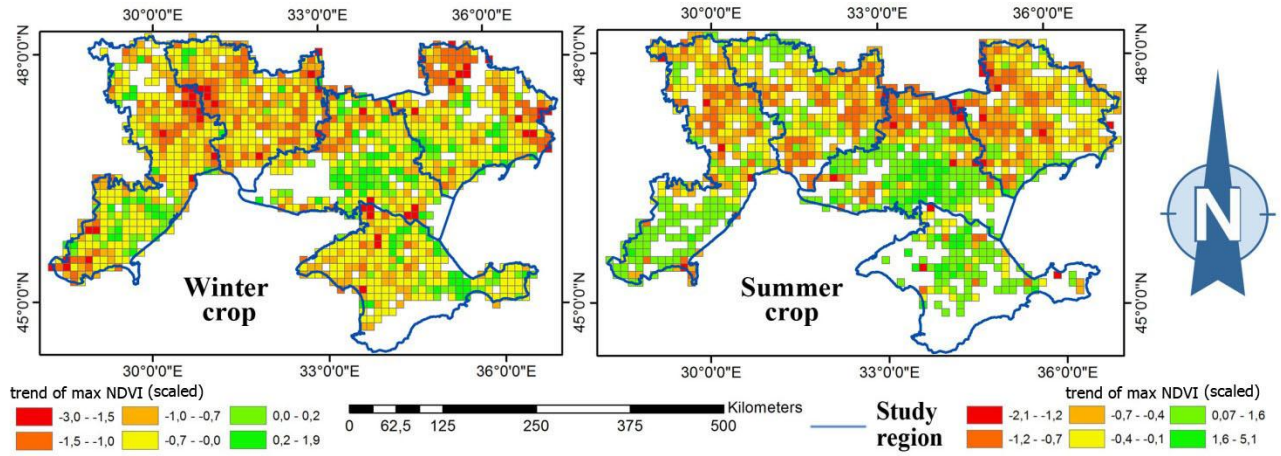

Figure 18. Inter annual trends for maximum NDVI values

4.3.2 Integral NDVI value of growing season

The integral NDVI value of the growing season was calculated using the *Linteg* parameters using the TIMESAT software package. Figure 22 shows inter-annual variations of this parameter for winter and summer crops and their spatial distribution are presented in Figure 23. As seen in Figure 22, integral NDVI varied around 1100 for winter crop and 1500 for summer crop. It can also be seen that in years 2003 and 2004, integral NDVI of winter crops varied with higher amplitude

around the mean value than during other years. For these years, it ranged from about 700 to almost 1600. It is also notable that for winter crops, integral NDVI values were the lowest in years 2007 and 2012 (700-1000). For winter crops, integral NDVI reaches its peak values in years 2004, 2008 and 2010. For summer crops, changes of integral NDVI over the study period are more gradual than for winter crops. It reaches maximum values in years 2003 and 2004, when it varied around 1700. Then it gradually decreased until the year 2008 to less than 1300. Similar minimum values can also be seen for years 2002 and 2011. The spatial distribution of unusually high and low integral NDVI values is illustrated in Appendix C (figures C.3, C.4).

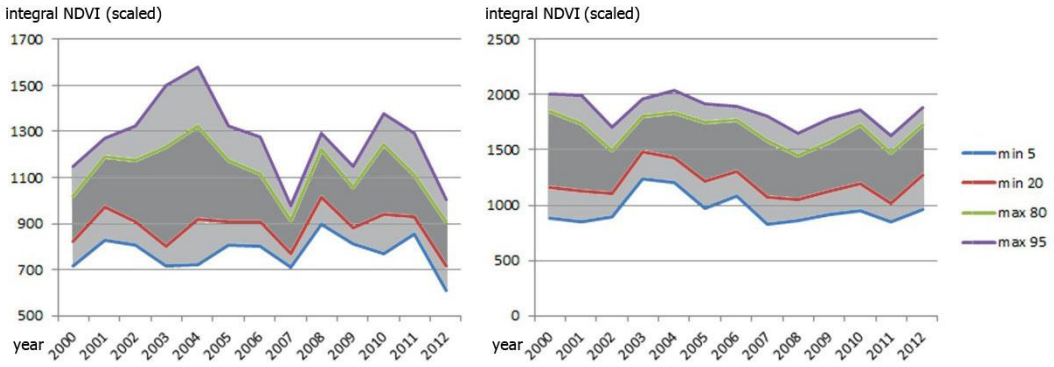

Figure 19. Integral NDVI value of growing season

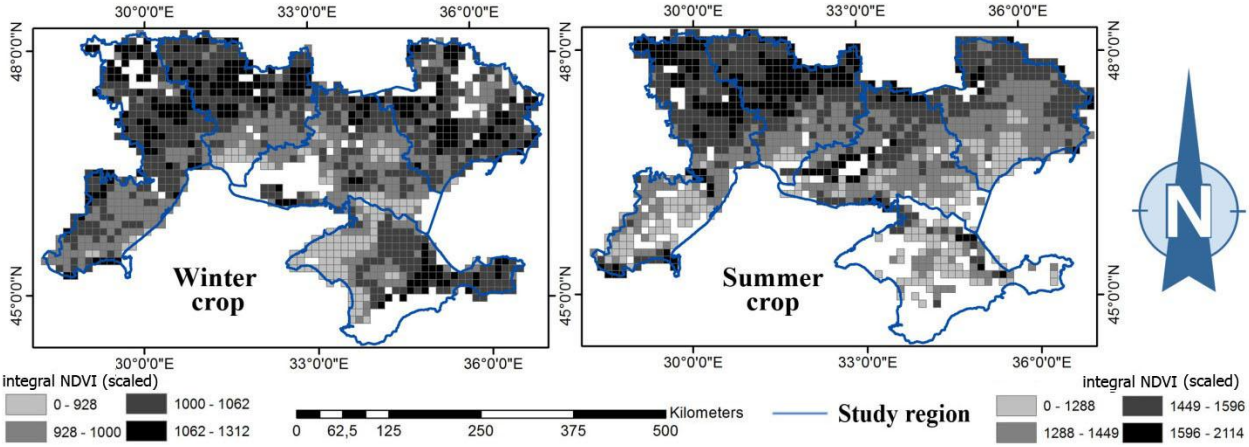

Figure 20. Mean max integral NDVI values for winter and summer crops

Figure 24 shows the standard deviation of integral NDVI for the study period. As seen in the figure, the highest amplitude of deviation of integral NDVI for winter crop was in year 2003. In this year the STD was equal to 300. The lowest STD is seen in year 2007, when it reached 100. For summer crops, the situation is the opposite. The lowest deviations were in year 2003 (240) and the highest in years 2007 and 2001 when it was around 350. Figure 25 shows the spatial distribution of inter-annual STD. As seen in the figure, STD is unevenly spread over the study area. The largest values were in the northern part of Odessa Oblast for both crop types, and highest values over Odessa Oblast and the Crimean Peninsula for summer crops.

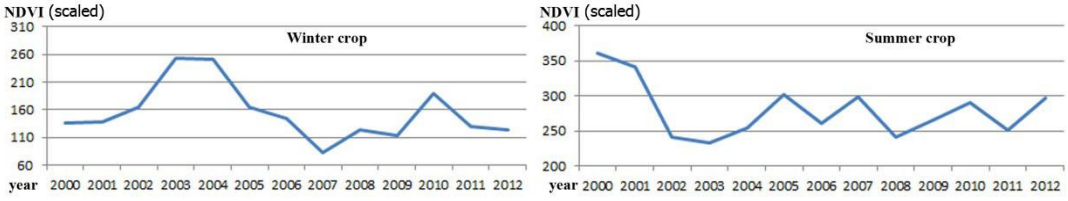

Figure 21. STD for integral NDVI values (*Linteg*) between grid cells

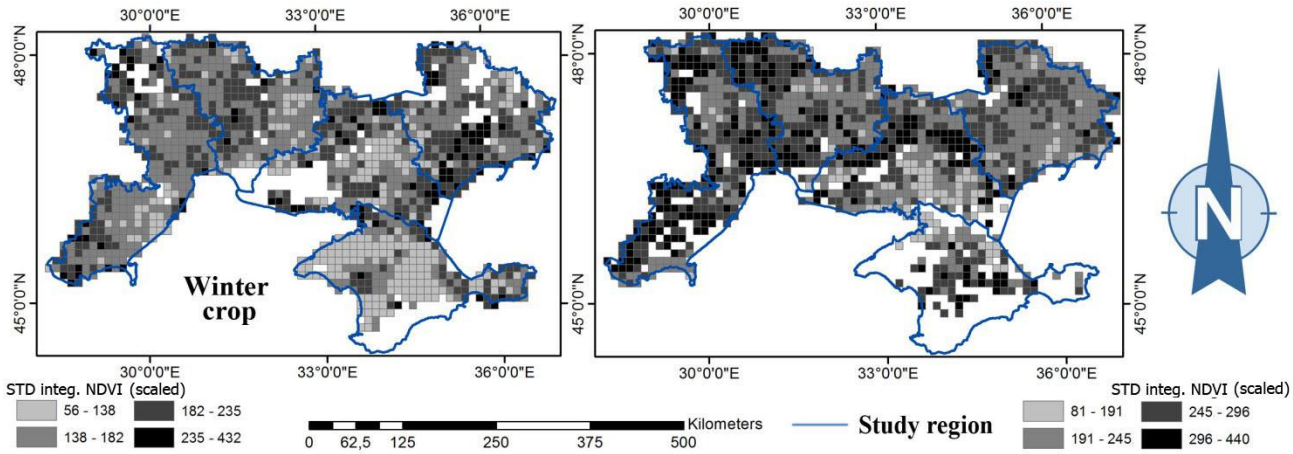

Figure 22. STD for integral NDVI values (*Linteg*) between years

In Figure 26, inter-annual trends of integral NDVI are shown. These trends are predominantly negative for both crop types over the study area. Trends have a positive direction in the northern part of Odessa Oblast, ranging from 1 to 22. Also a positive trend was found in the Crimean Peninsula for winter crops (1-10), and in the central part of Cherson Oblast for summer crops (1-10). Highly negative trends can be seen for summer crops in Zaporizhia Oblast, where they are smaller than -28 over the majority of the territory. Such negative trends are also seen in parts of Mykolaiv Oblast and in central and western parts of Zaporizhia Oblast. Trends covering the majority of study area for summer crops are smaller than -13. Such strong negative trends are also seen in Zaporizhia Oblast for winter crops.

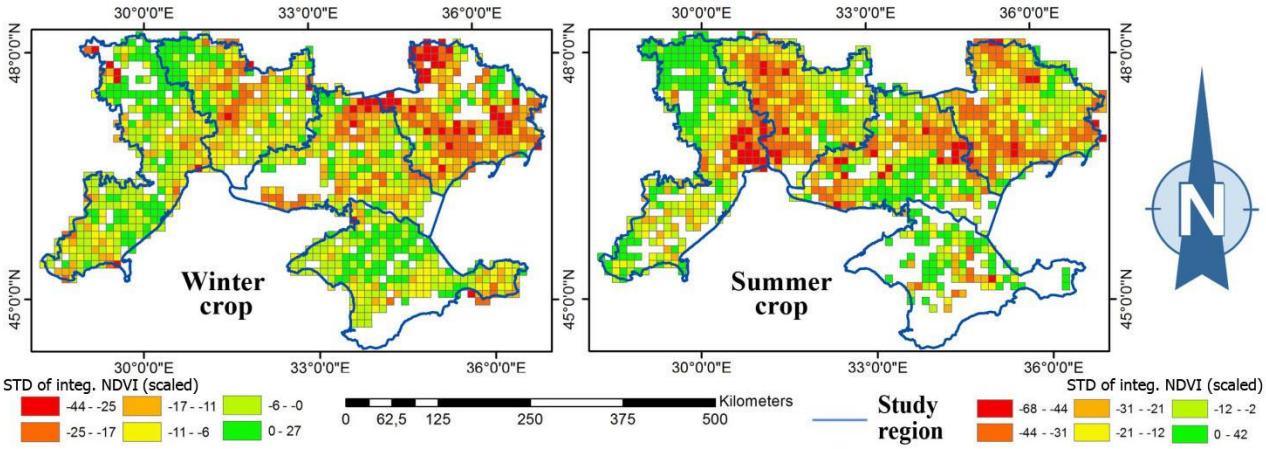

Figure 23. Trends integral NDVI values between years

4.4 TVDI calculations results

4.4 TVDI calculations results

In this research, time series of TVDI index was calculated for the study period, and the results of these calculations were summarized for each year. In order to analyze these results together with vegetation data, TVDI was sampled by grid cells used as a basis for vegetation data analysis. Figure 27 presents the results of TVDI calculations.

As seen in the figure, unlike vegetation data, TVDI is regularly distributed over the study area. Smaller TVDI values can be seen in the northern part of the study area. There are also small TVDI

values in the northern part of Odessa Oblast and the Crimean Mountains. The trend of TVDI between years 2000-2012 is positive (Figure 28), which means that moisture conditions became dryer during this period. Inter-annual standard deviation (STD) of TVDI is stronger in the eastern and central parts of the study area.

Inter-annual distribution of TVDI is more uneven than spatial. As seen in Figure 27, there were 3 occasions of strong surface dryness conditions during the study period in years 2001, 2007 and 2012. Also, dry conditions were seen in years 2003 and 2009. Figure D.1 in Appendix D illustrates the spatial distribution of unusually low and high surface humidity conditions. As seen in the figure, drought in year 2007 was the most severe in terms of extent. The extent of droughts in years 2000 and 2012 was also significant, while dryness in years 2003 and 2009 locally occurred in some parts of the study area.

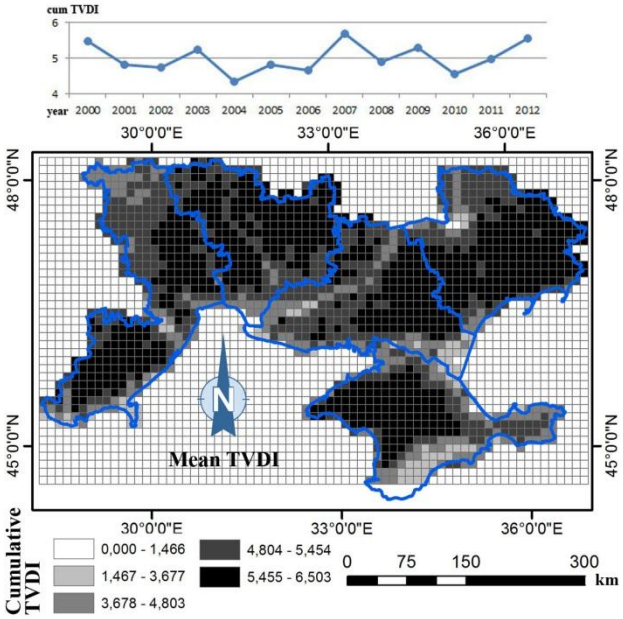

Figure 24. Distribution of cumulative TVDI over the study area and during the study period

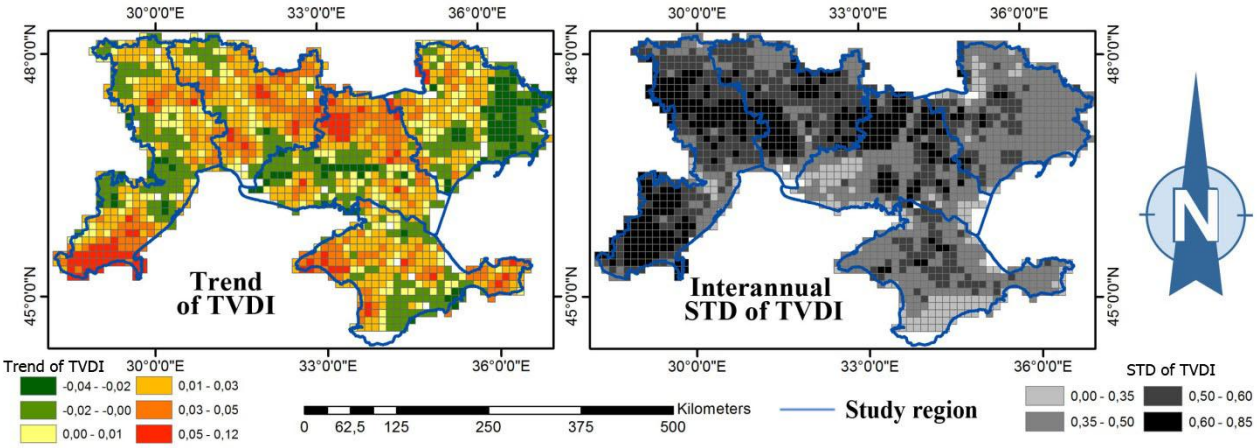

Figure 25. Spatial distribution of trend and standard deviation of TVDI

4.5 Impact of surface wetness conditions on conditions of agricultural vegetation

After climate and phenology variables were calculated, relations between them were assessed. In Figure 29, graphs are illustrated where cumulative TVDI (TVDI) was plotted against four phenology variables. As seen in the figure, TVDI and 3 phenology variables show opposite patterns of decrease and increase. Minimum and maximum values of phenology variables are related in time to maximum and minimum values of TVDI. In other words, phenology variables reach their minimum values when TVDI reaches its maximum, and vice versa. On the other hand, there is no such relation between TVDI and integral NDVI for the summer crops. Figure 30 shows that there is

statistically significant negative correlation between vegetation variables (except integral NDVI of summer crops) and TVDI. The strongest correlation is seen in Mykolaiv oblast and the weakest in the Crimean Peninsula. For winter crops, integral NDVI is better correlated with TVDI than maximum NDVI values. The situation is the opposite for the summer crops, where maximum NDVI is highly correlated with TVDI.

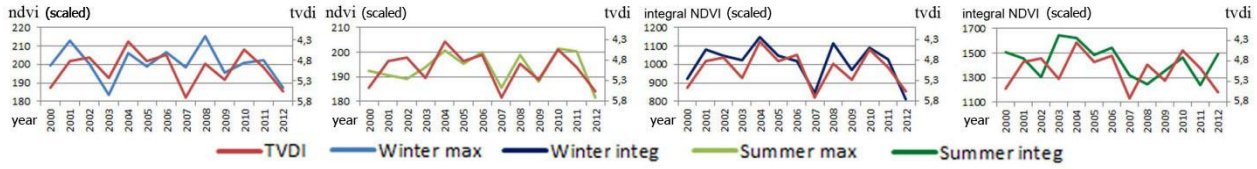

Figure 26. Variations of TVDI versus phenology variables

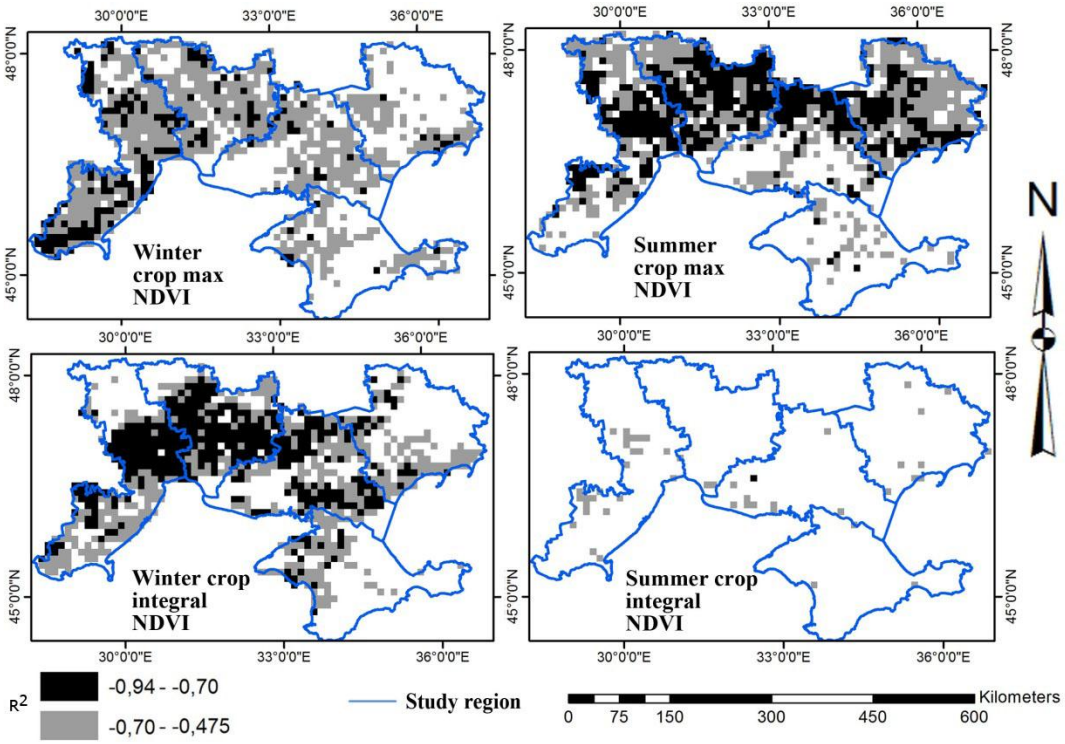

Figure 27. Correlation between TVDI and vegetation variables

Spatial distribution of Z-scores of TVDI smaller than "-1" are illustrated in Figure 31, which shows the extent of unusually dry surface moisture conditions in dry years (data for all years is illustrated in Appendix D). Also, this figure compares the extent of dryness to vegetation conditions, which are illustrated in Appendix C. As seen in the figure, unusually dry surface moisture conditions coincide with unusually low values of vegetation variables. However, the effects of lack of humidity on the surface are not seen in all three vegetation variables illustrated in the figure. Dryness in year 2000 had only limited influence on crop vegetation. In year 2003, winter crops were heavily impacted, which is seen by the broad spatial extent of Z-scores lower than -1 for maximum NDVI values. Droughts in years 2007 and 2009 impacted summer crops more than winter crops. Drought in year 2012 has evenly influenced both winter and summer crops.

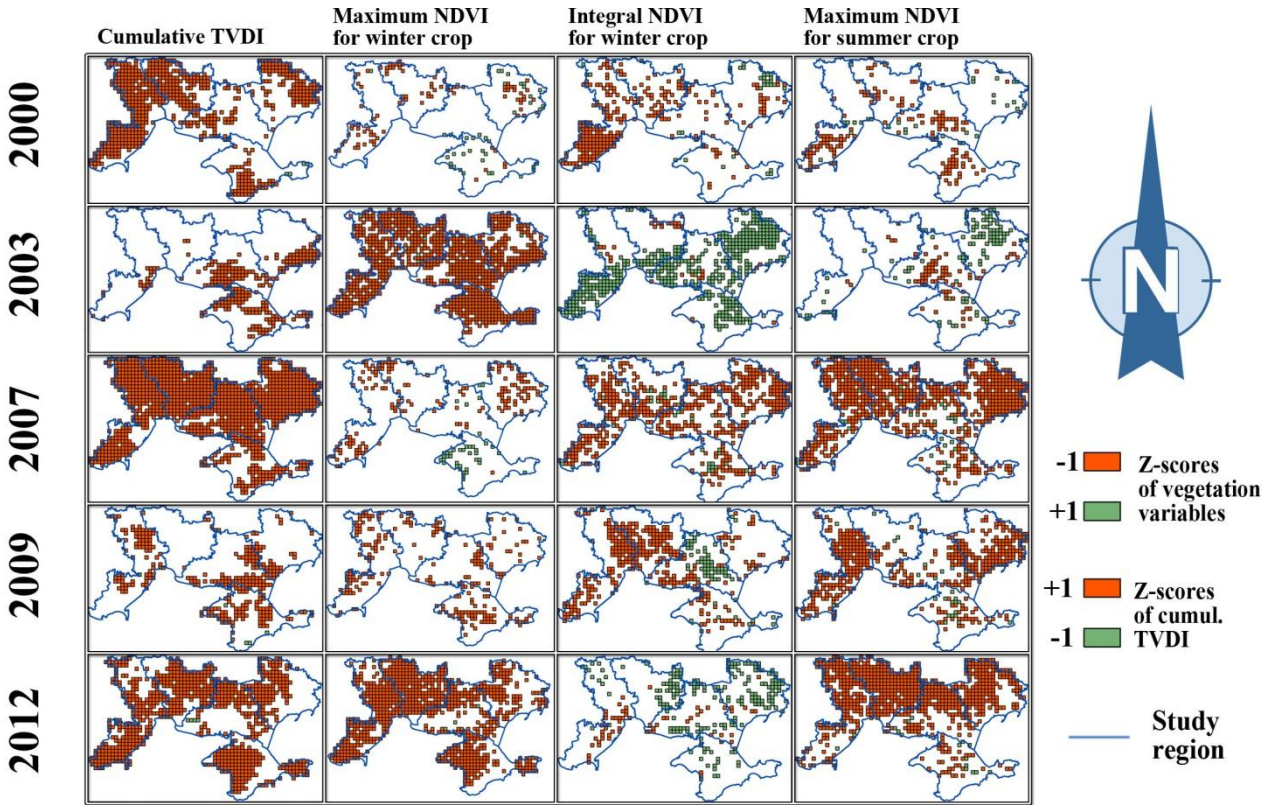

Figure 28. Scheme showing Z-scores of TVDI and of the three vegetation variables

5. Discussions

5.1 Classification of winter and summer crops

In each year, summer and winter crops were classified using two raster datasets (Equation 9) and the same threshold values for each year. Prior to classification using MODIS images, this approach was tested using Landsat images. Results illustrated in Figure 32 show the boundaries of fields covered with winter and summer crops classified in this research. There is no overlap between fields, and the shape of fields is generally well preserved. Fields classified using Landsat and Equation 8 for the year 2011 over Kryvoozersky district match the results of crop classification described in Grekov (2011).

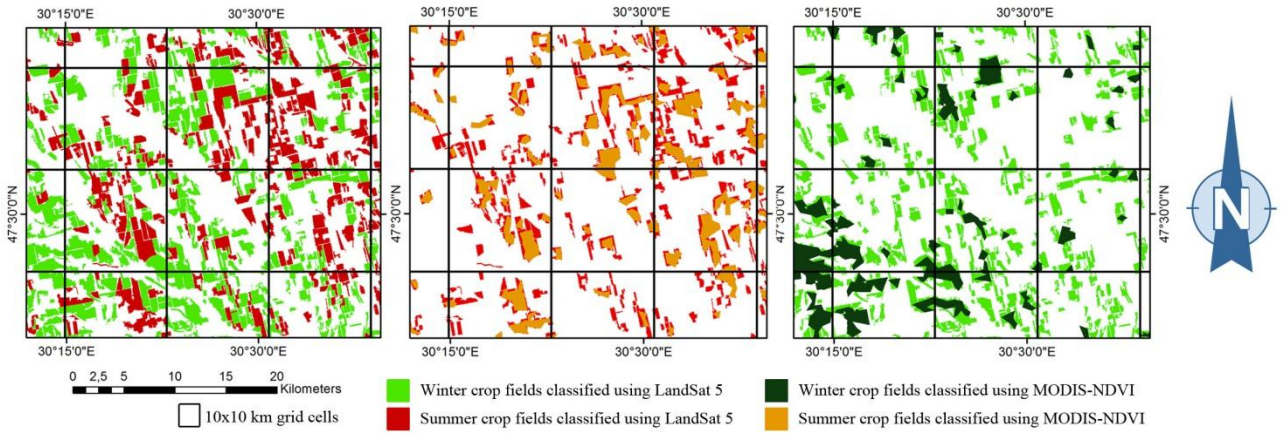

Figure 29. Comparison between classification results acquired using Landsat 5 TM imagery and MODIS-NDVI products

By comparison of classification results performed using MODIS and Landsat, it is evident that both winter/summer crop maps have generally similar field pattern. Due to coarse 250 meter pixel size, only large fields were classified with MODIS. Fields classified with MODIS-NDVI are located inside fields classified with Landsat, and there is only small area classified with MODIS which lay outside of Landsat classification results. In other words, almost all fields classified with MODIS are classified with Landsat, which is the evidence of high accuracy of crop classification which provided "pure winter/summer crop pixels" which were used in further analysis.

Crop classification for each year showed that winter crops are mainly planted in a southern part of the study area and the highest density of summer crop fields is seen in Zaporizhia Oblast (figure 24), which is consistent with the report of Cherenkov et al. (2013).

Current classification approach uses datasets related to the same dates for each year of the analysis (2000-2012). Even though climatic conditions can be different in these particular dates in different years, stages of summer and winter crops are the same. In each year in April, winter crop is fully emerged from the snow and starts growing, while summer crops is not yet or just planted. At the end of July and beginning of June, winter crop is usually cultivated and cultivation schedule differs insignificantly between years (Fedorenko, 2011). The same time summer crop reaches its vegetation peak values around these dates (Figure B.2). Thus, use of datasets related to the same periods (Apr-07 to Apr-22 and Jun-26 to Jul-11) for crop classification in different years is possible.

As seen from figure 15, total area of winter and summer crop fields classified in different years varies. Such deviations can be caused by utilization of the same thresholds values for classification in different years, whereas climatic conditions are different from year to year. By comparison of figures 15 and 29, it can be assumed that amount of fields classified depends on wetness conditions, since extremums of these values coincide in time with extremums of TVDI. In year 2000, TVDI reached maximum values while area of classified fields was low. In year 2003, TVDI has peaked while extremely low area of winter crop was classified. The same time, area of summer crops reached its all year peak in 2003. Small area of winter crop can be explained by the fact that a lot of agricultural fields were damaged by ice crust in winter (65% of winter crops was destroyed this year according to Yatsik et al., 2006) and extreme dry conditions in spring (Netis, 2007). Large area of summer crop can be the result of replanting of damaged fields with new summer crop plants. This can be proven by figure B.2, were in year 2003 there are apparently two growing seasons for winter crops. Such bimodal profile according to Wardlow et al. (2007) caused by cultivation of winter and summer crops at the same field at the same year. In year 2007 during extreme drought conditions, area of summer crops reached its minimum. Apparently, much of summer crops was damaged by the drought, and remained crop fields showed extremely low values of phenology variables.

The main drawback of the current classification approach is that the same threshold values were used over entire study area. This means that only crop species having strong seasonal variations are classified. By analyzing fields classified in this research and fields classified in Grekov (2011), it can be concluded that winter wheat, barley and rape and summer sunflower and soybean were classified. There is no other ground truth data which can prove that other crops were classified appropriately.

5.2 Calculations of phenology variables

In this research, conditions of vegetation were evaluated on an annual basis using two metrics derived from MODIS-NDVI datasets: annual maximum (peak) NDVI values and integral NDVI of the growing season. The first metric was derived directly from NDVI time series. The second metric was derived as an integral of Gaussian functions fitted to seasonal NDVI profiles using the TIMESAT software package. The function fitting approach provides the possibility “to effectively track high-order inter-annual variations in NDVI time series” (Hermance et al., 2007). This approach also reduces noise, which distorts values in NDVI time series (Eklundh et al., 2012). Thus, the NDVI metrics used in this research are represented by generally undistorted values.

In order to analyze vegetation changes, pixels representing NDVI metrics were sampled using a 10x10 kilometer grid. In the figure, crop classification results for years 2010 and 2011 are presented. As seen in the figure, the field fabric is not continuous, and has different patterns in different years. Unlike data represented by fields, data summarized by grid cells is continuous over the years. Thus, grid cells provide a basis for reasonable inter-annual statistical analysis.

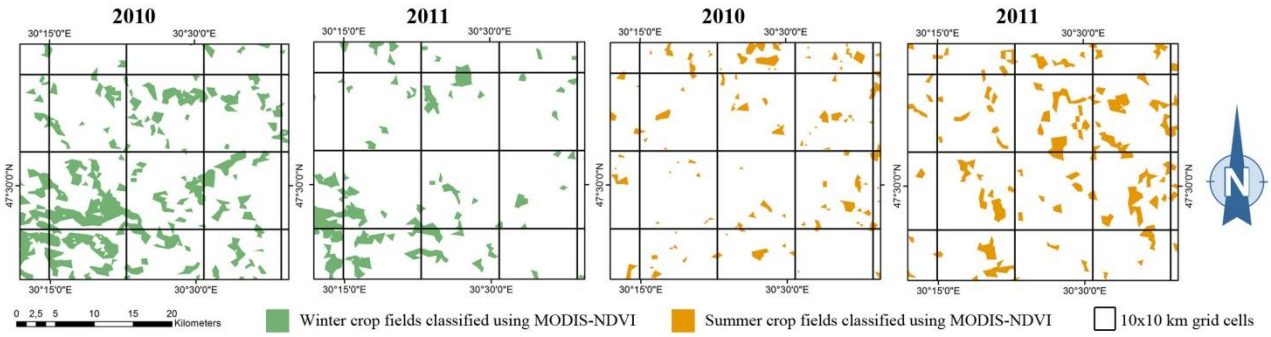

Figure 30. Average distribution of summer crop fields and winter crop fields over the study period

Phenology parameters used in the current research were also used in previous work to estimate and examine vegetation conditions. Although both parameters describe vegetation conditions, their values are not strongly related to each other. Figure 34 shows the spatial distribution of statistically significant correlation between the current phenology parameters. Correlation between these two variables for summer crops is only significant in limited areas in Odessa Oblast and in the Crimean Peninsula. There is a larger area where these parameters are correlated for winter crops. However, over the majority of the study area, there is no significant correlation between maximum and integral NDVI. This can be partially explained by the dependence of integral NDVI (calculated as an integral of a function fitted to growing season) on the length of growing season, which, among other factors, is determined by cultivation schedule.

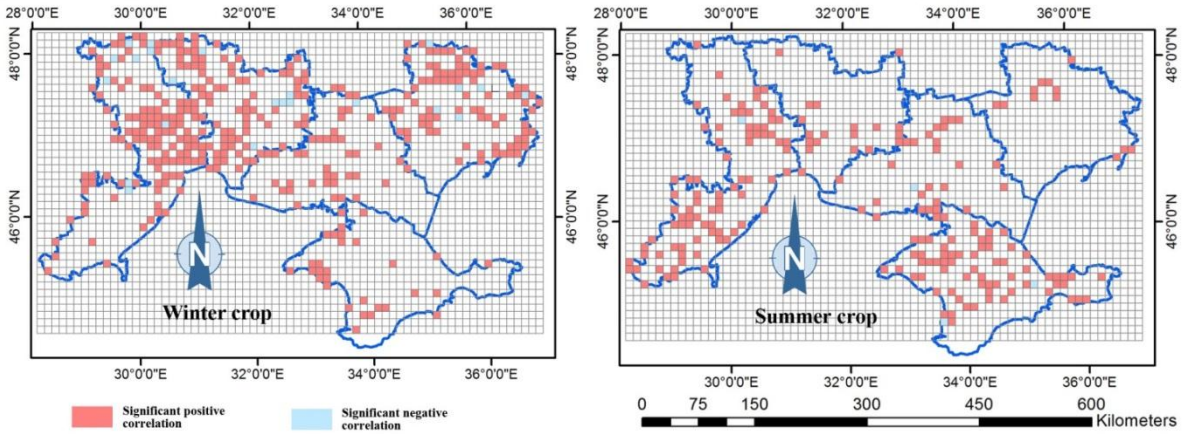

Figure 31. Pearson coefficient of correlation between integral and maximum NDVI

On average phenology parameters show higher values in north-eastern part of the study area. It can be seen for maximum NDVI values (figure 18) and for integral NDVI values (figure 23) of winter and summer crops. It is also evident that values of variables in north are slightly higher than in south. For summer crops, high values of maximum NDVI are seen in the central part of Zaporizhia Oblast and in Crimea Peninsula, were fields are irrigated.

Trends are generally negative for both phenology variables over the study area (figure 21; figure 26), which corresponds to findings in Wright et al. (2012). However, unlike findings of Wright et al. (2012), magnitude of the trend is not even over the study area. Especially, this is true for trends of integral NDVI, which are more unevenly spread then trends of maximum NDVI. Positive trends of vegetation variables can be seen in central part of Kherson Oblast where irrigation is used. Also positive trends for maximum NDVI are seen in the southern part of Odessa Oblast and for integral NDVI in the northern part of Odessa Oblast, which is situated in the forest-steppe agro-ecological

region (Gumeniuk et al., 2010) and were density of agricultural land is relatively low. One explanation for higher variation of trends calculated in the current research comparing to trend from Wright et al. (2012) is that current research was focused on agricultural areas and vegetation conditions in agricultural fields depends on cultivation practice. For example, high positive trend for summer crops in the central part of Kherson Oblast can be related to expansion of irrigation illustrated in figure 35, which was created in this reasearch using approximate classification method.

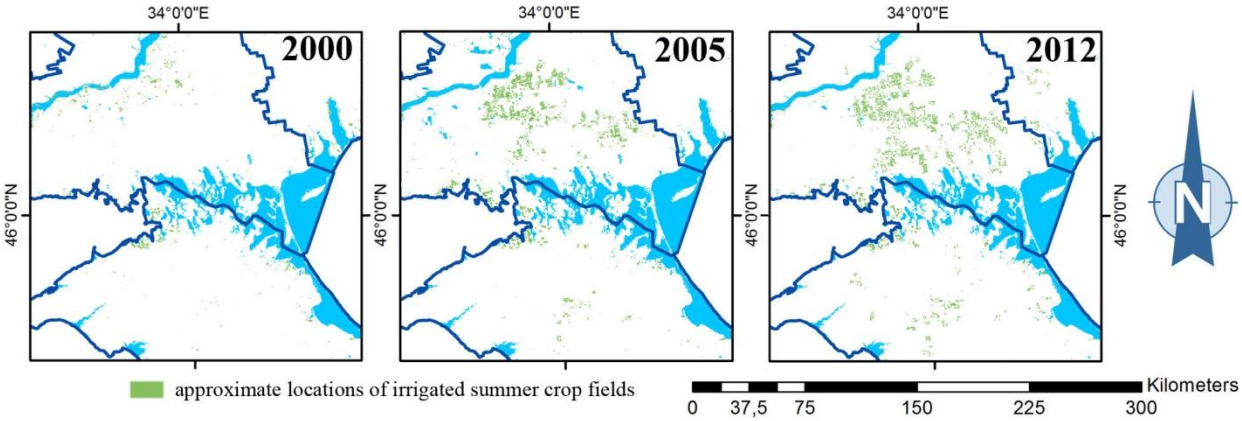

Figure 32. Extension of irrigated crop fields in Kherson Oblast and Crimea Peninsula

In this research, the variability of maximum and integral NDVI was estimated by standard deviation (STD). STD was calculated spatially (between grid cells) and between years. Temporal variability is illustrated in Figures 20 and 25. As seen in these figures, inter-annual variability of vegetation variables calculated for winter crops is higher than for summer crops. For summer crops variability of integral NDVI is higher in the eastern parts of study area, where density of summer crop fields is lower. According to Oindo et al. (2000), higher values of inter-annual standard deviation of NDVI may be evidence of heterogeneity of biodiversity. For winter crops, spatial standard deviation reaches its maximum around year 2003, and reaches its minimum around year 2007 for both integral NDVI and maximum NDVI. Distribution of spatial STD for summer crops is more regular between years. Although STD of agricultural vegetation is highly dependent on human activity, it is closely related to natural patterns and dependent on natural factors (Hall-Beyer et al., 2011).

Maximum NDVI and integral NDVI show different inter-annual patterns for both winter and summer crops over the study period (Figure 18; Figure 23). Spatial distribution of Z-scores, illustrated in figures in Appendix C, is also different for maximum and integral NDVI. The decrease in maximum NDVI values for winter crops in year 2003 was not followed by a high decrease in integral NDVI values, which can be explained by the presence of two peaks during the growing season in this year (Figure B.1) and by the replanting damaged crops. Similarly, minimum integral NDVI values for winter crops in year 2007 coincide with normal maximum NDVI values for winter crop in this year. The reason for this is seen in Figure B.1. As was mentioned in section 4.2, NDVI values were extremely low during the end of growing season in 2007. As seen in the plot, NDVI values in day 161 were lower than 150, which is the lowest for all years of study. During the same year, NDVI values before date 129 were normal, which explains normal peak values in this year. For summer crops, high NDVI values on day 145 in year 2012 may explain high values in integral NDVI for year 2012, when values of maximum NDVI were low. In this year, NDVI values in the

second part of the growing season (Figure B.2) were also extremely low, which can only be compared to values in year 2007.

5.3 TVDI calculations

In previous researches, TVDI index was used to compare moisture conditions in different locations of the large territory in one moment of time (Sandholt et al., 2002; Meng et al., 2010). In the present research, surface moisture changes both in space and in time were analyzed, which is similar to applications of CWSI index (Yuan et al., 2004; Gonzalez et al, 2005; USWCL, 2001). As in CWSI calculations, air temperature was used in the current approach for TVDI calculations in order to have account for changes of temperature of air over time. Inclusion of this variable helped to overcome time and regional dependence of TVDI values mentioned in Min et al (2010). However, it made calculations dependent on data from climate stations, network of which according to Kogan et al. (2009) is not sufficiently dense over Ukrainian territory. Although there is uncertainty caused by interpolation of temperature values between stations, difference of temperature values between stations are not larger than several degrees. Thus, network of climate stations may be sufficient in this case and interpolation of air temperature has not caused significant errors.

As was mentioned in section 3.2.2 and in Sandholt et al. (2002), variations in surface temperature are assumed to be related to changes in surface moisture conditions which influence energy balance (figure 4). However, energy balance depends also on factors not accounted in the research. These are surface type, presence of shadows and variations in sensor's viewing angle that influences visible proportion between bare soil and vegetation (Sandholt et al., 2002).

Calculations of TVDI depend on the shape of a Ts/NDVI space. In case a study area is large enough to represent different land cover and wetness conditions, the Ts/NDVI space can be modeled as a triangle or a trapezoid and wet and dry edges can be approximated by a linear model (Sandholt et al., 2002; Meng et al., 2010). If distribution of Ts/NDVI points forms an irregular shape, fixing dry and wet edges can be problematic and may lead to errors (Meng et al., 2010). In order to avoid these errors maximum and minimum Ts values were sampled for each NDVI value from Ts datasets, rather than approximated by a function. Thus, each Ts/NDVI space was limited by two contours of maximum and minimum Ts values, instead of lines.

Julian day		097	113	129	145	161	177	193	209	225	241	257	273
Dry edge	slope	-0,053	-0,038	-0,029	-0,036	-0,062	-0,090	-0,036	-0,061	-0,065	-0,077	-0,058	-0,072
	intercept	30,762	29,341	27,839	31,165	41,798	38,059	33,954	32,510	36,356	36,253	25,290	31,136
	R^2	0,744	0,757	0,710	0,596	0,372	0,894	0,126	0,763	0,682	0,760	0,694	0,724
Wet edge	slope	0,042	0,008	-0,022	-0,027	-0,036	-0,036	-0,037	-0,051	-0,040	-0,046	-0,010	-0,034
	intercept	-8,770	-2,257	2,994	2,463	5,240	3,082	4,596	6,965	4,567	6,395	-2,425	4,442
	R^2	0,612	0,079	0,474	0,548	0,744	0,642	0,699	0,823	0,721	0,723	0,139	0,565

Table 2. Parameters of linear regression fitted to the wet and dry sides of Ts/NDVI spaces

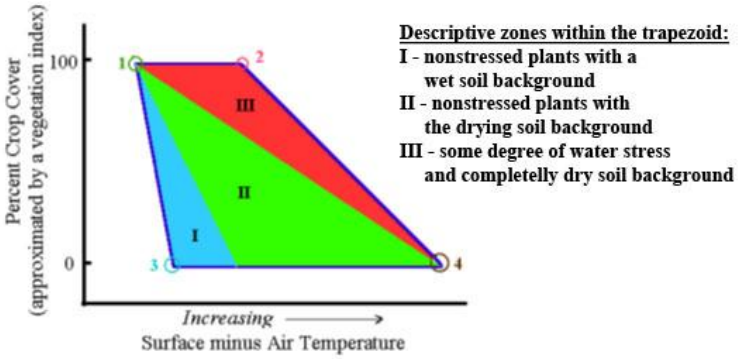

Figure 33. Zones of Ts/NDVI space (USWCL, 2001)

The majority of the contours of Ts/NDVI limits identified for each 16-day period have a shape close to linear and can be described as a linear distribution, the parameters of which are illustrated in Table 2. Large differences in intercept values between dry and wet edges and the relatively small slope of dry edges (Table 2) suggests that the third zone (III) (Figure 36) in Ts/NDVI space is quite large in calculated Ts/NDVI distributions. According to Clark (1997) and USWCL (2001), pixels falling in this zone represent dry soil, and different degree of water stress in plants.

As seen in Figure 27, moisture conditions are more favorable in forested areas. Particularly, TVDI is lower in the northern part of Odessa Oblast situated in the Forest Steppe agro-ecological region (Gumeniuk et al., 2010) and in the Crimean Mountains, which are also covered with forest. Deviations of TVDI values between years have higher amplitude in the central and eastern parts of the study area. As seen in Figure 28, areas with high values of standard deviation have also high positive trends of TVDI. This suggests that areas with higher variability of TVDI became dryer during the study period. This can be explained by findings from Gonzalez et al. (2005), where it was concluded that spatial variability of canopy temperature increases with the increase of water stress.

Overall, TVDI trends are positive over the study area. These findings suggest that the southern Ukraine become dryer over the period between the years 2000-2013, which is also confirmed by a negative trend in the Standardized Precipitation Index (SPI) calculated for the same area by Khokhlov et al. (2012). Khokhlov et al. (2012) also concluded that the frequency of droughts has increased in the southern Ukraine in the past decade. However, there is no empirical evidence which supports the claim that climate became dryer in the southern Ukraine (Yatsyk et al., 2006). The increased aridity of the surface found in this research may indicate human desertification processes, mentioned in Yatsyk et al. (2006) and Netis (2009).

According to findings in this research (Figure 27, Figure D.1), there were 5 years with unusually dry surface moisture conditions; 2000, 2003, 2007, 2009 and 2012. These findings confirm previous findings (Vojegova et al., 2013; Adamenko and Prokopenko, 2011) that indicate that drought is occurring every 2 or 3 years in the southern Ukraine.

5.4 Relations between climate and vegetation conditions

After vegetation and surface moisture variables were computed and analyzed, they were compared in order to find the impact of changes in moisture on vegetation conditions. As a result, a statistically significant negative correlation was found between integral NDVI of winter crop and

maximum NDVI of winter and summer crops. As seen in Figure 30, correlation with TVDI is especially strong for integral NDVI of winter crops and maximum NDVI of summer crops.

As mentioned by Hall-Beyer et al. (2011), NDVI variability of cropland is not always dependent on natural factors, since it is influenced by human controlled factors. For instance TVDI is not correlated with integral NDVI of summer crops over the entire study area. The reason for this is the dependence of integral NDVI on the length of growing season, which is influenced by cultivation practices. Date of planting is determined based on spring air temperatures and the presence or lack of snow on the ground. Although maximum NDVI for summer crops is highly correlated with TVDI, almost no correlation is found in the center of Kherson Oblast and in the Crimean Peninsula, where irrigation is practiced.

Integral NDVI of winter crops is less dependent on the length of the growing season, since only the spring and summer stages of the growing season are studied in this research, and winter crop is already grown when it emerges from snow. The length of the growing season is dependent on the date of cultivation only i.e. the date of the end of growing season. Integral NDVI has generally stronger correlation with TVDI than maximum NDVI values. For both metrics, correlation is insignificant in Kherson Oblast and the north of Odessa Oblast where, density of winter crop fields is low (Figure 16).

By comparing wetness conditions and vegetation performance (Figure 31), we find the most significant influence on agricultural vegetation was caused by droughts in years 2007 and 2012. Droughts in years 2000 and 2009 were rather mild. Although the effects of drought in year 2000 are not clearly seen in vegetation performance, they probably caused a smaller yield of winter wheat in this year (Figure 37A).

Drought in year 2012 had influence on both winter and summer crops. Its influence is clearly seen by low maximum NDVI values, which have almost the same spatial pattern as low TVDI values (Figure 31). According to Kytischeva (2012), air and soil moisture in this year was critically low in Zaporizhia Oblast, which caused substantial damage to sunflower.

In 2007, drought conditions have caused unusually low NDVI values for winter crops during the second half of the growing season (Figure B.1). At the same time, maximum NDVI values for winter crop were normal (Figure 31), but average yield of winter wheat was just a little lower than in other years (Figure 37a). For summer crops NDVI influence from drought was harder to see, since NDVI values were low during the entire year (Figure B.2) and the total area of summer crop in this year's fields was the smallest in the study period (Figure 16). This drought was also recognized as the most severe by Kogan et al. (2011).

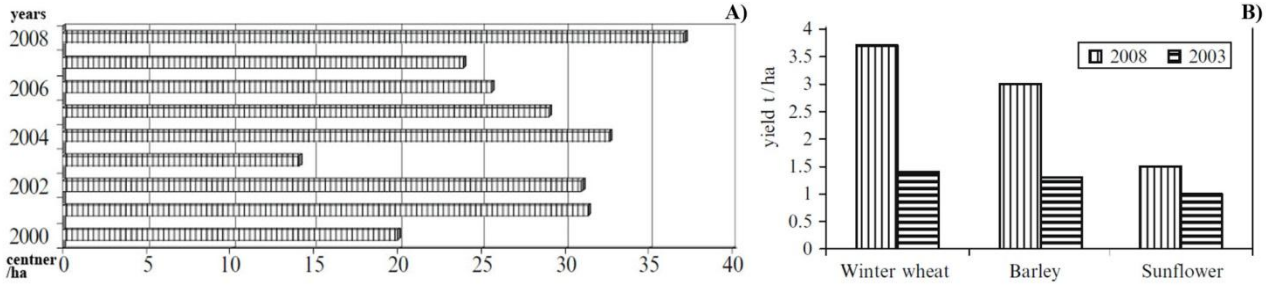

Figure 34. Average yield of winter wheat in different years a) and yield of different crops in years 2008 and 2003 b) (Adamenko and Prokopenko, 2011)

In year 2003, significant damage of winter crops was not apparently caused by extremely dry conditions during spring and summer. Only some parts of the study area were unusually dry (Figure 31) and the amount of rainfall registered by climate stations was around normal values in this year (Table E.1; Figure E.2). Due to this, the reasons for crop damage in year 2003 may be found during the winter, as suggested by Netis (2007). In this year, 65% of the winter crop was smothered by ice crust (FAO, 2005). Average winter wheat yield in this year was the lowest (Figure 37A). In the same year, damage to summer crops was found to be minimal (Figure 39), which coincides with only a small decrease in sunflower yield (Figure 37).

In his research, Kogan et al. (2011) concluded: The data shows that year "2003 indicates a very severe vegetation stress". The results of this research complements findings from Kogan et al. (2011). Since the surface was unusually dry only in limited locations, it was an extreme weather event in winter as specified by Netis (2007) and FAO (2005) that, according to the current research, damaged winter crops and had no effect whatsoever on summer crops.

6. Conclusion

In this research, vegetation conditions of summer and winter crops were analyzed and compared to surface moisture conditions during the study period (2000-2012) and over the study area, which include five administrative regions: Odessa Oblast, Mykolaiv Oblast, Kherson Oblast, Zaporizja Oblast and the Autonomous Republic of Crimea. Analysis was performed on a field-by-field basis and temporally on an inter-annual basis. Findings acquired in this research are listed below:

- Crop vegetation performance was generally negative over the study area. Some slightly positive trends were found in Zaporizja Oblast, Odessa Oblast and the Autonomous Republic of Crimea. Trends were highly negative in Mykolaiv and Kherson Oblasts.
- There is a strong variability of vegetation performance variables both inter-annually and spatially. Inter-annual variability of integral NDVI values is stronger than variability of maximum NDVI values.
- Crops cultivated in the northern parts of the study area are generally in better conditions than crops grown in the south.
- In years 2003, 2007 and 2012, conditions of winter crops were below average over the majority of the study area, while conditions of summer crops were unusually low in years 2007, 2009 and 2012. In other years, vegetation conditions were below normal for limited areas only.
- Surface moisture conditions are evenly spread over the study area. The surface is wetter near the seacoast, around major inland water bodies and in the part with a high proportion of forest; the northern part of Odessa Oblast and the Crimean Mountains.
- There was a negative trend of surface moisture (positive trend of TVDI) during the study period, which suggests that soil became dryer since the year 2000. Negative trends of surface moisture were found in areas with high variability of this parameter.
- There were five years, when the surface was unusually dry: 2000, 2003, 2007, 2009, and 2012.
- Statistically significant correlation was found between surface moisture and vegetation variables over the majority of the study area. Correlation was not found for integral NDVI of summer crops, due to its high dependence on the length of the growing season.
- It was found that unusually low agricultural vegetation performance coincides in time with unusually dry surface conditions. However, drought in year 2003 had no impact on summer crops and drought in year 2009 did not influence winter crops.

Based on the list above, it can be concluded that surface moisture has significant influence on both winter and summer crops. In years when the area became unusually dry, crop vegetation responded with lower vegetation performance. Although in comparison to research conducted by Kogan et al. (2011), the current research lacks the investigation of the duration of droughts, this research has complemented Kogan's research with an investigation of the driving forces of drought, and a specific focus on vegetation response from agricultural fields rather than the entire landscape. Beyond the study period of Kogan's research, two new years of unfavorable moisture conditions were found in the current research: year 2009 with limited impact on summer crops, and year 2012 with wide effects on summer and winter crops.

Appendix A. Data processing diagrams

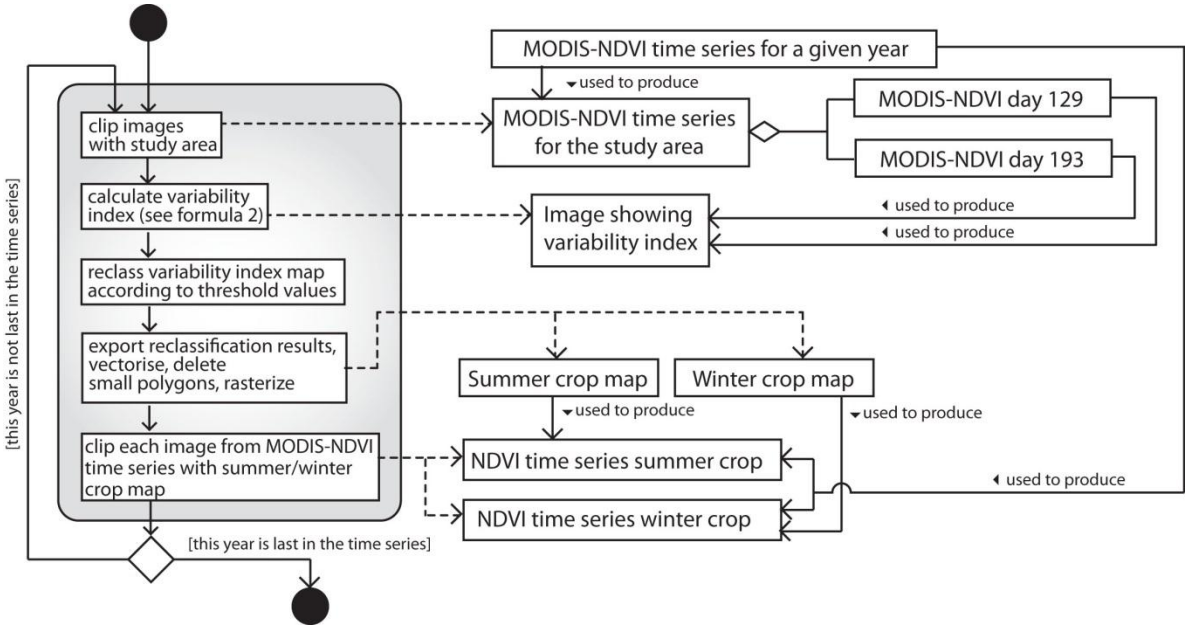

Figure A.1. Summer/winter crop classification procedure

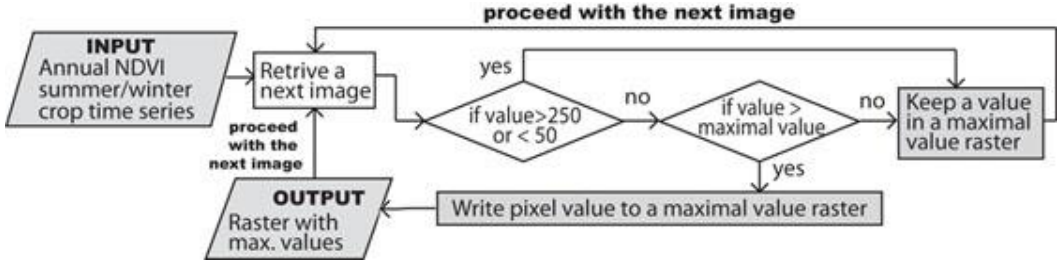

Figure A.2. Calculation of a maximal value raster

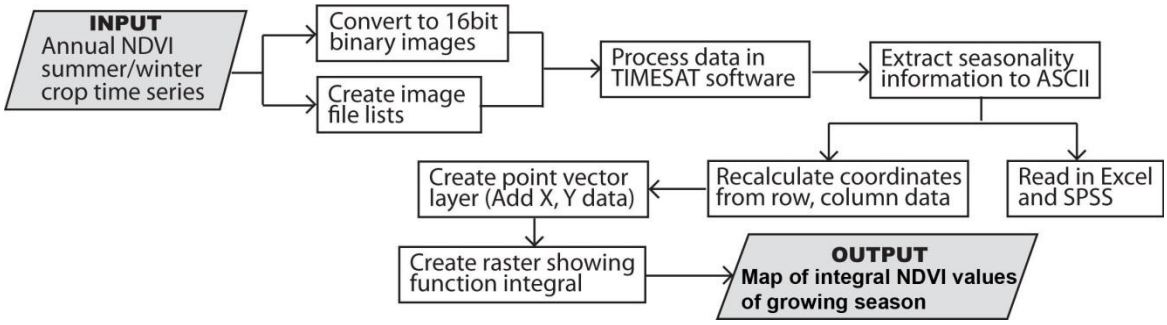

Figure A.3. Compilation of datasets showing integral values of growing season using the TIMESAT software

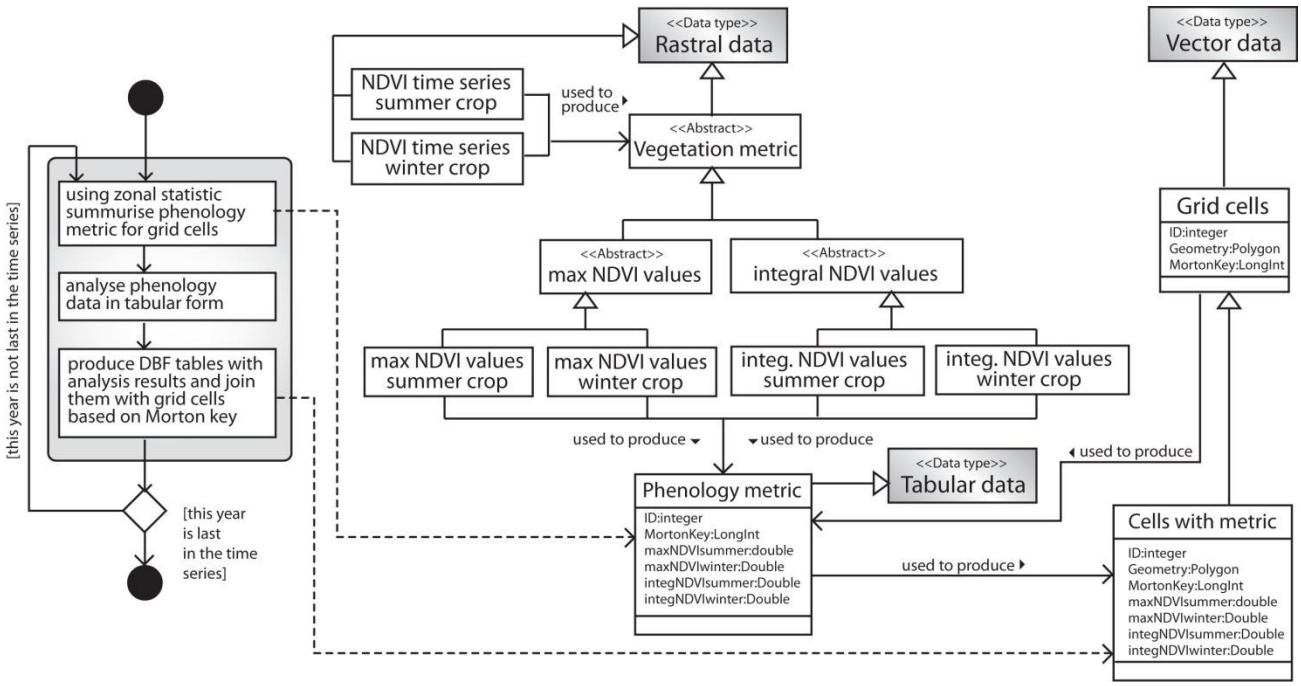

Figure A.4. Sampling phenology metrics to tabular form

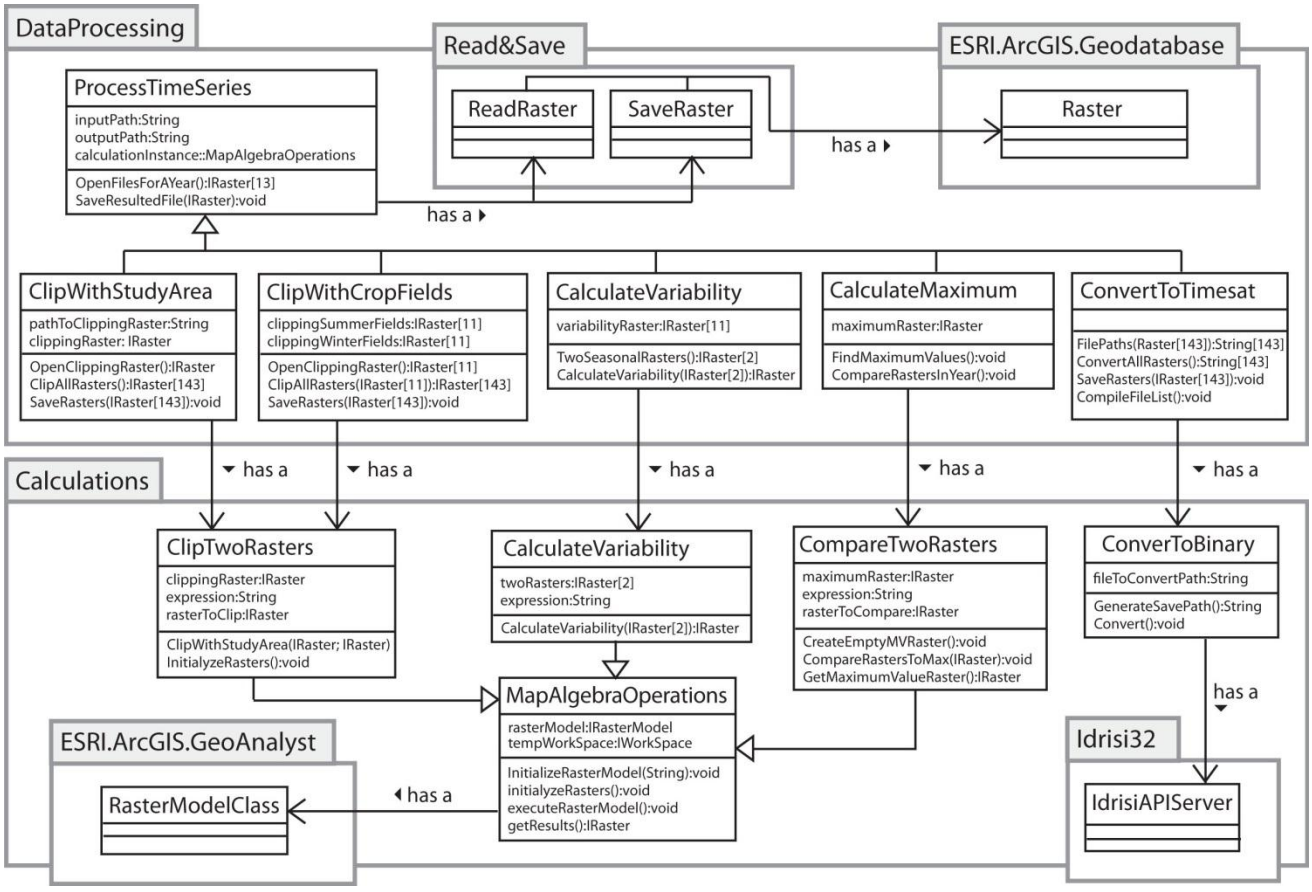

Figure A.5. Object oriented structure for data processing

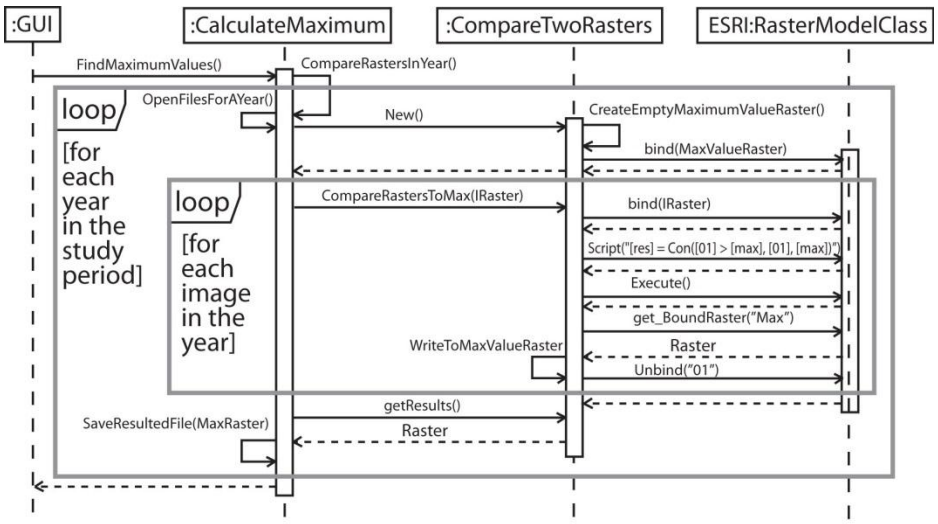

Figure A.6. Sequence for maximum value determination

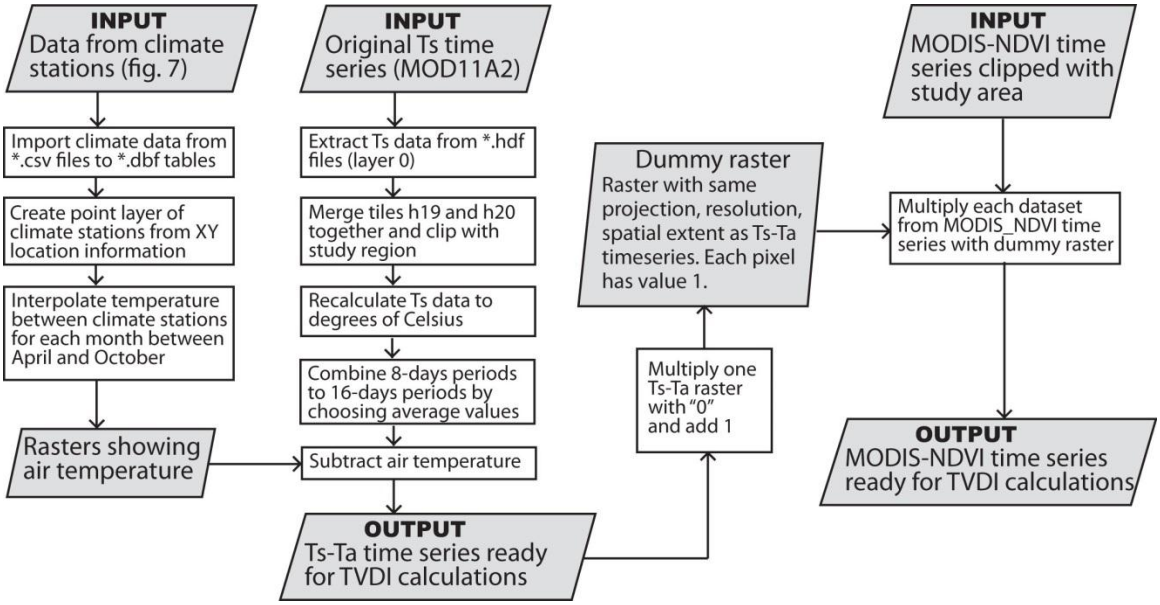

Figure A.7. Data processing for TVDI calculations

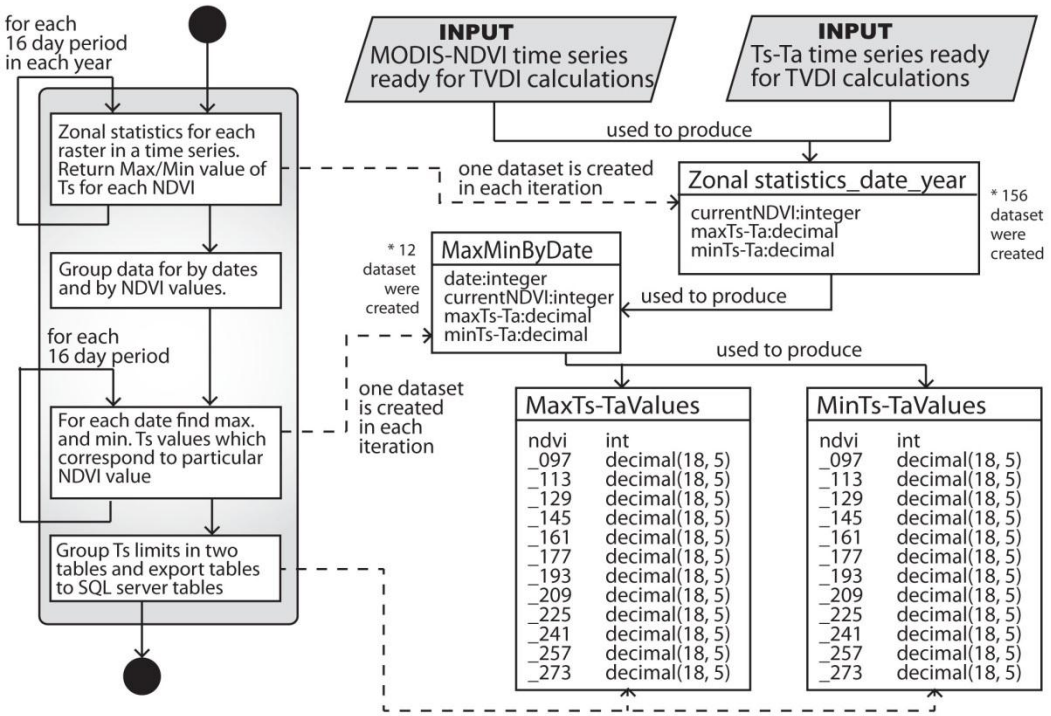

Figure A.8. Determining of limits of Ts-Ta values

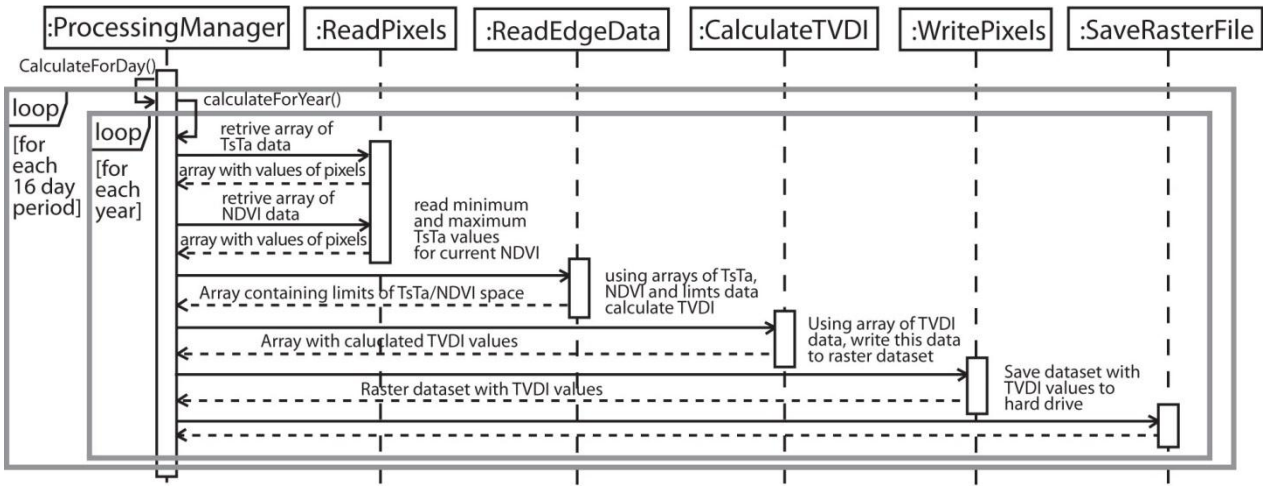

Figure A.9. Algorithm of TVDI calculations implemented in the software

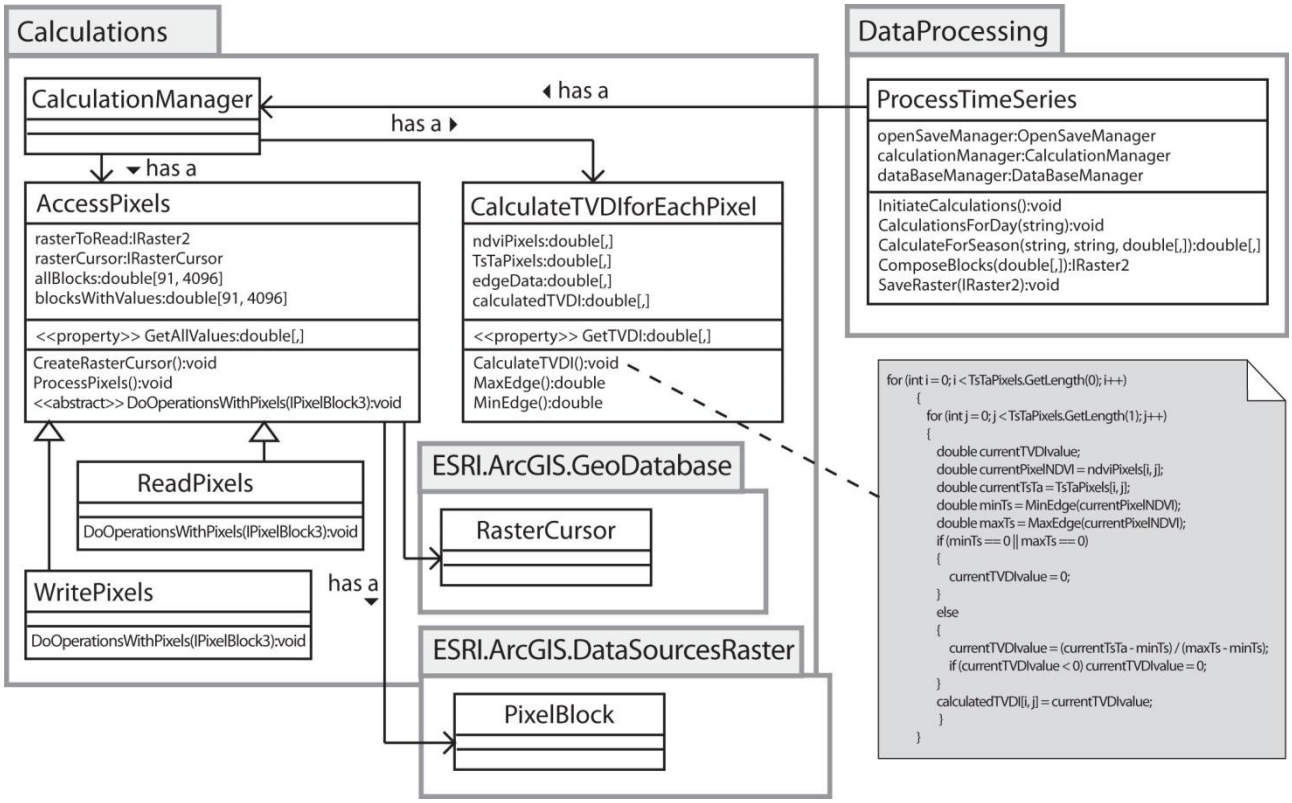

Figure A.10. Implementation of core functions of the software for TVDI calculations

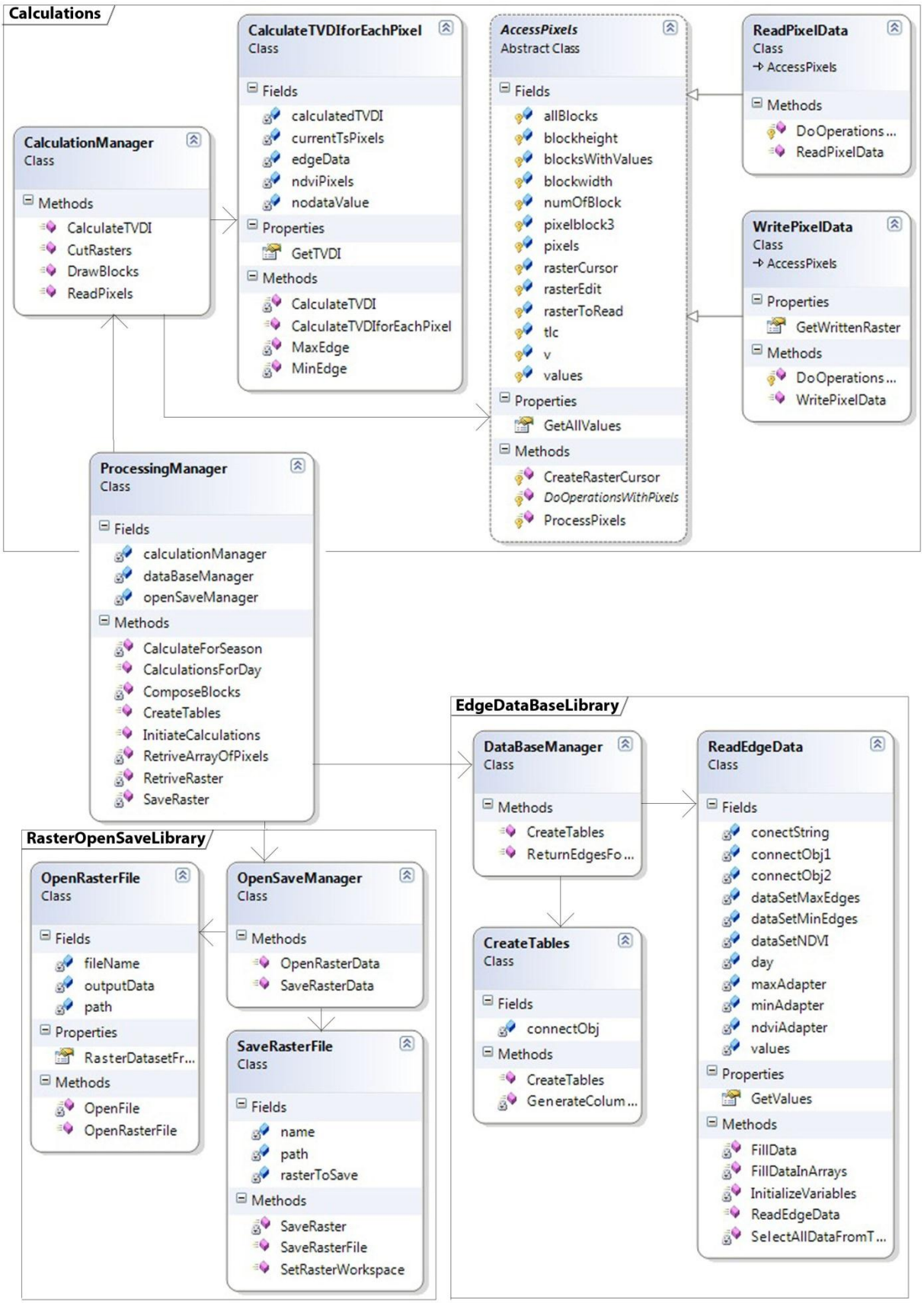

Figure A.11. UML class diagram of the software for TVDI calculations

Appendix B. Seasonal NDVI profiles for winter crop and summer crop areas

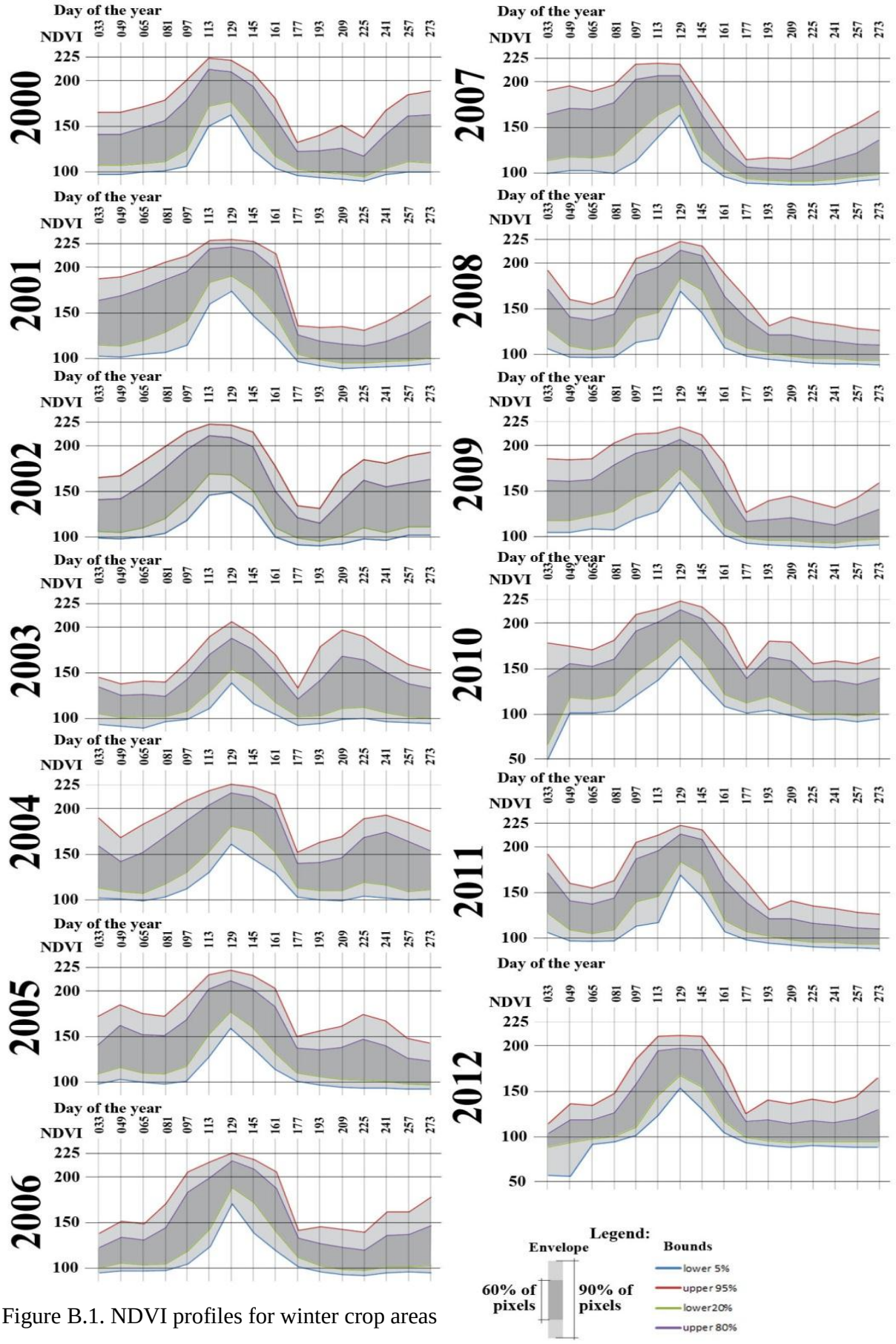

Figure B.1. NDVI profiles for winter crop areas

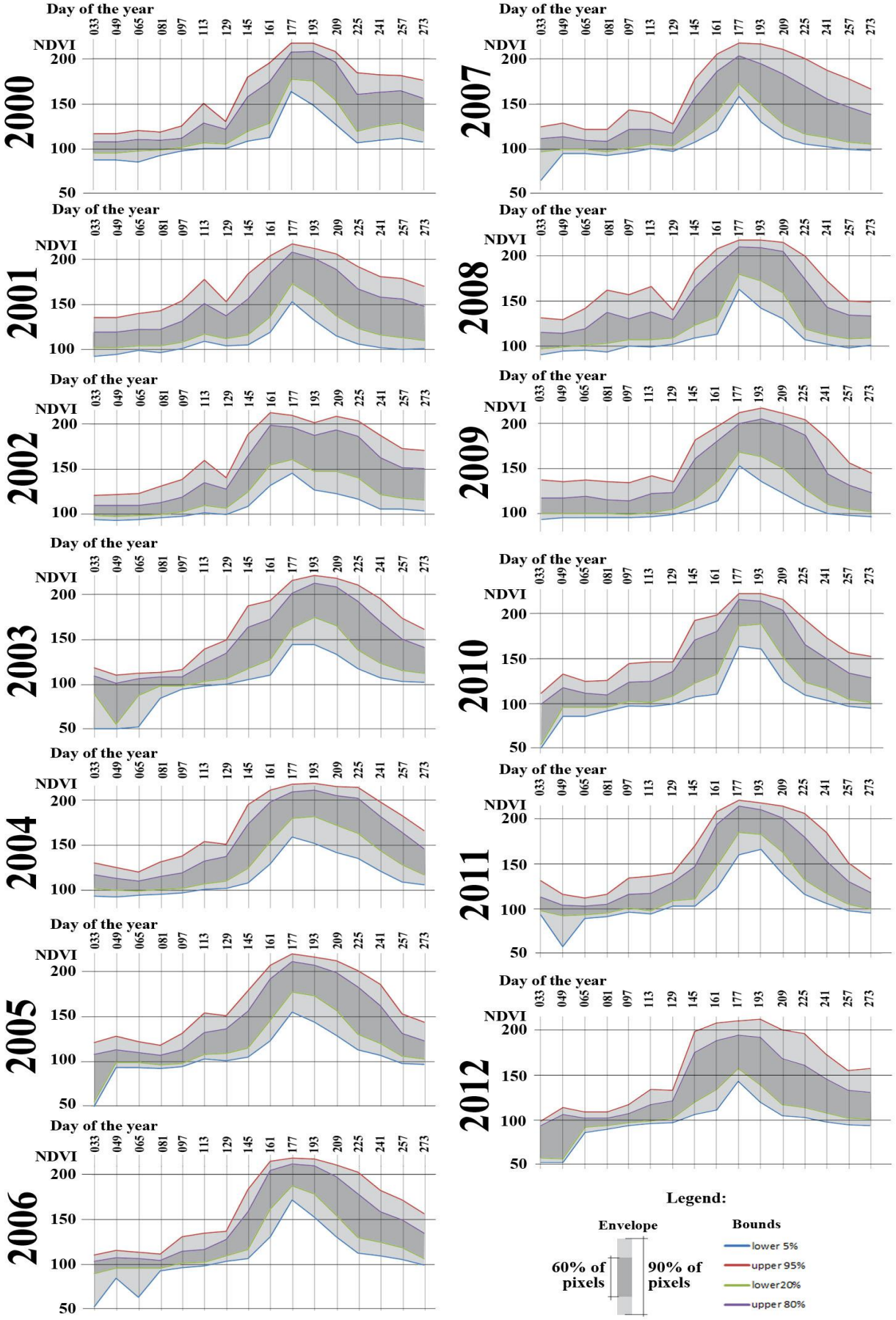

Figure B.2. NDVI profiles for summer crop areas

Appendix C. Z-scores of maximum and integral NDVI for growing season

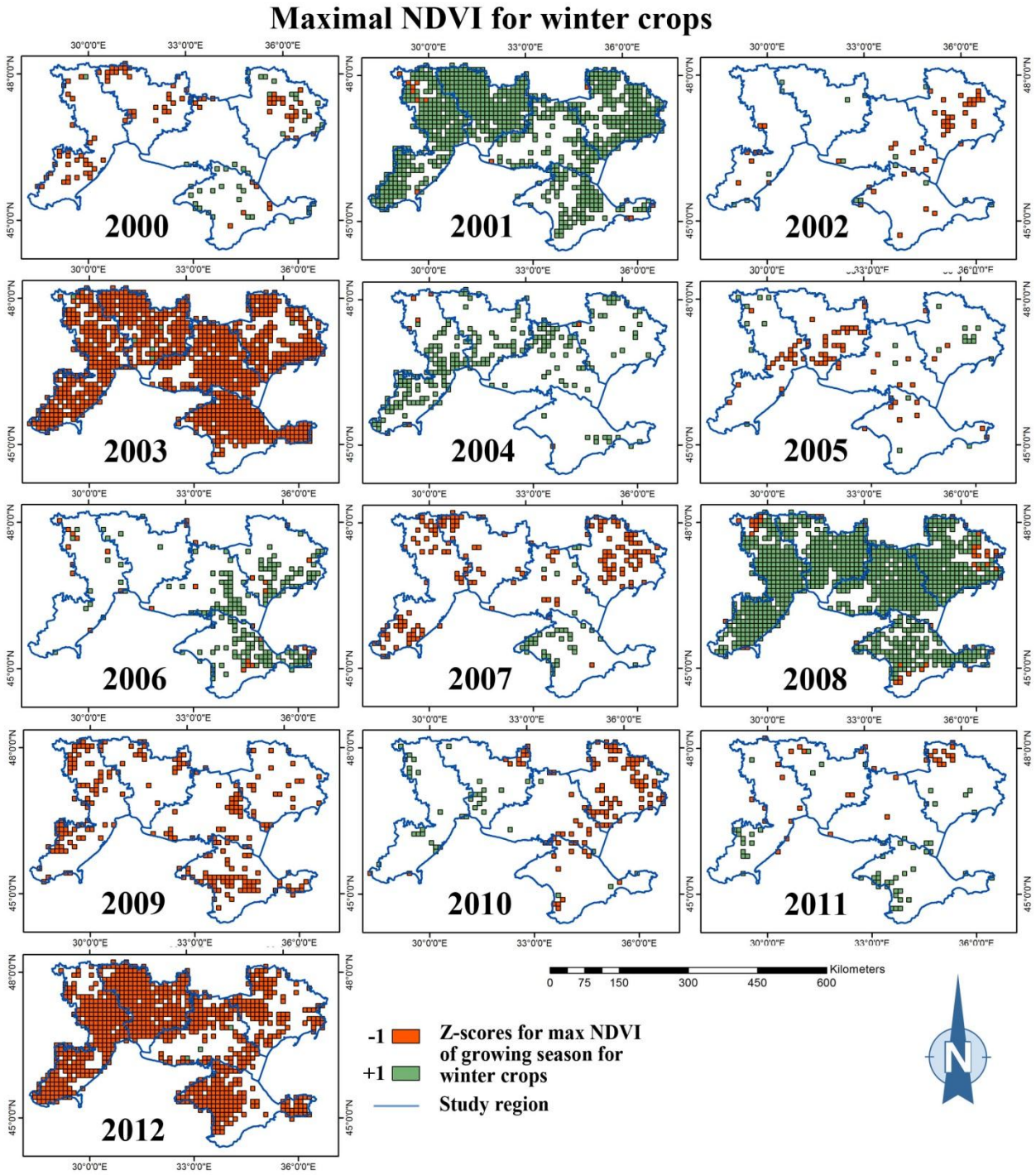

Figure C.1. Spatial distribution of Z-scores of maximum NDVI values for winter crops

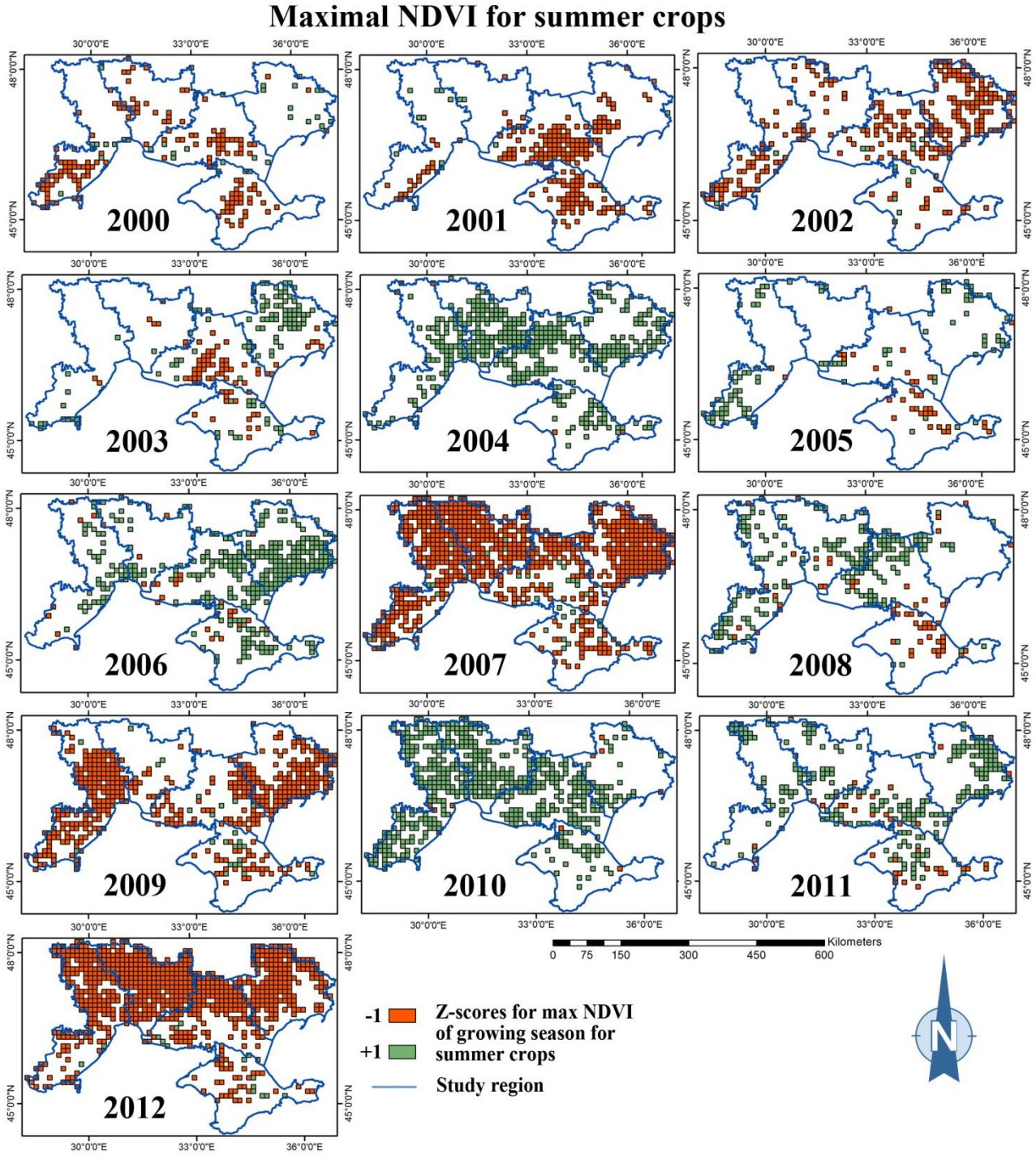

Figure C.2. Spatial distribution of Z-scores of maximum NDVI values for summer crops

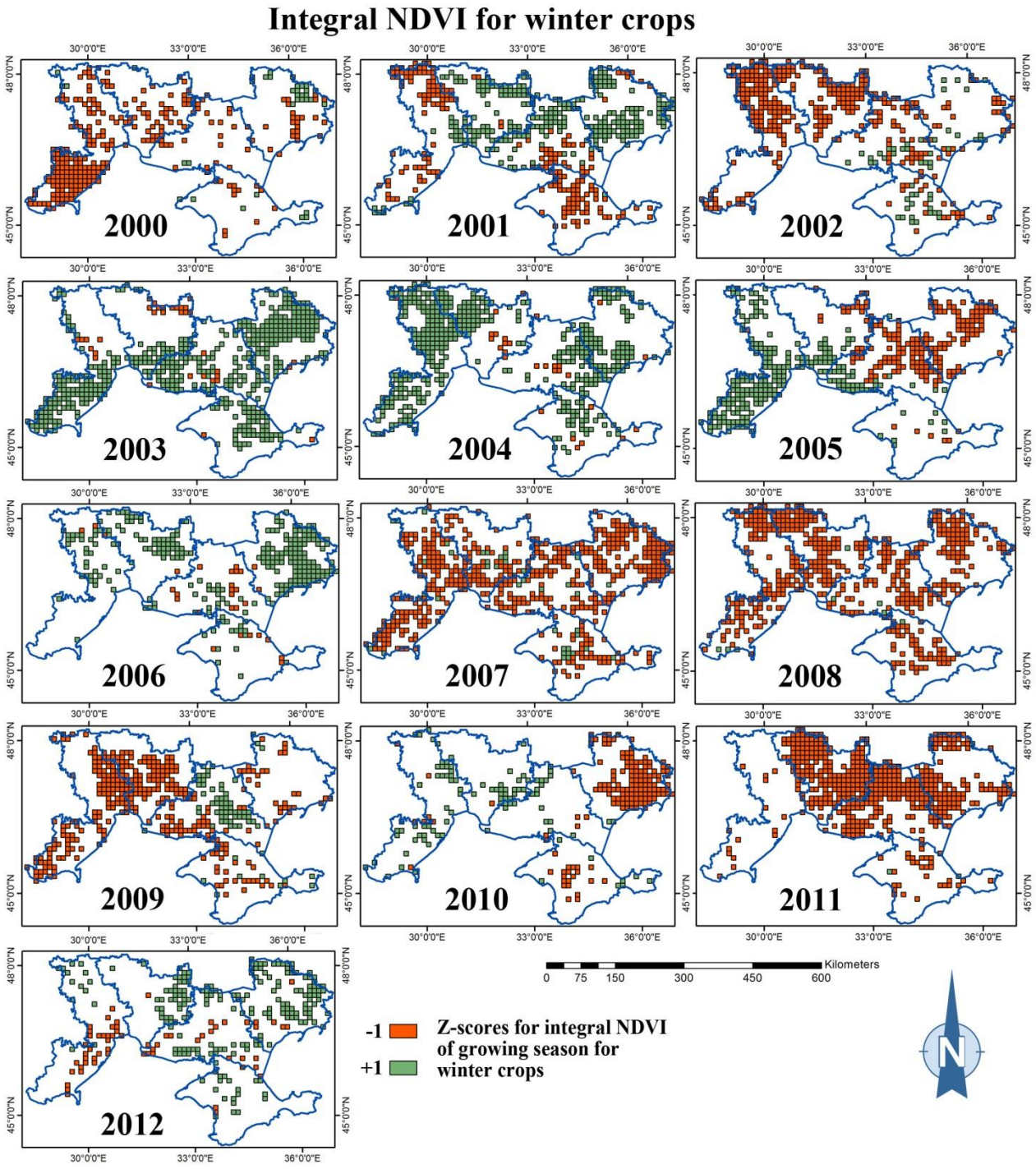

Figure C.3. Spatial distribution of Z-scores of integral NDVI values for winter crops

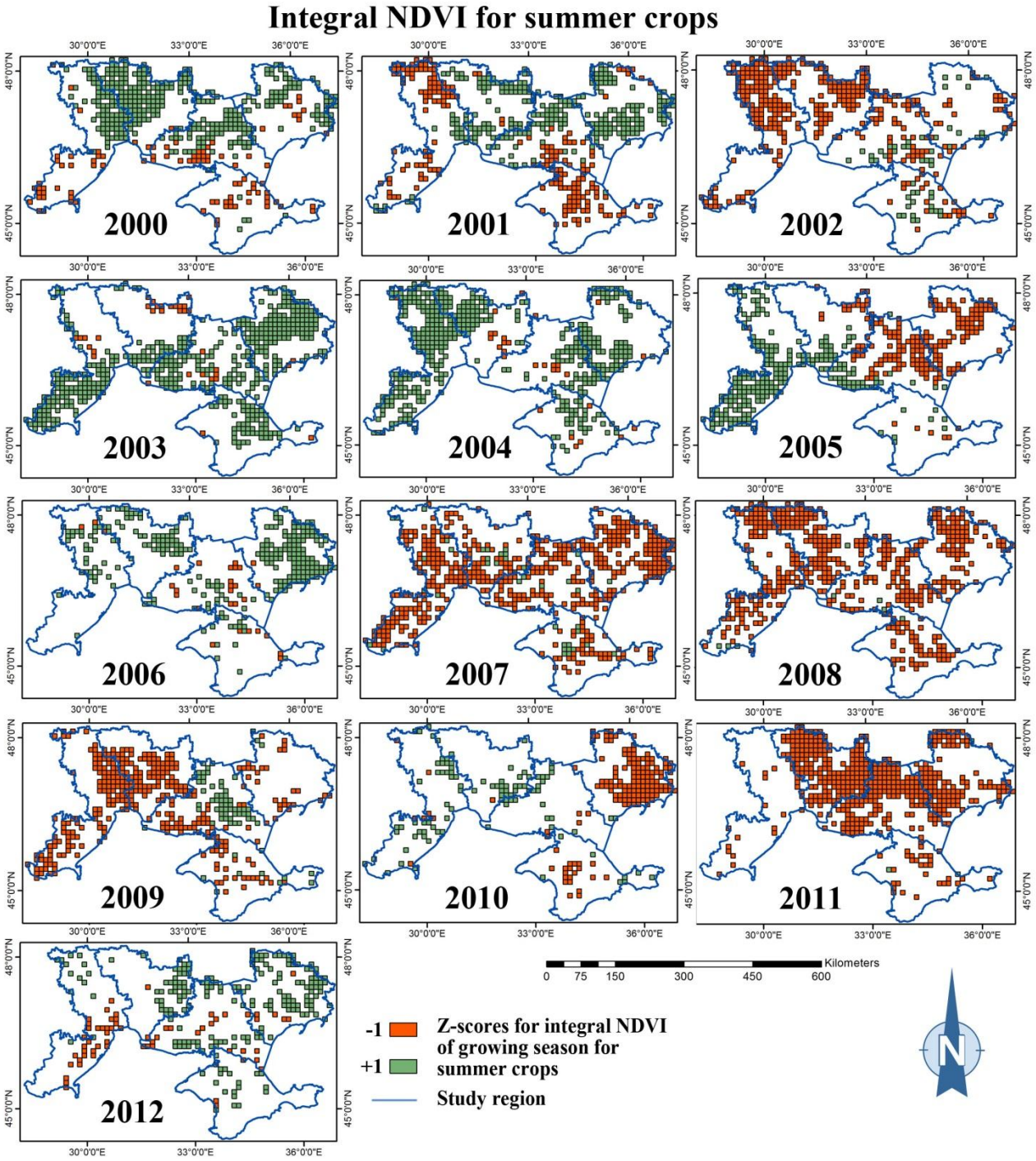

Figure C.4. Spatial distribution of Z-scores of integral NDVI values for summer crops

Appendix D. Z-scores of maximum and cumulative TVDI

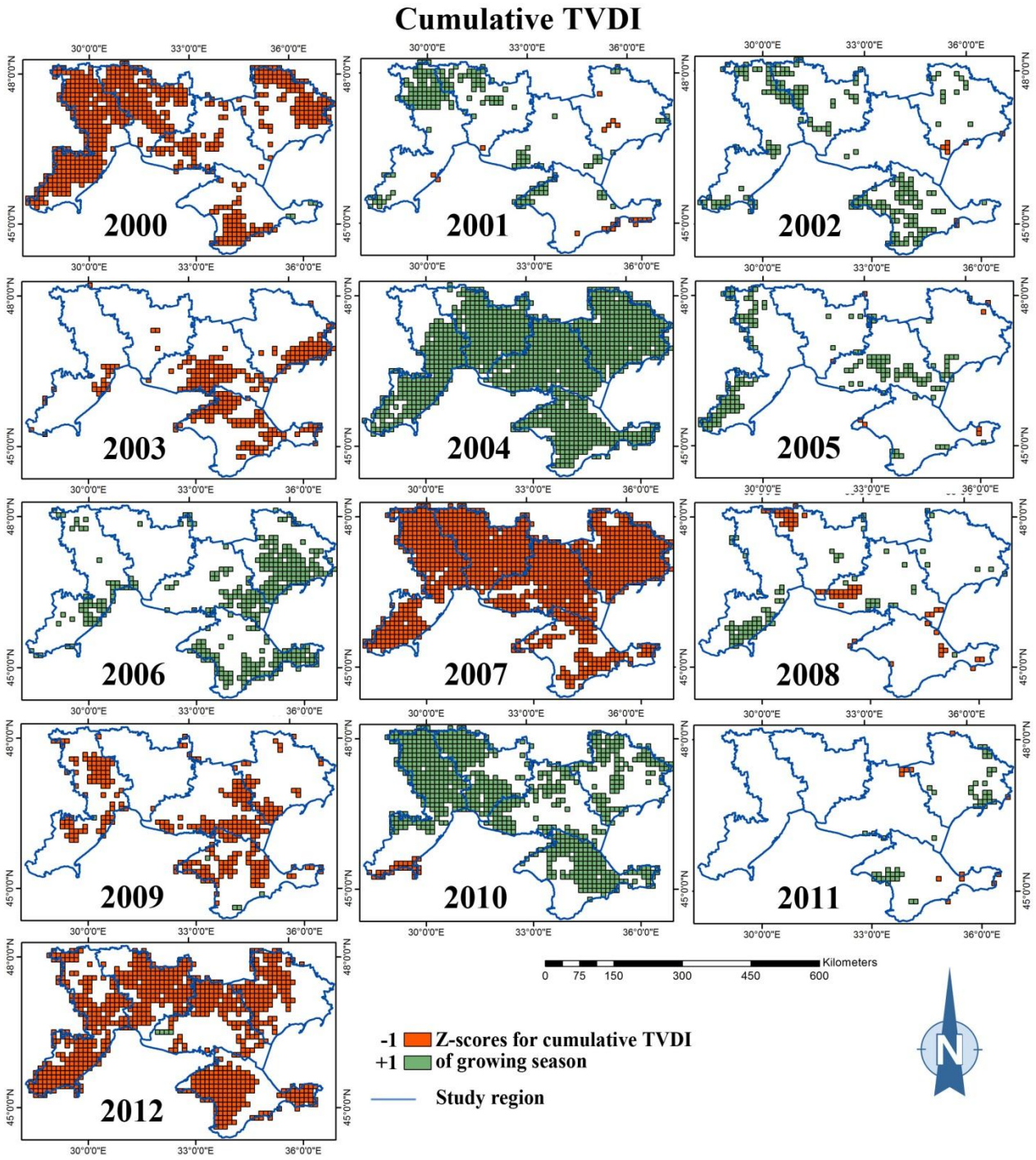

Figure D.1. Spatial distribution of Z-scores of cumulative TVDI values

Appendix E. Rainfall data from climate stations situated within study area.

LIUBASHIVKA UP

Month	2000	2001	2002	2003	2004	2005	2006	2007	2008	2009	2010	2011	2012
1	385	122	132	703	630	176	170	116	5	55	718	397	491
2	212	190	18	292	393	269	222	177	40	137	342	221	184
3	198	474	170	160	78	36	182	127	140	97	165	125	145
4	345	72	53	292	63	196	227	43	189	0	422	366	244
5	344	634	80	120	496	70	483	56	175	33	435	107	180
6	833	1018	119	452	0	133	694	50	10	7	389	1335	140
7	530	273	416	630	1431	29	200	0	1737	602	211	203	239
8	520	348	178	300	124	281	176	330	147	13	200	119	112
9	787	820	63	270	124	0	512	5	900	89	409	68	0
10	9	119	128	933	200	30	170	14	54	318	341	462	445
11	664	708	430	249	306	110	74	434	18	65	136	5	156
12	156	418	15	147	169	190	17	142	266	474	410	325	1046

KHERSON UP

Month	2000	2001	2002	2003	2004	2005	2006	2007	2008	2009	2010	2011	2012
1	253	167	16	468	605	176	172	199	0	100	505	168	698
2	196	366	201	295	320	486	65	221	20	174	348	35	210
3	239	509	77	447	143	104	283	100	154	40	76	23	176
4	303	365	51	146	138	8	46	192	146	6	97	342	40
5	210	316	16	543	543	110	153	7	8	93	160	249	35
6	652	478	350	381	234	27	174	110	190	5	341	256	170
7	415	186	92	411	409	333	50	520	327	102	170	20	0
8	110	148	192	553	297	441	286	3	506	63,5	330	50	513
9	1110	497	121	50	113	292	12	8	684	25	490	173	20
10	74	315	54	455	418	142	54	118	110	382	1169	90,5	38
11	17	401	366	282	154	111	126	418	160	238	294	8	43
12	146	211	19	190	317	286	1	32	3	650	565	241	309

CHORNOMORSKE

Month	2000	2001	2002	2003	2004	2005	2006	2007	2008	2009	2010	2011	2012
1	115	136	118	354	514	207	196	213	4	115	343	91	627
2	259	300	26	315	172	360	135	55	50	103	585	20	124
3	344	306	393	242	72	146	318	99	353	18	82	150	65
4	241	516	110	193	73	24	74	130	160	71	140	341	132
5	120	606	0	460	661	80	216	5	151	13	198	442	226
6	488	188	627	177	81	9	84	0	4	139	190	165	282
7	362	117	168	525	38	14	24	-	464	264	-	-	215
8	201	300	90	180	180	20	125	50	565	20	-	-	148
9	569	843	519	230	103	50	237	130	665	429	229	-	-
10	70	270	213	194	175	318	1464	63	28	46	353	282	0
11	123	356	341	634	45	166	98	465	153	179	229	59	-
12	320	209	40	235	258	1950	21	26	16	489	817	79	271

KERCH UP

Month	2000	2001	2002	2003	2004	2005	2006	2007	2008	2009	2010	2011	2012
1	448	125	165	425	668	440	107	303	10	42	482	196	396
2	358	417	288	233	807	278	65	27	20	280	96	99	124
3	528	532	317	300	97	307	83	54	106	228	142	35	170
4	89	603	282	249	131	288	72	250	48	63	101	386	183
5	210	318	178	0	805	172	200	43	20	56	361,5	94	450
6	1542	815	122	149	792	482	1377	0	56	103	622	-	140
7	12	0	105	624	129	422	90	20	555	150	-	-	76
8	1350	440	2031	159	1070	144	30	5	316	46	-	117	119
9	104	97	1557	258	326	178	86	71	76	450	208	20	10
10	223	152	683	411	228	696	80	6	38	51	490	496	8
11	9	413	474	370	414	601	430	454	95	594	521	122	140
12	173	389	32	409	296	671	55	152	146	358	600	286	135

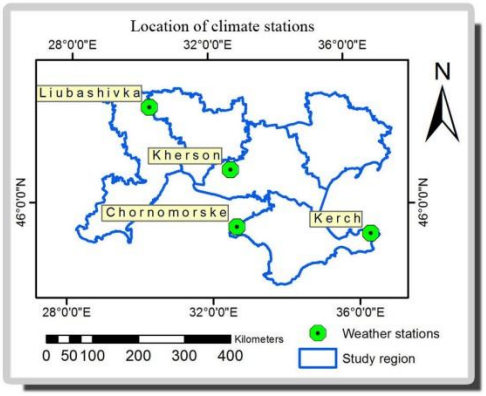

Figure E.1. Location of climate stations

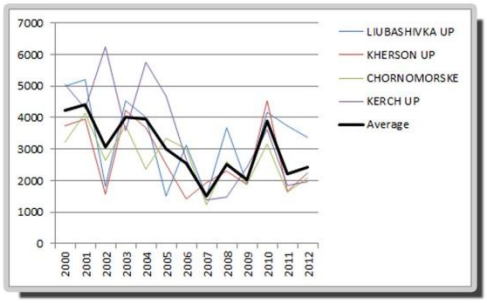

Figure E.2. Total annual precipitation

Table E.1. Total monthly rainfall data (tens of mm) for each year in the study period 2000-2012

References

Adamenko, T. and Prokopenko, A. (2011) Monitoring Droughts and Impacts on Crop Yield in Ukraine from Weather and Satellite Data. In F. Kogan et al. (eds.), *Use of Satellite and In-Situ Data to Improve Sustainability*, 3NATO Science for Peace and Security Series C: Environmental Security, DOI 10.1007/978-90-481-9618-0_1, Springer.

Aragón, l., M., Garza, E., J., T., Pérez, J., J., Calderón, O., A., A., Tagle, M., A., G., García, M., P. and Salado, C., A., A. (2012) NDVI-rainfall relationship using hyper-temporal satellite data in a portion of North Central Mexico (2000-2010). *African Journal of Agricultural Research*. Vol. 7(6), pp. 1023-1033.

Balint, Z., Mutua, F., M. and Muchiri, P. (2011): *Drought Monitoring with the Combined Drought Index*, FAO-SWALIM Nairobi, Kenya

Brown, J., F., Jenkerson, C. and Gu, Y. (2008) *Using eMODIS Vegetation Indices for Operational Drought Monitoring*. Submitted to: National Integrated Drought Information System Knowledge Assessment Workshop: Contributions of Satellite Remote Sensing to Drought Monitoring, February 6-8, 2008

Carroll, M.L., C.M. DiMiceli, R.A. Sohlberg, and J.R.G. Townshend (2004), *250m MODIS Normalized Difference Vegetation Index*, University of Maryland, College Park, Maryland. Retrieved 22.04.2013 from: http://glcf.umd.edu/data/ndvi/

Cherenkov, A.,V., Schevchenko, M., S., Lebid, E., M., Tsikov, V., C., Desjatnik, L., M., Lorinets, F., A., Fedorenko, I., E., Kotsuban, D., A. and Lib, I. M. (2013) *Structure of cultivated areas and crop rotation. (Scientific and practical recommendations).* Institute of agriculture of steppe zone, National Academy of Science of Ukraine. Dnipropetrovsk, Ukraine.

Clarke, T., R. (1997) An Empirical Approach for Detecting Crop Water Stress Using Multispectral Airborne Sensors. *HortTechnology*. Vol. 7 no. 1, pp. 9-16.

CRA-CIN (2009) Soil heat flux. *Agricultural Production and Externalties Simulator Help*. Research Centre for Industrial Crops, Bologna, Italy. Retrived 12.06.2013 from: http://www.apesimulator.org/help/models/evapotranspiration/Soil_heat_flux.html

Dou, Y., Chen, X., Bao, A., Luo, G., Jappar, G. and Li., J. (2008) *The Correlation Analysis of Vegetation Variable Process and Climate Variables in Alpine-Cold Wetland in Arid Area*. Paper presented in: Geoscience and Remote Sensing Symposium, 2008. IGARSS 2008. IEEE International

Eklundh, L. and Jönsson, P. (2012) *Timesat 3.1 Software Manual*, Lund University, Sweden.

EROS (2011,2012) *MOD11A2*, NASA Land Processes Distributed Active Archive Center (LP DAAC) as producer, USGS/Earth Resources Observation and Science (EROS) Center, Sioux Falls, South Dakota.

Enkhzaya, T. and Tateishi, R. (2011): Use of phenological features to identify cultivated areas in Asia. *International Journal of Environmental Studies*, 68:1, pp. 9-24.

European Environment Agency (EEA) (2008) *Global land cover - 250m*. Retrieved 22.04.2013 from: http://www.eea.europa.eu/data-and-maps/data/global-land-cover-250m

FAO (2004) *Drought-resistant soils. Optimization of soil moisture for sustainable plant production.* FAO Land and Water Bulletin 11. Food and Agriculture Organization of the United Nations, Rome, Italy. ISBN 92-5-105358-8.

FAO (2005) *Fertilizer use by crop in Ukraine.* Food and Agriculture Organization of the United Nations, Rome, Italy

FAO (2013) *Drought Facts.* FAO land and water. Food and Agriculture Organization of the United Nations, Retrieved 12.06.2013 from: http://www.fao.org/docrep/017/aq191e/aq191e.pdf

Fank, C. and Budde, M., E. (2009) Phenologically-tuned MODIS NDVI-based production anomaly estimates for Zimbabwe. *Remote Sensing of Environment*, Volume 113, issue 1 (January 15, 2009), pp. 115-125. ISSN: 0034-4257

Fedorenko, E., M. (2011) *Optimization of technological processes of harvesting and storage of grain yield in Dnipropetrovska oblast.* Institute of agriculture of Ukrainian steppe territories, National Academy of Science of Ukraine.

Frayer, O. (2012) *Agricultural production intensification in Ukraine: Decision support of agricultural policies based on the assessment of ecological and social impacts in rural areas*. Interim Report IR-11-037, International Institute for Applied Systems Analysis, Laxenburg, Austria

Funk, C. and Budde, M., E. (2009) Phenologically-tuned MODIS NDVI-based production anomaly estimates for Zimbabwe. *Remote Sensing of Environment*. Vol 113, pp. 115-125

GEOG (2013) *250-meter MODIS/NDVI Time Series Database from the Global Agriculture Monitoring (GLAM) Project, Version 0.3.13.* Department of geographical sciences, University of Mariland. Retrieved 12.06.2013 from: http://pekko.geog.umd.edu/usda/test/

Giarolla, A., Baethgen, W., E. and Ceccato, P. (2010) *NDVI (MODIS sensor) response to interannual variability of rainfall and evapotranspiration in a soybean producing region, southern Brazil*. Presented in: ISPRS TC VII Symposium – 100 Years ISPRS, July 5–7, 2010, Vienna, Austria.

Gonzalez-Dugo M., P., Moran, M., S., Meteos, L. and Bryan, R. (2005) Canopy temperature variability as an indicator of crop water stress severity. *Irrigation Science.* Vol. 24, issue 4, pp. 233-240.

Grekov, L., D. (2012) *Regional monitoring system for agricultural land and agro resources*. Presented in: XVII technical scientific symposium "Geo-information monitoring of environment: GNSS and GIS technologies" 10-15 September, Alushta, Ukraine

Gu, Y., Brown, J., F., Verdin, J., P. and Wardlow, B. (2007) A five-year analysis of MODIS NDVI and NDWI for grassland drought assessment over the central Great Plains of the United States. Geophysical Research Letters, vol. 34, L06407, doi:10.1029/2006GL029127

Gumeniuk, K., Mishchenko, N., Fischer, G. and van Velthuizen, H. (2010) *Agro-ecological Assessment for the Transition of the Agricultural Sector in Ukraine. Methodology and Results for Baseline Climate*. IIASA, Laxenburg, Austria. Retrieved 02.11.2012 from: www.iiasa.ac.at/Publications

Hall-Beyer, M. (2011) Patterns in the yearly trajectory of standard deviation of NDVI over 25 years for forest, grasslands and croplands across ecological gradients in Alberta, Canada. *International Journal of Remote Sensing*. 33:9, pp. 2725-2746

Hermance, J., F., Jacob, R., W., Bradley, B., A. and Mustard, J., F. (2007) Extracting Phenological Signals From Multiyear AVHRR NDVI Time Series: Framework for Applying High-Order Annual Splines With Roughness Damping. *IEEE Transactions On Geoscience And Remote Sensing*, vol. 45, no. 10.

Hird, J., N. and McDermid, G. (2011) *Dealing with noise in multi-temporal NDVI datasets for the study of vegetation phenology: Is noise reduction always beneficial?* Paper presented in: Proceedings of Spatial Knowledge and Information - Canada (SKI-Canada) 2011, March 3-6 in Fernie BC, Canada.

Huete A., Didan K., Miura T., Rodriguez E.P., Gao X., Ferreira L.G. (2002) Overview of the radiometric and biophysical performance of the MODIS vegetation indices. *Remote Sensing of Environment* Vol.83 pp.195-213.

Huete A., Liu, H., Q., Batchily, K. and van Leeuwen, W. (1997) A Comparison of Vegetation Indices over a Global Set of TM Images for EOS-MODIS. *Remote Sensing of Environment*. Volume 59, Issue 3, pp. 440–451.

Ichii, K., Kawabata, A. and Yamaguchi, Y. (2002) Global correlation analysis for NDVI and climatic variables and NDVI trends: 1982–1990. *International Journal of remote Sensing*. vol. 23, no. 18, 3873–3878.

Jönsson, P. and Eklundh, L. (2002). Seasonality extraction by function fitting to time-series of satellite sensor data. *IEEE Transactions on Geoscience and Remote Sensing* 40 (8), pp. 1824-1832.

Jönsson, P. and Eklundh, L. (2003). Seasonality extraction from satellite sensor data. *Frontiers of Remote Sensing Information Processing*, edited by Chen, C.H. World Scientific Publishing. pp. 487-500.

Jönsson, P. and Eklundh, L. (2012) *TIMESAT 3.1 - Software Manual*. Lund University, 82 pp.

Kastens, J. H., Kastens, T. L., Kastens, D. L. A., Price, K. P., Martinko, E. A. and Lee, R. Y. (2005). Image masking for crop yield forecasting using AVHRR NDVI time series imagery. *Remote Sensing of Environment*, 99(3), 341−356.

Khokhlov, V., Yermolenko, N. and Ivanov, A. (2012) *Spatiotemporal features of droughts in Ukraine under climate change.* Paper presented in: Workshop on the Development of an Experimental Global Drought Information System (GDIS), 11-13 April 2012, Frascati (Rm) – Italy.

Kogan, F. (2007) *Drought Ukraine 2007*. National Oceanic and Atmospheric Administration (NOAA), National Environmental Satellite Data and Information Services (NESDIS),USA Retrieved 22.04.2013 from: http://www.star.nesdis.noaa.gov/smcd/emb/vci/VH_doc/2007_Ukraine07agWEB.pdf

Kogan, F., Adamenko, T. and Kulbida, M. (2011) Satellite-Based Crop Production Monitoring in Ukraine and Regional Food Security. In *Use of Satellite and In-Situ Data to Improve Sustainability*. NATO Science for Peace and Security Series C: Environmental Security. pp. 99-105. ISBN 978-90-481-9618-0.

Kogan, F. and Guo, W. (2011) Early Detection and Monitoring Droughts From NOAA Environmental Satellites. In *Use of Satellite and In-Situ Data to Improve Sustainability*. NATO Science for Peace and Security Series C: Environmental Security. pp. 99-105. ISBN 978-90-481-9618-0.

Kul'bida (2009) *Weather risks, connected with agro production in Ukraine*. Retrieved 2012-12-02 from: http://www.agroinsurance.com/en/risks_management/?pid=5174&print=1

Kytischeva, N. (2012) Drought and sunflower. In *"The Ukrainian Farmer"* september, 2012. Retrieved 02.06.2013 from: http://www.agrotimes.net/posuha-sonyashnik.html

Lawder, J., K. and King, P., J., H. (2000) *Using Space-filling Curves for Multi-dimensional Indexing*. School of Computer Science and Information Systems, Birkbeck College, University of London.

Liu, Y, Guo, M., Wang, X., Tani, H. and Yi, K. (2011) *Analysis the Impact of Drought on NDVI in Drought Periods Combined with Climate factors and Land Cover in Southwest China*. Presented in: 34th International Symposium on Remote Sensing of Environment. Sydney, Australia 10-15 April

Martynenko, O., Kobzev, O. and Oginskiy, A. (2001) Transformation of farming systems in southern Ukraine and soil degradation. *Farming Systems and Poverty, improving farmers' livelihoods in a changing world*. Food and Agriculture Organization of the United Nations, Rome, Italy. ISBN 92-5-104627-1.

Meng, L., Li, J., Chen, Z., Xi, W., Chen, D. and Duan, H. (2010) The calculation of TVDI based on the composite time of pixel and drought analysis. *The International Archives of the Photogrammetry, Remote Sensing and Spatial Information Sciences*, Vol. 38, Part II

Min, Y. and Minghu, C. (2010) *Ts /NDVI Space Based Drought Monitoring Study from Satellite Remote Sensing Data in Heilongjiang*. Paper presented in: World Automation Congress (WAC), Kobe, 19-23 Sept.

Nemani, R., Pierce, L. and Running, S. (1992) Developing Satellite-derived Estimates of Surface Moisture Status. *Journal of Applied Meteorology*, vol. 32, pp. 548 – 557.

Netis, I. (2007) Drought – the lesson for the future. *Ukrainian journal of agribusiness issues*. Number 2007'07. Retrieved 2012-12-02 from: http://www.propozitsiya.com/?page=149&itemid=2400&number=75

Netis, I., T. (2009) Changes of moisture conditions of soil in southern Ukraine. *Taurian Science Journal*. Vol.64. Registration number: КВ № 13543-2508 ПР.

NOAA (2008) *Drought. Public fact sheet.* National Weather Service. Retrieved 12.06.2013 from: http://www.nws.noaa.gov/om/brochures/climate/Drought.pdf

NOAA (2013) *GHCND (GlobalHistorical ClimatologyNetwork)-Monthly Summaries*. CSV datasets. Retrieved 12.06.2013 from: ftp://ftp.ncdc.noaa.gov/pub/data/cdo/documentation/GHCNDMS_documentation.pdf

Oindo, B., O., Skidmore, A., K. and de By, R., A. (2000) Interannual variability of NDVI and species richness in Kenya. *International Archives of Photogrammetry and Remote Sensing.* Vol. XXXIII, Part B7., Amsterdam.

Oliver, S., A., Oliver H., R., Wallace, J., S. and Roberts A.M. (1987) Soil heat flux and temperature variation with vegetation, soil type and climate. *Agricultural and Forest Meteorology*, 39 pp. 257-269

PELCOM (2001) Pan-European Land Use and Land Cover Monitoring, *1-km pan-European land cover database.* Retrieved 22.04.2013 from: http://www.geo-informatie.nl/projects/pelcom/public/index.htm

Peng, S., Chen, A., Xu, L., Cao, C., Fang, J., Myneni, R.B., Pinzon, J.E., Tucker et al. (2011) *Recent change of vegetation growth trend in China*. Environmental Research Letters 6: 10.1088/1748-9326/6/4/044027.

Peters, A., J., Walter, E., A., Ji, L., Vlina, A., Hayes, M. and Sodova, M., D. (2002) Drought Monitoring with NDVI-Based Standardized Vegetation Index. *Photogrammetric Engineering & Remote Sensing*. Vol. 68, No. 1. pp. 71-75

Pinnok, D., R., Bugbee, B. and Morrow, R., C. (2002) *Leaf Temperature: Applying the CWSI to Controlled Environments.* Utah State University, Crop Physiology Laboratory, Logan, UT, U.S.A.

Propastin, P. and Kappas, M. (2008) *Spatio-temporal drifts in AVHRR/NDVI-precipitation relationships and their linkage to land use change in central Kazakhstan*. EARSeL eProceedings, 7(1): 30-45

Reed, B., C., Brown, J., F., VanderZee, D., Loveland, T., Merchant, J., W. and Ohlen, D., O. (1994) Measuring Phenological Variability from Satellite Imagery. *Journal of Vegetation Science*, Vol. 5, No. 5, Applications of Remote Sensing and Geographic Information Systems in Vegetation Science (Nov., 1994), pp. 703-714, Willey

Ricotta, C., Avena, G. and de Palma, A. (1999) Mapping and monitoring net primary productivity with AVHRR NDVI time-series: statistical equivalence of cumulative vegetation indices. *ISPRS Journal of Photogrammetry & Remote Sensing* 54 pp. 325–331

Rogerson, P., A. (2001) *Statistical methods for geography*. SAGE Publications, London, Thousand Oaks, New Delhi. ISBN 0 76196287 5.

Rudenko, L., G. (Eds.) (2007) *National Atlas Of Ukraine*, SSPE "Kartographia", Kiev, Ukriane, ISBN: 978-966-475-067-4.

Runnström, M. (2000). *Is northern China winning the battle against desertification?* Ambio, Vol.29, No.8, (April 2000), pp. 468-476, ISSN 0044-7447

Saiko ,V., F. (1995) Problems of Rational Agricultural Land Use in Ukraine. Working Paper 95-WP 145, Center for Agricultural and Rural Development Iowa State University, Ames, U.S.A.

Sandholt, I., Rasmussen, K. and Andersen, J. (2002) A simple interpretation of the surface temperature/vegetation index space for assessment of surface moisture status. *Remote Sensing of Environment*, vol. 79, pp. 213-224

Solodushko, M., M. (2011) Features of wintering and productivity of winter wheat. Institute of agriculture of steppe zone, National Academy of Science of Ukraine. Dnipropetrovsk, Ukraine.

UNFCCC (1998) *The First National Communication on Climate Change, Ukraine*. The United Nations Framework Convention on Climate Change. Retrived 22.07.2013 from: http://unfccc.int/resource/docs/natc/ukrnc1.pdf

USGS (2011) *Deriving Phenological Metrics from NDVI. U.S.* Department of the Interior and U.S. Geological Survey. Retrieved 22.04.2013 from: http://phenology.cr.usgs.gov/methods_metrics.php

USWCL (2001) Thermal Crop Water Stress Indices. U.S. Water Conservation Laboratory, Phoenix, Arizona. Retrieved 12.06.2013 from: http://www.plantstress.com/articles/drought_i/drought_i_files/cwsi_phoenix.pdf

van Leeuwen, W., J., D., Hartfield, K., Miranda, M. and Meza, F., J. (2013) *Trends and ENSO/AAO Driven Variability in NDVI Derived Productivity and Phenology alongside the Andes Mountains*. Remote Sensing 2013, 5, pp. 1177–1203

van Leeuwen, M., Salamon, P., Fellmann, T., Banse, M., von Ledebur, O., Salputra, G. and Nekhay, O. (2012) *The agri-food sector in Ukraine: Current situation and market outlook until 2025*. Scientific and Policy Report by the Joint Research Centre of the European Commission. Publications Office of the European Union, Luxembourg. ISBN 978-92-79-25742-1.

Verheye, W. (2006) Dry lands and desertification. *Land use, land cover and soil sciences*. Vol. 5. UNESCO - encyclopedia of life support system. Retrieved 2012-12-02 from: http://www.eolss.net/Sample-Chapters/C19/E1-05-06.pdf

Vojegova, R., A., Zayiets, S., O. and Kovaenko, A., M. (2013) Irrigated agriculture and agro-technology in case of climate changes in Ukrainian steppe zone. *Manual for Ukrainian farmer*. Chapter 4. Irrigation and melioration. National registration: КВ № 14171-3142 P. pp. 162-164

Vrieling, A., de Beurs, K., M., and Brown, M., E. (2011) Variability of African farming systems from phenological analysis of NDVI time series. *Climatic Change*. Vol.109 pp. 455-477

Wang, J., Prince, K., P. and Rich, P., M. (2001) Spatial patterns of NDVI in response to precipitation and temperature in the central Great Plains. *International Journal of Remote Sensing.* vol. 22, no. 18, pp. 3827–3844

Wang, J., Rich, P., M. and Price, K., P. (2003) Temporal responses of NDVI to precipitation and temperature in the central Great Plains, USA. *International Journal of Remote Sensing*. Vol. 24, No. 11, pp. 2345–2364

Wardlow, B., D. and Egbert, S., L. (2008) Large-area crop mapping using time-series MODIS 250 m NDVI data: An assessment for the U.S. Central Great Plains. *Remote Sensing of Environment.* Vol.112, pp. 1096-1116

Weier, J. and Herring, D. (2000) *Measuring Vegetation (NDVI & EVI)*. NASA Earth Observatory. Retrieved 22.04.2013 from: http://earthobservatory.nasa.gov/Features/MeasuringVegetation/printall.php

World Bank (2004) *Achieving Ukraine's Agricultural Potential*. *Stimulating Agricultural Growth and Improving Rural Life.* Joint Publication by the Organization for Economic Co-operation and Development and the Environmentally and Socially Sustainable Development Unit, Europe and Central Asia Region, The World Bank. Washington, DC. U.S.A.

World Bank (2007*) Integrating Environment into Agriculture and Forestry Progress and Prospects in Eastern Europe and Central Asia*, Volume II, Country Review, Ukraine

Yatsyk, A., Kublanov, S., Kh., Oleksiyenko, o., V., Tregubova, O., O., Tararyko, O., G., Bulygin, S., Y. et al. (2006) *Synergy report on the research of interaction and the status of implementation in Ukraine of the UN Framework Convention on Climate Change, the UN Convention on Biological Diversity and the UN Convention to Combat Desertification*. Retrieved 14.05.2012 from: http://www.thegef.org/gef/sites/thegef.org/files/documents/document/768.pdf

Yin, H., Udelhoven, T., Fensholt, R., Pflugmacher, D. and Hostert, P. (2012) How Normalized Difference Vegetation Index (NDVI) Trends from Advanced Very High Resolution Radiometer (AVHRR) and Système Probatoire d'Observation de la Terre VEGETATION (SPOT VGT) Time Series Differ in Agricultural Areas: An Inner Mongolian Case Study. *Remote Sensing*. Vol. 4, pp. 3364-3389. ISSN 2072-4292.

Yuan, G., Luo, Y., Sun, X. and Tang, D. (2004) Evaluation of a crop water stress index for detecting water stress in winter wheat in the North China Plain. *Agricultural Water Management*, vol. 64 pp. 29-40.

Yuan, F. and Roy S., S. (2007) *Analysis of the relationship between NDVI and climate variables in Minnesota using geographically weighted regression and spatial interpolation.* Paper presented in ASPRS 2007 Annual Conference Tampa, Florida

Series from Lund University

Department of Physical Geography and Ecosystem Science

Master Thesis in Geographical Information Science (LUMA-GIS)

1. *Anthony Lawther:* The application of GIS-based binary logistic regression for slope failure susceptibility mapping in the Western Grampian Mountains, Scotland. (2008).

2. *Rickard Hansen:* Daily mobility in Grenoble Metropolitan Region, France. Applied GIS methods in time geographical research. (2008).

3. *Emil Bayramov:* Environmental monitoring of bio-restoration activities using GIS and Remote Sensing. (2009).

4. *Rafael Villarreal Pacheco:* Applications of Geographic Information Systems as an analytical and visualization tool for mass real estate valuation: a case study of Fontibon District, Bogota, Columbia. (2009).

5. *Siri Oestreich Waage:* a case study of route solving for oversized transport: The use of GIS functionalities in transport of transformers, as part of maintaining a reliable power infrastructure (2010).

6. *Edgar Pimiento:* Shallow landslide susceptibility – Modelling and validation (2010).

7. *Martina Schäfer:* Near real-time mapping of floodwater mosquito breeding sites using aerial photographs (2010)

8. *August Pieter van Waarden-Nagel:* Land use evaluation to assess the outcome of the programme of rehabilitation measures for the river Rhine in the Netherlands (2010)

9. *Samira Muhammad:* Development and implementation of air quality data mart for Ontario, Canada: A case study of air quality in Ontario using OLAP tool. (2010)

10. *Fredros Oketch Okumu*: Using remotely sensed data to explore spatial and temporal relationships between photosynthetic productivity of vegetation and malaria transmission intensities in selected parts of Africa (2011)

11. *Svajunas Plunge:* Advanced decision support methods for solving diffuse water pollution problems (2011)

12. *Jonathan Higgins:* Monitoring urban growth in greater Lagos: A case study using GIS to monitor the urban growth of Lagos 1990 - 2008 and produce future growth prospects for the city (2011).

13. *Mårten Karlberg:* Mobile Map Client API: Design and Implementation for Android (2011).

14. *Jeanette McBride:* Mapping Chicago area urban tree canopy using color infrared imagery (2011)

15. *Andrew Farina:* Exploring the relationship between land surface temperature and vegetation abundance for urban heat island mitigation in Seville, Spain (2011)

16. *David Kanyari*: Nairobi City Journey Planner An online and a Mobile Application (2011)

17 *Laura V. Drews:* Multi-criteria GIS analysis for siting of small wind power plants - A case study from Berlin (2012)

18 *Qaisar Nadeem:* Best living neighborhood in the city - A GIS based multi criteria evaluation of ArRiyadh City (2012)

19 *Ahmed Mohamed El Saeid Mustafa:* Development of a photo voltaic building rooftop integration analysis tool for GIS for Dokki District, Cairo, Egypt (2012)

20 *Daniel Patrick Taylor*: Eastern Oyster Aquaculture: Estuarine Remediation via Site Suitability and Spatially Explicit Carrying Capacity Modeling in Virginia's Chesapeake Bay (2013)

21 *Angeleta Oveta Wilson:* A Participatory GIS approach to *unearthing* Manchester's Cultural Heritage '*gold mine'* (2013)

22 *Ola Svensson:* Visibility and Tholos Tombs in the Messenian Landscape: A Comparative Case Study of the Pylian Hinterlands and the Soulima Valley (2013)

23 *Monika Ogden:* Land use impact on water quality in two river systems in South Africa (2013)

24 *Stefan Rova:* A GIS based approach assessing phosphorus load impact on Lake Flaten in Salem, Sweden (2013)

25 *Yann Buhot:* Analysis of the history of landscape changes over a period of 200 years. How can we predict past landscape pattern scenario and the impact on habitat diversity? (2013)

26 *Christina Fotiou:* Evaluating habitat suitability and spectral heterogeneity models to predict weed species presence (2014)

27 *Inese Linuza:* Accuracy Assessment in Glacier Change Analysis (2014)

28 *Agnieszka Griffin:* Domestic energy consumption and social living standards: a

GIS analysis within the Greater London Authority area (2014)

29 *Brynja Guðmundsdóttir* Detection of potential arable land with remote sensing and GIS - A Case Study for Kjósarhreppur (2014)

30 *Oleksandr Nekrasov* Processing of MODIS Vegetation Indices for analysis of agricultural droughts in the southern Ukraine between the years 2000-2012 (2014)

31 *Sarah Tressel* Recommendations for a polar Earth science portal

in the context of Arctic Spatial Data Infrastructure (2014)